Population genetics theory of natural selection

Takahiro Sakamoto

Doctor of Philosophy

Department of Evolutionary Studies of Biosystems

School of Advanced Sciences

SOKENDAI

2023

Abstract

One of the ultimate goals of population genetics is to understand how changes in DNA sequences are influenced by various evolutionary factors. Natural selection is a very powerful evolutionary force that determines the direction of evolution. How natural selection affects evolution is of great interest for researchers in population genetics and has been a subject of many studies. Most previous theoretical studies have considered simple situations where selection pressure is homogeneous across multiple populations and interactions between different loci are negligible. These studies have revealed how natural selection affects various properties such as mutation fixation probability and allele frequency distribution. However, recent advances in DNA sequencing technology have made it possible to obtain large amounts of sequence data across multiple loci from many populations, demanding new theories that take into account more complex selection pressures involving multiple loci and multiple populations. It is not yet clear how such complex natural selection affects the temporal changes of DNA sequences. In this thesis, I develop theories to explore the effects of complex natural selection on molecular evolution.

In Chapter 2, I focus on the evolutionary process of genome divergence in a local adaptation process. In local adaptation, the direction of natural selection could differ among populations. Using a two-population model, I quantitatively evaluate the establishment probability of a locally adaptive allele and the level of nucleotide diversity after the establishment. The results show that the combination of diffusion and effective migration approximations describes the dynamics well. The probability of establishment of a new locally adaptive allele is obtained as a function of selection coefficient, migration rate, and population sizes of the two populations. The expected patterns of nucleotide diversity are also derived. It is found that nucleotide diversity changes significantly when a new locally adaptive allele is established, and then the pattern changes gradually through a joint work of migration, selection, recombination, and mutation.

In Chapter 3, I incorporate sexual selection into the model of local adaptation described in Chapter 2 and examine the effect of sexual selection on the establishment of locally adaptive alleles. First, an approximate expression of the probability of establishment is derived. It is found that assortative mating enhanced by sexual selection inhibits the establishment of locally adaptive alleles. The probability of establishment depends mainly on the relative strength of natural and sexual selection, but random genetic drift also affects the dynamics when the population size is small. I also describe the expected trajectory of allele frequency during the establishment process.

In Chapter 4, I examine how a turnover of sex-determining loci is driven by sexually antagonistic selection at linked loci. Turnovers of sex-determining gene are often observed in amphibians and teleost fishes, and sexually antagonistic selection is thought to be one of

the driving forces. Previous studies have investigated this process in deterministic models, whereas I use a more realistic stochastic model and demonstrate that the stochasticity of random genetic drift essentially changes the establishment dynamics of a new sex-determining allele. The mode of sexually antagonistic selection is a key determinant of the establishment probability. The establishment probability is high when linked selection works as balancing selection, while it is low when selection works as directional selection. I also use simulations to illustrate how the mode of selection affects the pattern of nucleotide diversity following the turnover process.

In Chapter 5, I study the degenerative process of Y chromosomes. It is theoretically known that in non-recombinant chromosomes such as the Y chromosome, the interaction between multiple deleterious mutations makes them easily fix. Recent genome analyses have revealed that Y chromosomes retain duplicated genes in many species and that gene conversion between homologous sequences occurs frequently. However, previous models of the degenerative process of the Y chromosome have not taken this into account. Therefore, I construct a new model of Y chromosome evolution that takes gene duplication and gene conversion into account and analyze its evolutionary dynamics. The results show that gene duplication and gene conversion affect the evolutionary dynamics in a complex manner.

In summary, in this thesis, I developed new theories of natural selection for local adaptation and the evolution of sex chromosomes. To understand these processes, it is necessary to consider multiple-loci models or multiple-population models, which made detailed theoretical analysis difficult. I introduced new approximation methods to make these models tractable and clarified the evolutionary dynamics in these processes. In Chapter 6, I systematically organized the approximations used in this thesis and discussed their usefulness. This thesis demonstrates how useful various approximation methods can be in the analysis of multi-loci multi-population models with natural selection.

Contents

Chapter 1

General Introduction

Theoretical population genetics studies how the population dynamics of DNA sequences are determined by the interaction of various evolutionary forces, including mutation, natural selection, recombination, population structure, and random genetic drift. Of these factors, natural selection would be one of the most important forces because it determines the direction of evolution. Natural selection works when multiple genotypes with different survival and reproductive abilities are present in a population, and it favors the spread of more favorable genotypes. Natural selection tends to fix beneficial mutations in a population and to purge harmful ones. The dynamics of evolution under such selection pressures has been a major interest of researchers in population genetics.

Previous theories have successfully revealed the effects of selection in a simple one-locus one-population model. However, to fully understand the mechanism behind molecular evolution, it is required to consider the interactions of selection at multiple loci and in multiple populations. Many species live in geographically extended spaces, and population structure is an important factor to determine the evolutionary dynamics. Recent developments in DNA sequencing technologies have made it easier to obtain large amounts of sequence data from many populations. These data can reveal how genome is shaped in the face of interactions of multiple loci and multiple populations, and there is need to develop multi-locus multi-population theories to infer evolutionary history from genomic data. It is particularly important to consider the interactions of multiple loci because linkage is a fundamental property of the DNA sequences in all species. However, theoretical studies of selection in multi-locus/multi-population models have not been fully explored due to technical difficulties in mathematical analysis.

The aim of this thesis is to construct theories for evolutionary processes that inherently involve selection at multiple loci and/or in multiple populations. As examples, I especially focus on local adaptation and the evolution of sex chromosomes. Although the analysis of the multi-locus and multi-population models is generally difficult, I successfully derive theoretical expressions for these evolutionary processes with several approximations. These theories show that developing useful approximations is a powerful strategy for overcoming theoretical difficulties and exploring multi-locus multi-population models.

In this chapter, I briefly explain the theoretical background of natural selection. First, I review the results of one-locus, one-population models. In such simple models, diffusion approximation often allows us to obtain analytical results, and the effect of selection is well understood. Next, I consider multi-locus multi-population models. In such complex models, mathematical analysis is more difficult than in one-locus one-population models, and analyt-

ical results can be obtained only in limited situations. I review these studies and explain how theoretical difficulties arise in these models. Finally, I explain how local adaptation and the evolution of sex chromosomes, that are topics I focus on in this thesis, are inherently involved in selection at multiple loci and selection in multiple population.

1.1 Natural selection in one-locus one-population model

The effects of natural selection have been extensively studied using one-locus one-population models. In this section, I briefly review the results of these studies.

Consider a biallelic locus A/a at which allele A and allele a coexist. Let x be the frequency of allele A. It is assumed that allele A has fitness $1 + s(x)$ while the fitness of wild type allele a is fixed to 1. Under the Wright–Fisher model (Fisher 1930, Wright 1931), the expected change of x in one generation, $M(x)$, is given by

$$M(x) \approx s(x)x(1-x). \tag{1.1}$$

Well known classic results are as follows. Haldane (1927) derived the fixation probability of an allele A as $P_{\text{fix}} \approx 2s$ for constant $s(x) \equiv s > 0$ using a branching process approximation. Allowing for mutation between the two alleles, Wright (1938) derived the equilibrium distribution of x, $\phi(x)$, as:

$$\phi(x) \propto \frac{1}{V(x)G(x)}, \tag{1.2}$$

where $G(x) = \exp\left(\int -\frac{2M(x)}{V(x)}dx\right)$, $V(x) = \frac{x(1-x)}{2N}$ and N being the population size of diploid species. These results illustrate how natural selection interacts with mutation and random genetic drift to affect evolution in the Wright–Fisher model.

Later, Motoo Kimura have developed various mathematical methods based on the diffusion approximation, which is very powerful in the analysis of allele frequency dynamics. Using the diffusion approximation, the evolutionary process is described by the Kolmogorov forward equation:

$$\frac{\partial\phi(p,x,t)}{\partial t} = \frac{1}{2}\frac{\partial^2}{\partial x^2}[V(x)\phi(p,x,t)] - \frac{\partial}{\partial x}[M(x)\phi(p,x,t)] \tag{1.3}$$

and Kolmogorov backward equation:

$$\frac{\partial\phi(p,x,t)}{\partial t} = \frac{V(p)}{2}\frac{\partial^2\phi(p,x,t)}{\partial p^2} + M(p)\frac{\partial\phi(p,x,t)}{\partial p}, \tag{1.4}$$

where $\phi(p,x,t)$ is the probability density that the allele frequency is x at time t when the allele frequency at $t = 0$ is p (Crow and Kimura 1970). From this equation, many evolutionary properties can be obtained in a more general form. For example, the fixation probability is derived for arbitrary s and dominance as:

$$P_{\text{fix}} = \frac{\int_0^p G(x)dx}{\int_0^1 G(x)dx}, \tag{1.5}$$

where p is the initial allele frequency (Kimura 1962). Other various properties are also derived using the diffusion approximation such as average allele age (Maruyama 1974), average

fixation time (Kimura and Ohta 1969) and temporal change of allele frequency distribution (Kimura *et al.* 1955, Song and Steinrücken 2012). In summary, the diffusion approximation is applicable to general situations and is very useful for studying the evolutionary dynamics in the one-locus one-population model.

While the diffusion approximation is the most common way to incorporate selection in the one-locus one-population model, some theories have been constructed based on the coalescent theory. The coalescent theory considers the evolutionary history of samples taken from current populations. This approach is very useful to handle neutral mutations, and most studies of the coalescent theory have focused only on neutral mutations. However, several studies have attempted to incorporate selection into the coalescent theory framework. Krone and Neuhauser developed an ancestral selection graph to simulate selection by permitting bifurcations of genealogy (Krone and Neuhauser 1997, Neuhauser and Krone 1997), but this approach is suitable for a computational use and may not be useful for deriving analytical results (but see Wakeley 2009).

1.2 Natural selection in more complex models

When selection operates in multi-population or multi-locus models, theoretical description of the evolutionary dynamics becomes much more difficult. In this section, I briefly review the theories of such complex natural selection and point out the difficulties in theoretical construction.

1.2.1 Diffusion approximation

The diffusion approximation is still a useful framework in multi-population multi-loci models. First, I focus on the effect of population structure. The Kolmogorov forward equation for the two-population model is given by:

$$\frac{\partial \phi}{\partial t} = \frac{1}{2}\frac{\partial^2}{\partial x_1^2}[V_1\phi] - \frac{\partial}{\partial x_1}[M_1\phi] + \frac{1}{2}\frac{\partial^2}{\partial x_2^2}[V_2\phi] - \frac{\partial}{\partial x_2}[M_2\phi], \tag{1.6}$$

where x_i, V_i and M_i are x, V and M in population i, respectively (Ewens 2004). Compared to Equation 1.3, Equation 1.6 has two additional terms because the dimension of the diffusion process is increased. This increase in dimension makes it very difficult to obtain analytical expressions.

A similar difficulty of increased dimension arises when we consider a multi-locus model. Consider a two-locus model consisting of loci A/a and B/b, and let x_1, x_2, and x_3 be the frequency of genotypes AB, Ab, and aB, respectively. The frequency of genotype ab is given by $1 - x_1 - x_2 - x_3$. The Kolmogorov forward equation for this two-locus model is given by:

$$\frac{\partial \phi}{\partial t} = -\sum_i \frac{\partial}{\partial x_i}[M_i\phi] + \frac{1}{2}\sum_i \frac{\partial^2}{\partial x_i^2}[V_i\phi] + \frac{1}{2}\sum_i \sum_{j\neq i} \frac{\partial^2}{\partial x_i \partial x_j}[C_{ij}\phi], \tag{1.7}$$

where M_i is the expected change of x_i in one generation, V_i is the variance of x_i in one generation, and C_{ij} is the covariance between x_i and x_j in one generation (Ewens 2004). We can see that the number of terms in Equation 1.6 has increased considerably compared to Equation 1.3. Thus, the theoretical description of the process is again difficult.

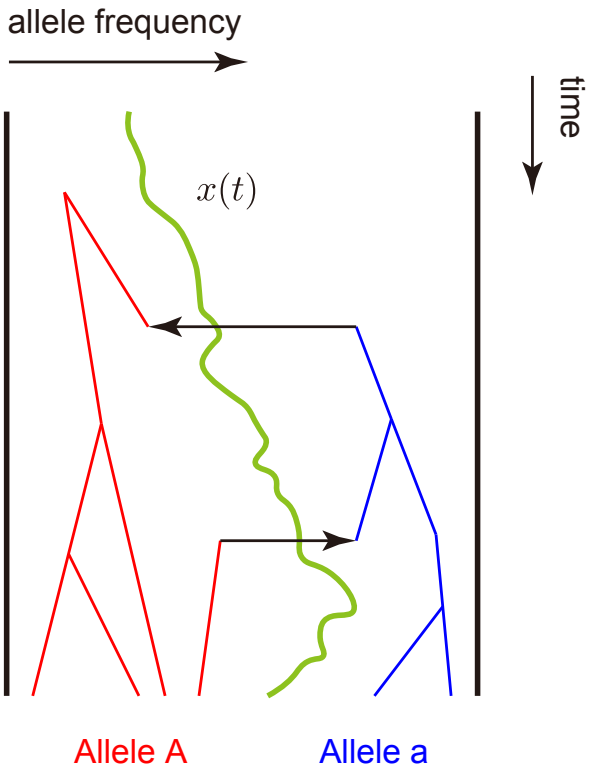

Figure 1.1: Summary of the structured coalescent approximation. First, $x(t)$ is determined (green line). Next, assuming that alleles linked to each selected allele belong to different populations, standard structured coalescent theory is applied, in which mutation at locus A/a and recombination function as "migration" events (black arrows).

In some special cases, analytical results can be obtained even in multi-population models. Maruyama (1970) considered a multi-populations model of haploid species where selection pressure s is homogeneous in all populations. Then, Maruyama (1970) mathematically showed that the fixation probability is the same as the fixation probability in an unstructured population with the same total population size. In the case of low migration limit, where the evolution in each population can be considered independent, Slatkin (1981) obtained analytical expressions for the fixation probability and the average fixation time. However, in general situations in which selection pressure differs between populations and migration is not negligible, solving the diffusion equation is still very difficult.

1.2.2 Structured coalescent approximation

Another approach to handle a multi-locus multi-population model is the structured coalescent approximation. It was developed to consider the amount of neutral polymorphism in the vicinity of selected locus (Kaplan *et al.* 1988, Hudson and Kaplan 1988). The basic scheme is explained in Figure 1.1. Let us consider the evolutionary history of a neutral locus that is close to a selected locus. First, the allele frequency dynamics at the selected locus, $x(t)$, is determined. Both simulations and analytical formula can be used to determine $x(t)$. Next, we consider that alleles linked to different selected alleles (alleles A and a) belong to different "subpopulations", and that mutations at the selected locus and recombination between the linked neutral locus and the selected locus work as "migration" between the different subpopulations. Then, standard structured coalescent theory can be applied.

This technique has been used to investigate various topics such as the effect of balancing

selection (Hudson and Kaplan 1988), selective sweep (Kaplan *et al.* 1989), and background selection (Charlesworth *et al.* 1993a, Hudson and Kaplan 1995) (see also Nordborg 1997, Wakeley 2009). Some analytical results are obtained when $x(t)$ can be considered as a constant (see Hudson and Kaplan 1988, for example). However, when x changes dynamically, it is generally difficult to obtain analytical results in a closed form. In summary, while the diffusion approximation and structured coalescent approximation are very useful frameworks, multi-locus multi-population models are complex and generally not possible to obtain mathematical expressions in an exact manner.

1.3 The content of this thesis

In this thesis, I develop a new theory of selection involving multiple loci and multiple populations. Since such complex models cannot be analyzed in a rigorous manner as I reviewed above, I take a different approach, using approximations to describe the evolutionary dynamics. These approximations may not be valid in the full range of parameters, but they work well in specific situations that are biologically significant. Then, such theories are very useful to understand the evolutionary dynamics.

I especially focus on two processes; local adaptation and the evolution of sex chromosomes. Local adaptation occurs when the direction of selection pressure is different among multiple populations. Since this process inherently involves multiple populations, our knowledge from the one-population model should not be applied. In Chapter 2, I develop a new theoretical framework to understand local adaptation process using a two-population model. In Chapter 3, this framework is extended to incorporate the effect of assortative mating driven by sexual selection.

The evolution of sex chromosomes is a situation in which linkage between different loci becomes very important. In Chapter 4, I focus on the evolution of young sex chromosomes in which recombination between two sex chromosomes (X/Y or Z/W) is ongoing. In such cases, linkage to sex-determining alleles has large effects on the evolutionary process. I investigate how such linkage affects the dynamics of turnover of sex-determining genes. In Chapter 5, I focus on later stages of sex chromosomes in which recombination between the two chromosomes is suppressed. In this situation, it is well known that multiple deleterious mutations arise in linkage, affecting the evolutionary dynamics of Y and W chromosomes. I study the degeneration speed of the sex chromosomes in such situation. My theories which I describe in this thesis demonstrate how complex natural selection affects the evolutionary dynamics and how useful approximation techniques can be in analyzing evolutionary dynamics.

Chapter 2

The Evolutionary Dynamics of a Genetic Barrier to Gene Flow: From the Establishment to the Emergence of a Peak of Divergence

2.1 Introduction

A genomic island of divergence could arise when a locally adapted allele establishes in a certain subpopulation (e.g., Wu 2001, Turner *et al.* 2005, Nosil 2012). This local establishment could be stably maintained by divergent selection if the allele confers sufficient benefit in the subpopulations in which it is adaptive, but not in the ones in which it is deleterious. Such a locus works as a genetic barrier to gene flow or a barrier locus because migrants are maladaptive. Due to recombination, the genomic region that is affected by divergent selection is limited, thereby creating a peak of divergence along the chromosome (i.e., a genomic island of divergence). Further development of multiple barrier loci in the genome might initiate ecological speciation (Turner *et al.* 2005, Nosil 2012). In this study, I am interested in the evolutionary dynamics of a barrier locus, from its establishment via a partial local sweep, the emergence of a peak of divergence to its stable preservation.

I consider theoretically the process by dividing into three phases, the establishment, consolidation and equilibrium phases, as illustrated in Figure 2.1. I consider a simple situation with two subpopulations, I and II. Assuming a relatively high migration rate between them, the levels of polymorphism within the two subpopulations are similar to each other (measured by the heterozygosities, h_{w1} and h_{w2}, for subpopulations I and II). In the meantime, the population divergence (measured by h_b, the heterozygosity between the two subpopulations) is very low (Figure 2.1A). Then, a *de novo* mutation (the star in Figure 2.1A) arises in subpopulation I, in which the mutation is advantageous, but it is maladaptive (or deleterious) in subpopulation II. In the establishment phase, the mutation spreads in subpopulation I and nearly fixes (Figure 2.1B), but its frequency in subpopulation II is low because it should be selected against if migrated into subpopulation II. In a strict sense, this is not a fixation that can be mathematically treated as an absorbing state, because migration keeps providing maladaptive alleles. Therefore, after Kimura (1954), I hereafter use the terminology of "quasi-fixation" for this nearly fixed state. The quasi-fixation should occur quickly, and a partial local selective sweep occurs in subpopulation I (Figure 2.1B), thereby establishing a barrier locus. Around the barrier locus, it is typical to observed a "block" of region with low genetic variation in subpopulation I with a slightly elevated F_{ST}. The consolidation

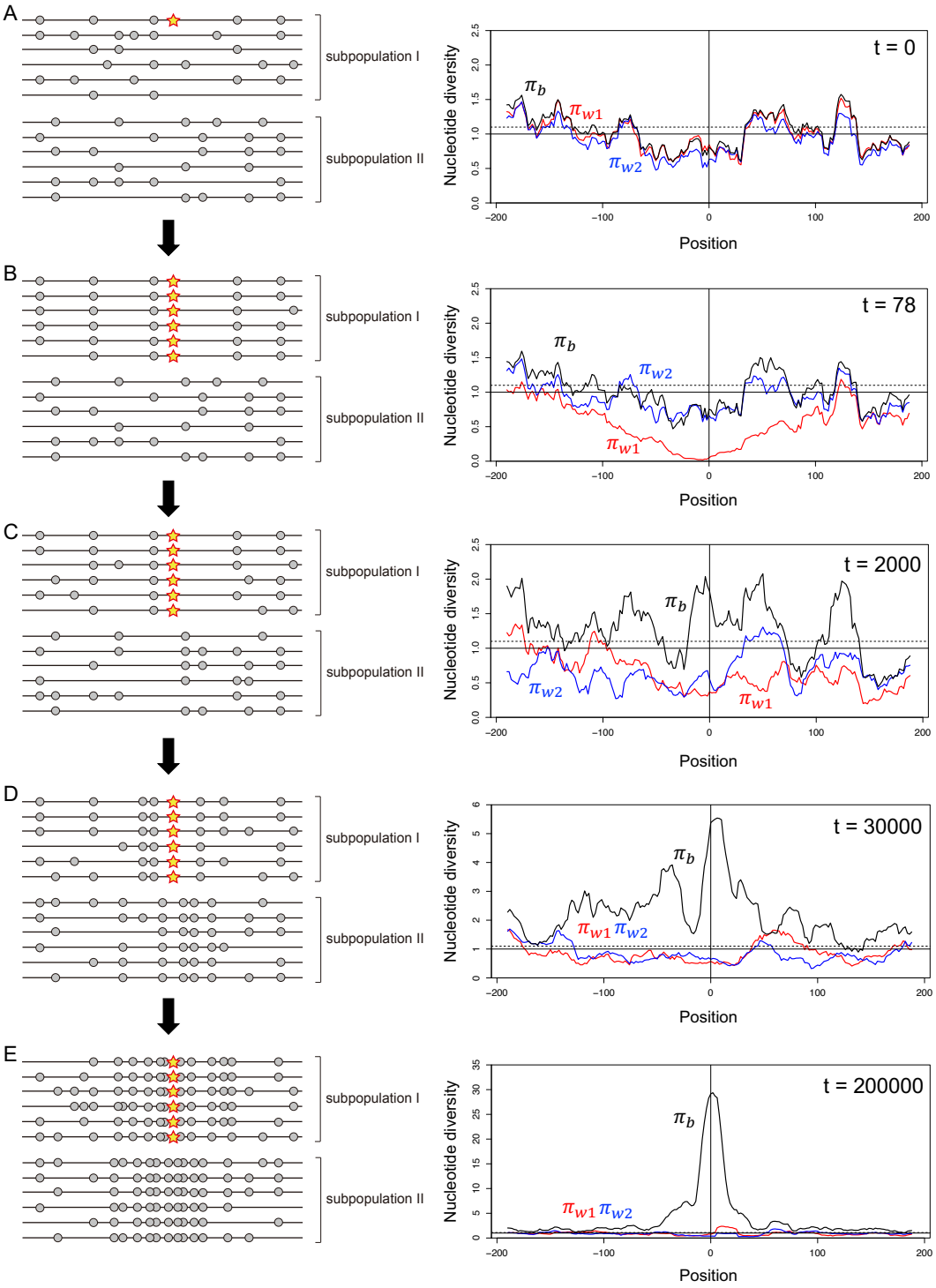
A
subpopulation I
subpopulation II
t = 0
B
t = 78
C
t = 2000
D
t = 30000
E
t = 200000
Nucleotide diversity
Position
π_b
π_{w1}
π_{w2}

Figure 2.1: Illustrating the evolution of a barrier locus in a simple two-population model with fairly high migration between them. (A) A locally adaptive de novo mutation arises in subpopulation I at position 0. A typical pattern of polymorphism is shown in left. The star is the locally adaptive mutation and gray circles are neutral polymorphism in the surrounding region. The right panel shows the spacial distributions of nucleotide diversity obtained by a simulation. The simulation considers two subpopulations with population sizes are $2N_1 = 2N_2 = 2000$, between which symmetric migration is allowed at rate $4N_1m_1 = 4N_2m_2 = 5.0$. I assume selection intensity $s_1 = 0.2$ and $s_2 = -0.2$. The entire simulated region is 400 kb if a population recombination rate of $4Nr = 0.001$ per site is assumed. See Appendix A for details about the simulation. The polymorphism levels within the two populations (π_{w1} and π_{w2}) are in red and blue, and divergence between the two populations (π_b) is in black. π_{w1}, π_{w2} and π_b can be considered as the averages of h_{w1}, h_{w2} and h_b in a 20 kb window. The y-axis is adjusted such that $E(\pi_{w1}) = E(\pi_{w2}) = 1$ under neutrality (the solid line) and the broken line exhibits $E(\pi_b)$, (i.e., = the genomic average). (B) The mutation quasi-fixes in subpopulation I, causing a drastic reduction in π_{w1}. (C) Migration shuffles polymorphisms in the two subpopulations, while selection works to maintain the quasi-fixation of the mutation. (D) The divergence gradually increases around the mutation, and (E) a clear peak of divergence arises. It should be noted that the star is fixed in the sample (left panes in B-E), but it does not necessarily mean that it is fixed in subpopulation I because there should be maladaptive immigrant alleles at a low frequency.

phase starts after the initial establishment of the barrier locus, during which the block of low genetic variation gradually shrinks in length over time by recombination and migration, while new mutations accumulate and the divergence between two subpopulations increases particularly near the barrier locus (Figure 2.1C). Then, at the end, a stable sharp peak of divergence arises in the equilibrium phase (Figure 2.1D). The equilibrium shape of the peak of divergence is mainly determined by the balance between selection intensity and the rates of recombination and migration.

The scope of this work is to provide a unified and comprehensive theoretical understanding of the evolution of a new peak of divergence, from its birth to stable preservation in equilibrium. I use a simple two-population model, where migration is allowed between subpopulations I and II. Suppose a de novo mutation arises that confers a selective advantage specific to subpopulation I, which is the initial state of my system. Under this model, I derive the following:
for the establishment phase,

(i) The establishment probability of the de novo mutation, that is, the probability that the mutation quasi-fixes in subpopulation I.

(ii) The expected reduction of genetic variation within subpopulations I and II after the quasi-fixation (i.e., partial local sweep).

for the consolidation phase,

(iii) the evolutionary dynamics at both the barrier locus and the linked neutral sites since the quasi-fixation.

and for the equilibrium phase,

(iv) The expected shape of the peak of divergence at equilibrium.

There have been several theoretical works that focused on a specific part of these aspects. For (i) the establishment probability, perhaps the most flexible, useful theoretical framework

was introduced by Barton (1987) in a general multiple-island-model. By using a diffusion approximation, Barton (1987) derived a partial differential equation for the establishment probability. Essentially the same result was obtained by Pollak (1966), who used a branching process and the establishment probability was derived from a probability generating function. Barton's differential equation was solved and closed forms of the establishment probability have been available only in several specific situations in *continuous* habitat models. In a one-dimensional continuous habitat model, Barton (1987) solved his partial differential equation analytically assuming two forms of fitness gradient (linear and pocket). Kirkpatrick and Peischl (2013) used a branching process, from which they obtained a partial differential equation that is similar to that of Barton (1987). Then, the authors successfully incorporated changes in fitness gradient along time, and derived an approximate establishment probability.

In *discrete* population models, Barton's general formula (and also Pollak's one) is difficult to handle, and it has not been fully explored even in a simple two-population model with symmetric migration. Therefore, the currently available theoretical results are not based on Barton's differential equation, and have some limitations. In a continent-island model with *unidirectional* migration, Aeschbacher and Bürger (2014) solved the establishment probability of a locally beneficial mutation linked to another locally beneficial mutation that was already established, where mathematical treatment is facilitated by unidirectional migration (see also Yeaman *et al.* 2016). Yeaman and Otto (2011) obtained an approximate establishment probability by using a heuristic approach that is a combination of the leading eigenvalue of the transition matrix of deterministic process and Kimura's formula of fixation probability (Kimura 1962). As shown in their paper, this formula well describes the establishment probability when a de novo mutation arises in the adapted subpopulation (i.e., subpopulation I in my model), but it does not work when it arises in the maladapted subpopulation (i.e., subpopulation II in my model). Recently, Tomasini and Peischl (2018) provided an approximate establishment probability by assuming a slightly supercritical branching process. Their formula works well under the assumption of slightly supercritical approximation, namely, the leading eigenvalue of the transition matrix of deterministic model is not large, but it may not work well when the selection intensity in the adapted subpopulation is very large.

In this work, I derive a closed form formula of the establishment probability in a two-population model with bidirectonal migration along the formulation of Barton (1987). I extend Barton's derivation with simultaneous quadratic equations and solve them allowing unequal subpopulation sizes. My formula is more general than previous ones (Yeaman and Otto 2011, Tomasini and Peischl 2018); it works with strong selection and it allows that a de novo mutation can arise either subpopulation I or II.

To my best knowledge, there is no theoretical work on the hitch-hiking process of a partial local sweep in a two-population model. With regard to a single population model, many studies theoretically investigated the reduction of polymorphism due to a selective sweep. These studies considered a selected site and a linked neutral site, and assumed that a sufficiently advantageous mutation arises and goes to fixation in the population. Along this fixation, they derived how much polymorphism can be reduced at the linked site. Maynard Smith and Haigh (1974) first obtained the reduction of polymorphism, where the stochastic effect of genetic drift at the linked site was ignored. The model was extended to include the stochastic effect by using a coalescent approach (Kaplan *et al.* 1989) and by using a diffusion method

(Stephan *et al.* 1992) (see also Barton 1998, Etheridge *et al.* 2006). Durrett and Schweinsberg (2004) used a different approach for a faster approximate simulation of a selective sweep and derived some analytical expressions (see also Schweinsberg and Durrett 2005).

There are several theoretical studies on a sweep in multi-population models available, but these considered a fixation across multiple subpopulations, not a local fixation. In a model with multiple subpopulations, Slatkin and Wiehe (1998) and Santiago and Caballero (2005) considered the process where a beneficial mutation fixes in the entire population through weak migration. Kim and Maruki (2011) allowed stronger migration and derived an analytical expression in a two-population model. My interest is different from these studies in that I consider a locally beneficial mutation that can quasi-fix only in the subpopulation in which it is beneficial (not in the entire population). I here extend the theory of Stephan's diffusion model (Stephan *et al.* 1992) to a two-population model, and consider how much polymorphism can be reduced locally at a linked site after a partial local sweep.

I then turn to the evolutionary dynamics at both the barrier locus and the linked neutral sites after the completion of the partial local sweep. I here consider this process after a local sweep as described in Figure 2.1. A local sweep creates a "block" of a fairly long region with almost no genetic variation within the subpopulation in which the new mutation is adaptive (i.e., subpopulation I in my model). In this work, given an arbitrary configuration of genetic variation after a local sweep, I analytically obtain the moments of allele frequency at a linked site, with which I describe how a genomic island decays. Yeaman *et al.* (2016) investigated a similar problem in a different situation, where an genomic island evolves due to the clustering of two barrier loci. In their model, considering a secondary contact, erosion starts when there already are a large number of fixed sites that spread over the genome, and islands appear because selection works to maintain divergence at selected site(s), while losing divergence in other regions through homogenization by migration. By using the structured coalescent, they obtained the expected spacial distribution of F_{ST} (in terms of relative coalescent time) around selected sites as a function of the time since the secondary contact. They also considered the scenario where a de novo mutation broadens a genomic island which has been created by a barrier locus and revealed the final shape of a two-barrier island is the same as the genomic island under the secondary-contact scenario. However, their derivation did not consider the effect of selective sweep of the de novo mutation. It should be noted that, because my derivation accepts any arbitrary initial allele frequency at a linked site, it can be applied to any situation, not only that after a secondary contact but also that after a local sweep.

In the equilibrium phase, the balance between selection, migration, recombination and mutation holds. Theoretical treatment at equilibrium is relatively straightforward, and there are several theoretical studies on the spacial distribution of F_{ST} (Charlesworth *et al.* 1997, Akerman and Bürger 2014, Yeaman *et al.* 2016). Under my framework for the consolidation phase, essentially the same result can be provided as a special case with time going to infinity.

2.2 Model and Results

I consider a two-population model with discrete generations and monoecious diploid individuals that mate at random. The diploid population sizes of subpopulations I and II are assumed to be constant at N_1 and N_2, respectively. As illustrated in Figure 2.1, I am specifically interested in selection for local adaptation in subpopulation I. I consider a genomic

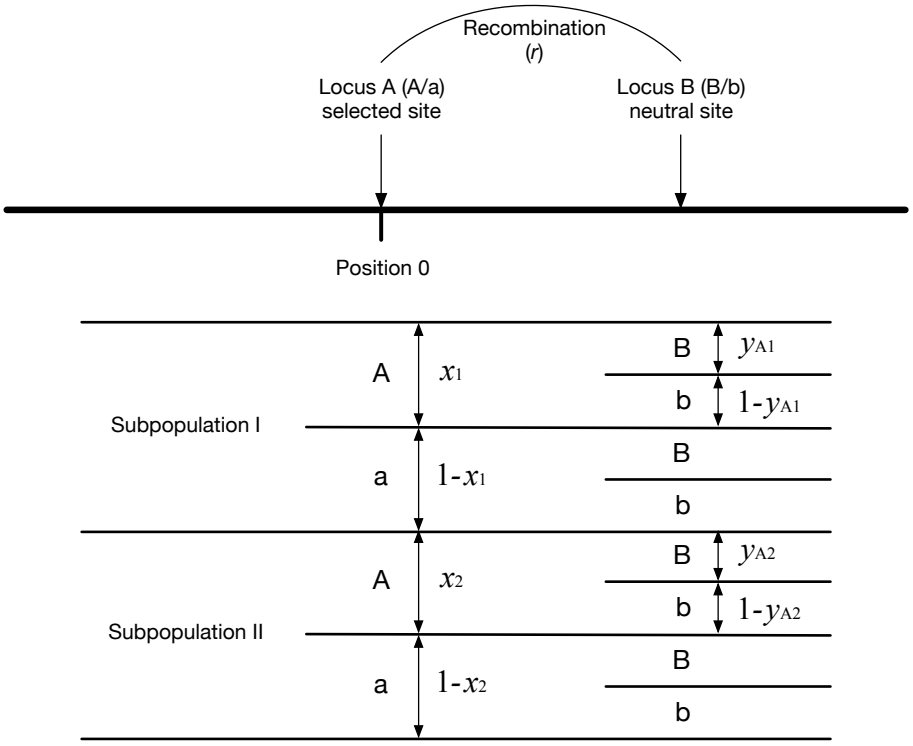

Figure 2.2: Two-locus model used in this work. Locus A targeted by divergent selection is placed at position 0, and a linked neutral locus B can be placed at an arbitrary position. The frequencies of allele A and allele a at locus A and those of allele B and allele b at locus B in the two subpopulations are illustrated.

region encompassing a selected site at position 0, which is referred to as locus A (Figure 2.2). At locus A, two alleles (A/a) are allowed with no recurrent mutation between them. Allele A confers a selection coefficient s_1 in subpopulation I and s_2 in subpopulation II (I assume $s_1 > 0$ and $s_2 < 0$). Additive selection is assumed so that the fitness of individuals with AA, Aa and aa are given by $1 + 2s_1$, $1 + s_1$ and 1 in subpopulation I, and $1 + 2s_2$, $1 + s_2$ and 1 in subpopulation II. Selection works only at this selected site, and all remaining sites are assumed to be neutral. For the following derivation under a two-locus model, I consider a secondary neutral site (locus B), at which two alleles (B/b) are allowed with recurrent mutation between them (Figure 2.2). The mutation rate from allele B to allele b is u and that from allele b to allele B is v. The recombination rate between the two loci, A and B, is r.

The system starts when a de novo mutation (allele A) arises in a single individual either in population I or II, where allele a is fixed in both subpopulations. Therefore, the initial state is $(x_1, x_2) = (1/2N_1, 0)$ or $(0, 1/2N_2)$, where x_1 and x_2 are frequencies of the new allele A in subpopulations I and II, respectively. Throughout this article, I assume strong selection and weak migration so that maladapted individuals are rare in each subpopulation once the initial establishment is achieved.

2.2.1 Establishment probability

I derive the establishment probability of a new de novo allele using the general framework of Barton (1987), who derived a simultaneous quadratic equation from the diffusion theory. This section focuses only on the selected locus A (see Figure 2.2), at which I am interested in the probability that allele A quasi-fixes in subpopulation I. Following Haldane (1927), I

approximate the establishment probability by the probability that the new mutation increases in frequency and escapes from immediate extinction. This is because, under the assumption of strong selection, the behavior of such a mutation is almost deterministic once it escapes from extinction by genetic drift.

Let $F(x_1, x_2)$ be the establishment probability when the frequencies of allele A are x_1 and x_2 in the two subpopulations. By using an analogous procedure to Barton (1987), I derive $p_1 = F(1/2N_1, 0)$ and $p_2 = F(0, 1/2N_2)$, the establishment probability when the new allele arises in subpopulations I and II, respectively. According to the diffusion theory, F satisfies the Kolmogorov backward equation:

$$0 = \frac{x_1}{4N_1}\frac{\partial^2 F}{\partial x_1^2} + \frac{x_2}{4N_2}\frac{\partial^2 F}{\partial x_2^2} + \{s_1 x_1 + m_1(x_2 - x_1)\}\frac{\partial F}{\partial x_1} + \{s_2 x_2 + m_2(x_1 - x_2)\}\frac{\partial F}{\partial x_2}, \quad (2.1)$$

where $m_1(m_2)$ is the proportion of immigrant individuals just after migration in subpopulation I (II). To keep the subpopulation sizes constant, I assume $N_1 m_1 = N_2 m_2$, and I ignore higher order terms of $o(x_i)$ (i.e., x_1^2, x_2^2). This is reasonable because of the assumption that the establishment probability is mainly determined at low frequencies. Because the extinction probabilities of individual mutations are independent, we can write F as

$$F(x_1, x_2) = 1 - \exp(-2N_1 x_1 \psi_1 - 2N_2 x_2 \psi_2) \quad (2.2)$$

where $\exp(-\psi_i)$ is the extinction probability of a new mutant in subpopulation i, therefore, p_i is determined as $p_i = 1 - \exp(-\psi_i)$. After substitution of Equation 2.2 into Equation 2.1, one can show that solutions to Equation 1 can be obtained by solving the following system of equations:

$$\begin{aligned} \psi_1^2 &= 2(s_1 - m_1)\psi_1 + 2\frac{N_2}{N_1}m_2\psi_2 \\ \psi_2^2 &= 2\frac{N_1}{N_2}m_1\psi_1 + 2(s_2 - m_2)\psi_2, \end{aligned} \quad (2.3)$$

which corresponds to Equation 4b in Barton (1987). Equation 2.3 can be rearranged to

$$\psi_1(\psi_1^3 - 2a\psi_1^2 + (a^2 - bd)\psi_1 + b(ad - bc)) = 0 \quad (2.4)$$

$$\psi_2 = \frac{\psi_1^2 - a\psi_1}{b}, \quad (2.5)$$

where $a = 2(s_1 - m_1)$, $b = 2\frac{N_2}{N_1}m_2 = 2m_1$, $c = 2\frac{N_1}{N_2}m_1 = 2m_2$, and $d = 2(s_2 - m_2)$. Equation 2.4 can be solved by using the solution of a cubic equation. Equations 2.4 and 2.5 have at most one solution which fulfills $p_1 > 0$ and $p_2 > 0$. The condition where Equations 2.4 and 2.5 have such a solution is $a + d > 0$ or $ad - bc < 0$, which corresponds to the situation where the deterministic growth rate of the mutant allele is positive (see Appendix B for details).

Figure 2.3 shows the establishment probability from Equations 2.4 and 2.5 as a function of migration rate. I first consider a symmetric model ($N_1 = N_2 = 1000$), and two selection intensities ($s_1 = 0.02$ and $s_1 = 0.1$) are assumed, while $s_2 = -0.01$ is fixed (Figures 2.3A and B). The establishment probability can be computed when a locally adaptive mutation arises either in subpopulation I or II, represented as $F(1/2N_1, 0)$ and $F(0, 1/2N_2)$, respectively. I

performed a forward simulation to check the performance of my analytical result (Appendix A). For each parameter set, I ran 1,000,000 independent replications of the simulation and counted the number of replications where the new allele A was preserved in 10,000 generations. The establishment probability was then obtained as the proportion of such replications. Therefore, it includes replications where two alleles (A and a) coexisted (case C) and those where allele A is completely fixed in both subpopulations (case F). The proportion of case C in the established replications (Pc) decreases with increasing migration rate (see below).

The result (red in Figure 2.3) is in excellent agreement with the simulation result: $F(1/2N_1, 0)$ is approximately $F_{m=0} = \frac{1-\exp(-2s_1)}{1-\exp(-4N_1 s_1)}$ when the migration rate is very low, consistent with the prediction in a single population model (Kimura 1957). As the migration rate increases, $F(1/2N_1, 0)$ decreases and $F(0, 1/2N_2)$ increases, and they become similar to each other. With a very high migration rate ($m \sim 0.5$), the two subpopulations can be considered as a single random-mating population, and the fixation probability of a single mutation is mainly determined by the average selection coefficient, $\bar{s} = \frac{s_1 N_1 + s_2 N_2}{N_1 + N_2}$, namely, $F_{m=0.5} = \frac{1-\exp(-2\bar{s})}{1-\exp(-4N_T \bar{s})}$ where $N_T = N_1 + N_2$ (Nagylaki 1980). Indeed, in the simulations, allele A was fixed in both populations in almost all established cases ($Pc = 1$). In each panel in Figure 2.3, a gray region is placed such that $Pc > 0.9$ in the left, while $Pc < 0.1$ in the right. It has been demonstrated that, under a deterministic model, the condition where two alleles (A and a) coexist is $s_1 s_2 < 0$ and

$$\left| \frac{m_1(1+s_1)}{s_1} + \frac{m_2(1+s_2)}{s_2} \right| < 1 \tag{2.6}$$

(Nagylaki and Lou 2008). The critical migration rate predicted by this equation is shown by the vertical lines in Figure 2.3, which roughly agrees with the line of $Pc = 0.9$ (see Yeaman and Otto 2011). It is indicated that the pattern dramatically changes in a short range of m_1, and the left side is the scope of this article. Similar results were also obtained in asymmetric models ($N_1 = 3N_2$ in Figure 2.3C and $N_1 = N_2/3$ in Figure 2.3D).

Figure 2.3 quantitatively compares my analytical results with those of previous studies (Tomasini and Peischl 2018, Yeaman and Otto 2011). It is found that $F(1/2N_1, 0)$ from Yeaman and Otto (2011) is almost as good as the present one, but unfortunately $F(0, 1/2N_2)$ was not provided by Yeaman and Otto (2011). It seems that Tomasini and Peischl (2018) overestimates $F(1/2N_1, 0)$ and underestimates $F(0, 1/2N_2)$.

2.2.2 Reduction of genetic variation due to a selective sweep

When a new locally adaptive mutation (a→A) arises and quasi-fixes in subpopulation I, genetic variation in the surrounding region in subpopulation I should be dramatically reduced due to the hitch-hiking effect. In this section, I consider a two-locus model as defined in Figure 2.2. I derive the degree of reduction in heterozygosity at a linked neutral site (locus B) in subpopulation I, D_{LS}, by extending the diffusion approach of Stephan *et al.* (1992), who investigated the effect of hitch-hiking in a single population model with no population structure.

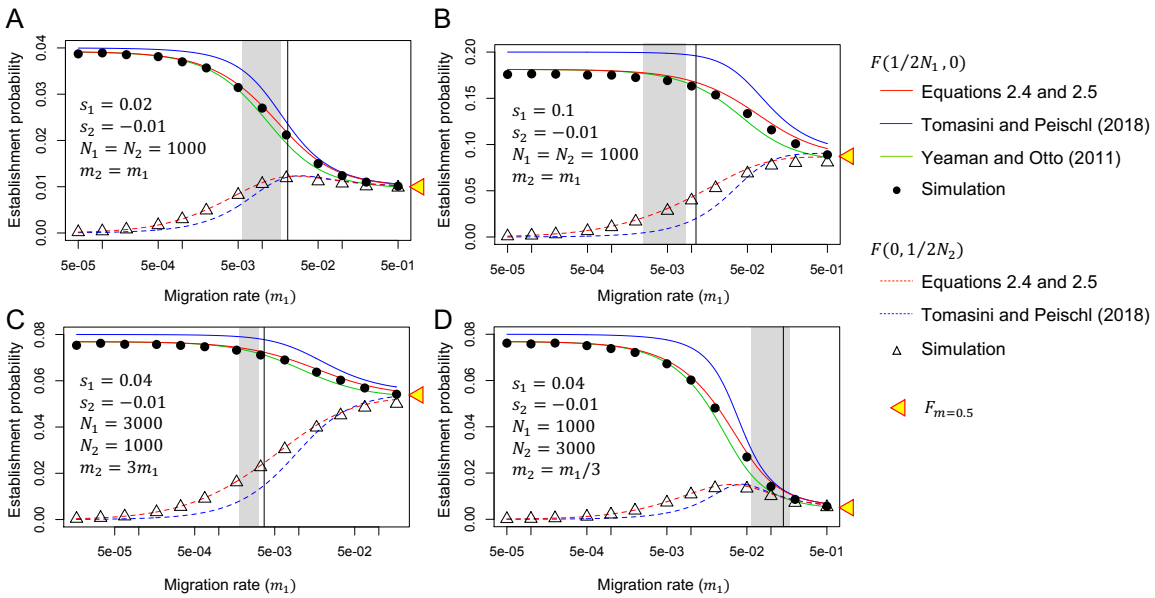

Figure 2.3: Establishment probability as a function of migration rate. (A) Weak selection ($s_1 = 0.02$ and $s_2 = -0.01$) and (B) strong selection ($s_1 = 0.1$ and $s_2 = -0.01$) are assumed in a symmetric model ($N_1 = N_2$). (C, D) Asymmetric population settings are considered ($N_1 = 3N_2$ in C and $N_1 = N_2/3$ in D). my result in red is compared with those of Tomasini and Peischl (2018) and Yeaman and Otto (2011), together with the result of my forward simulation. The establishment probability for a mutation that arises in subpopulation I ($F(1/2N_1, 0)$) is shown by solid lines and closed circles, and that for a mutation that arises in subpopulation II ($F(0, 1/2N_2)$) is shown by broken lines and open triangles. The establishment probability at the high migration limit ($m = 0.5$) is shown by a yellow triangle. In each panel, a gray region is placed such that the proportion of the replications where two alleles (A and a) coexisted (Pc) > 0.9 in the left, while $Pc < 0.1$ in the right. The vertical line presents the critical migration rate above which allele A fixes in the entire population, obtained by Equation 2.6 (see text for detail).

Overview of Stephan *et al.* (1992)

I first introduce the approach of Stephan *et al.* (1992) briefly, which provides the basis of my derivation below. The expected reduction of heterozygosity at locus B for a single population model with diploid size N is denoted by D_0. With the assumption of strong selection, Stephan *et al.* (1992) assumed that the behavior of the frequency (x) of the beneficial allele A with selection coefficient, s, follow a deterministic function:

$$\frac{dx}{dt} = sx(1-x), \tag{2.7}$$

where selection is additive. This deterministic treatment works once the frequency of allele A exceeds a certain threshold such that it escapes from immediate extinction by genetic drift, as mentioned in the previous section. This treatment makes the following derivation much easier because the dynamics can be described by a two-dimensional diffusion equation. It should be noted that x with no subscript denotes the frequency of allele A in the single population model, whereas in my two-population model, the frequencies of allele A in subpopulations I and II are denoted by x_1 and x_2, respectively (see Figure 2.2). I consider another biallelic neutral locus (B/b), and the recombination rate between this neutral locus and the selected locus is assumed to be r. y_A is the frequency of allele B among A-chromosomes and y_a is the frequency of allele B among a-chromosomes. Then, the expected changes of an arbitrary

function $f(y_A, y_a)$ is described as the following ordinary differential equation:

$$\frac{d}{dt}E(f) = E(L(f)), \tag{2.8}$$

where L is a differential operator of the Kolmogorov backward equation:

$$L = \frac{y_A(1-y_A)}{4Nx}\frac{\partial^2}{\partial y_A^2} + r(1-x)(y_a - y_A)\frac{\partial}{\partial y_A} + \frac{y_a(1-y_a)}{4N(1-x)}\frac{\partial^2}{\partial y_a^2} + rx(y_A - y_a)\frac{\partial}{\partial y_a}. \tag{2.9}$$

By using this formula, Stephan *et al.* (1992) solved the first and second moments of y_A and y_a after a sweep, from which the expected reduction of heterozygosity at the linked site can be computed numerically. With some approximation, Stephan *et al.* (1992) further obtained a nice closed form of the solution:

$$D_0 = \frac{2r}{s}(2Ns)^{-2r/s}\Gamma\Big(-\frac{2r}{s}, \frac{1}{2Ns}\Big). \tag{2.10}$$

In this work, I found that this equation somehow undervalues the effect of random genetic drift at the linked neutral locus perhaps due to the approximation of Stephan *et al.* (1992). I noted that, in Equation 2.10, D_0 goes to $\exp(-1/2Ns)$ in the limit of $r \to \infty$, whereas heterozygosity should decrease by genetic drift by a factor of $1/2N$ per generation even in the absence of the hitch-hiking effect. I here consider the expected reduction of heterozygosity along the quasi-fixation as $\exp(-\log(2N)/Ns)$, because the fixation time is approximately given by

$$T = \int_{1/2N}^{1-1/2N} \frac{dx}{sx(1-x)} \approx \frac{2\log(2N)}{s}.$$

This equation means that the expected reduction of heterozygosity due to genetic drift, $\exp(-\log(2N)/Ns)$, is not negligible compared to $\exp(-1/2Ns)$. To correct for this factor, I add this into Equation 2.10:

$$D_0' = \frac{2r}{s}(2Ns)^{-2r/s}\Gamma\Big(-\frac{2r}{s}, \frac{1}{2Ns}\Big)\exp\Big(-\frac{\log(2N)}{Ns}\Big). \tag{2.11}$$

I found that this heuristic approach is in very good agreement with the numerical solution obtained by directly computing Equation 2.9.

Local sweep in the two-population model

In this work, I extend Stephan *et al.*'s derivation (1992) to the two-population model defined above. I first consider the dynamics of the new mutant allele frequency (x_1) at the selected locus (position 0) in the subpopulation I. The major difference from the corresponding formula in Stephan *et al.* (1992) (i.e., Equation 2.7) is that the effect of migration should be considered in the two-population model. Because allele A is very rare in subpopulation II under the assumption of strong selection and low migration, I can ignore migrants with A allele from subpopulations II to I. Then, the dynamics of x_1 can be approximated by a deterministic function:

$$\frac{dx_1}{dt} = s_1 x_1(1-x_1) - m_1 x_1. \tag{2.12}$$

I set the time such that $t = 0$ when the mutation arises and $t = \tau$ when the mutation quasi-fixes.

I next consider the neutral locus B (B/b). As illustrated in Figure 2.2, y_{A1} (y_{A2}) is the frequency of haplotype A-B among A-chromosomes in subpopulation I (II), and y_{a1} (y_{a2}) is the frequency of haplotype a-B among a-chromosomes in subpopulation I (II). I assume that y_{A2} is very small throughout the sweep process. Then, the expected changes of an arbitrary function $f(y_{A1}, y_{a1}, y_{a2})$ is described as the following ordinary differential equation:

$$\frac{d}{dt}E(f) = E(L(f)), \tag{2.13}$$

where L is a differential operator of the Kolmogorov backward equation. Following Ohta and Kimura (1969), I obtain L for my model as

$$\begin{aligned} L =& \frac{y_{A1}(1-y_{A1})}{4N_1 x_1(t)}\frac{\partial^2}{\partial y_{A1}^2} + r(1-x_1(t))(y_{a1}-y_{A1})\frac{\partial}{\partial y_{A1}} \\ &+ \frac{y_{a1}(1-y_{a1})}{4N_1(1-x_1(t))}\frac{\partial^2}{\partial y_{a1}^2} + \{r x_1(t)(y_{A1}-y_{a1}) + \frac{m_1}{(1-x_1(t))(1-m_1)+m_1}(y_{a2}-y_{a1})\}\frac{\partial}{\partial y_{a1}} \\ &+ \frac{y_{a2}(1-y_{a2})}{4N_2}\frac{\partial^2}{\partial y_{a2}^2} + \{x_1(t)m_{e,1\to 2}(y_{A1}-y_{a2}) + (1-x_1(t))m_2(y_{a1}-y_{a2})\}\frac{\partial}{\partial y_{a2}}. \end{aligned} \tag{2.14}$$

This equation is derived such that several terms are added to Equation 2.9 for incorporating random genetic drift within subpopulation II (first term on the third line) and the effect of migration. The second term of $\partial/\partial y_{a1}$ (second line) is for migration from subpopulation II to subpopulation I, and the term of $\partial/\partial y_{a2}$ (third line) is for migration from subpopulation I to subpopulation II. Due to the assumption of strong selection, migrant A-chromosomes from subpopulation I to subpopulation II should be selected out immediately. Therefore, the migration rate of locus B can be *effectively* considered as the product of migration rate and the probability that at least one recombination event occurs before selection purges allele A, $m_{e,1\to 2}$:

$$m_{e,1\to 2} = \frac{(1+s_2)r}{1-(1+s_2)(1-r)}m_2 \tag{2.15}$$

(Bengtsson 1985). Then, Equation 2.13 directly allows us to compute the first and second moments of y_{A1} and y_{a2} after the quasi-fixation of allele A (i.e., $y_{A1}(\tau)$ and $y_{a2}(\tau)$). I obtain heterozygosity within each subpopulations (h_{w1} and h_{w2}) and between them (h_b) at $t = \tau$ as

$$\begin{aligned} h_{w1}(\tau) &= 2E(y_{A1}(\tau)) - 2E(y_{A1}(\tau)^2), \\ h_{w2}(\tau) &= 2E(y_{a2}(\tau)) - 2E(y_{a2}(\tau)^2), \\ h_b(\tau) &= E(y_{A1}(\tau)) + E(y_{a2}(\tau)) - 2E(y_{A1}(\tau)y_{a2}(\tau)), \end{aligned} \tag{2.16}$$

from which the expected reduction of heterozygosity is obtained as

$$D_{LS} = h_{w1}(\tau)/h_{w1}(0). \tag{2.17}$$

Generally, D_{LS} involves the initial frequencies, $y_{a1}(0)$ and $y_{a2}(0)$. However, it should be noted that their quantitative effect on D_{LS} is not large unless $y_{a1}(0)$ and $y_{a2}(0)$ are not very

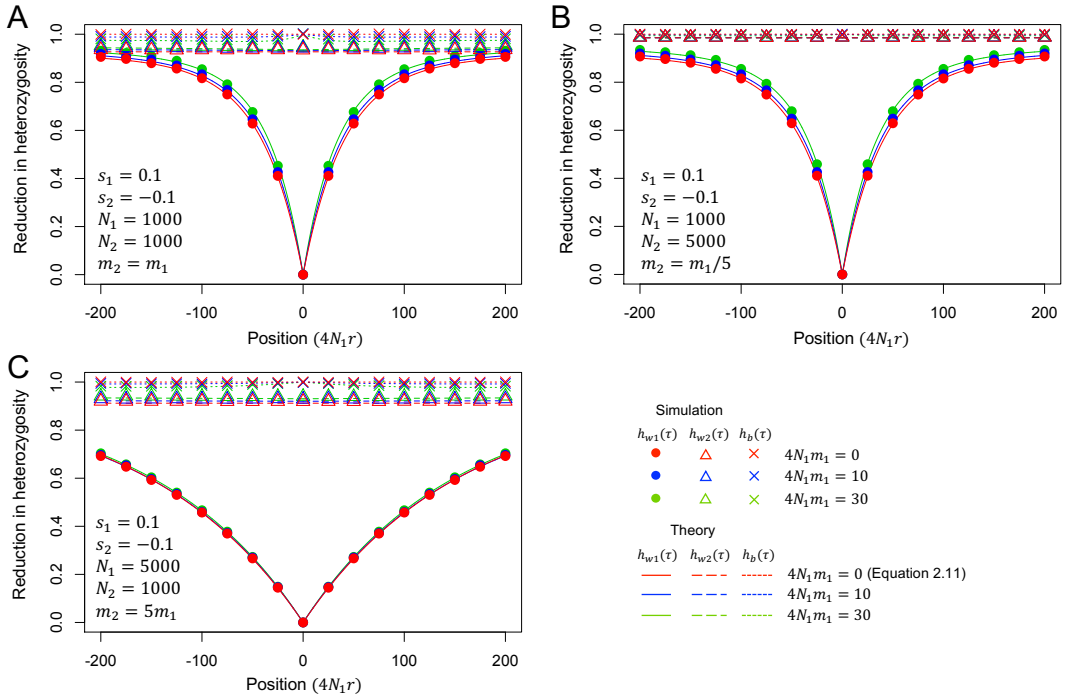

Figure 2.4: The expected reduction of heterozygosity after a local partial sweep in the two-population model. Position is shown in $4N_1r$ from the selected site. Theoretical results for $h_{w1}(\tau)$ $h_{w2}(\tau)$ and $h_b(\tau)$ computed from 2.14-2.17 by assuming $y_{a1}(0) = y_{a2}(0) = 0.3$ for convenience, but very similar results were obtained for other values of $y_{a1}(0)$ and $y_{a2}(0)$. In the case of no migration (red), my results is identical to Stephan *et al.* (1992) (i.e., Equation 2.11)

similar.

Figure 2.4 shows the effect of migration on the reduction in heterozygosity. The plot in red is the case of no migration, where my result is essentially identical to Stephan *et al.* (1992), and the plots in blue and green are for migration cases. I consider three pairs of population sizes, $N_1 = N_2 = 1000$ in A, $N_1 = 1000, N_2 = 5000$ in B, and $N_1 = 5000, N_2 = 1000$ in C. For each parameter set, filled circles represent the average over 100,000 replications of forward simulation (See Appendix A). In Figure 2.4, $h_{w1}(\tau)$, $h_{w2}(\tau)$ and $h_b(\tau)$ are plotted such that $h_{w1}(0) = h_{w2}(0) = 1$ before the sweep, so that $h_{w1}(\tau)$ directly corresponds to D_{LS}. In all cases, my theoretical result from Equation 2.14 is in excellent agreement with the simulation results. It is found that the effect of a local partial sweep seems to be only on subpopulation I, and there is almost no effect on the variation in subpopulation II. Moving away from the selected site at position 0, D_{LS} is larger for a higher migration rate. This is because that migration brings standing variation maintained in subpopulation II into subpopulation I, thereby increasing the polymorphism level in subpopulation I. I observed $h_b(\tau)$ is slightly elevated around the selected site at position 0. If I assume $1 - h_w(\tau)/h_{all}(\tau)$ roughly approximates F_{ST} where h_{all} is heterozygosity when the two subpopulations are merged together, it can be said that a local sweep creates a relatively wide block of region with elevated F_{ST}, which can be considered as an initial peak of divergence.

2.2.3 Consolidation of a barrier locus with a peak of divergence

When a new locally adaptive mutation (a→A) quasi-fixes in subpopulation I, a block of region with elevated F_{ST} arises, where genetic variation in subpopulation I is dramatically reduced (Figure 2.1B). In this section, by using the two-locus model defined in Figure 2.2, I consider the process after this state, but my derivation is flexible enough to plug in any initial state.

I use a similar diffusion approach to the previous section but I focus on the behavior of y_{A1} and y_{a2}. The expected changes of an arbitrary function $f(y_{A1}, y_{a2})$ is described as the following ordinary differential equation:

$$\frac{d}{dt}E(f) = E(L(f)), \tag{2.18}$$

where L is a differential operator of the Kolmogorov backward equation, which is given by

$$\begin{aligned} L =& \frac{y_{A1}(1-y_{A1})}{4N_1}\frac{\partial^2}{\partial y_{A1}^2} + \frac{y_{a2}(1-y_{a2})}{4N_2}\frac{\partial^2}{\partial y_{a2}^2} \\ &+ [v-(u+v)y_{A1} + m_{e,2\to1}(y_{a2}-y_{A1})]\frac{\partial}{\partial y_{A1}} + [v-(u+v)y_{a2} + m_{e,1\to2}(y_{A1}-y_{a2})]\frac{\partial}{\partial y_{a2}}. \end{aligned} \tag{2.19}$$

The two terms in the first line of Equation 2.19 are for random genetic drift within subpopulation I and II, and the terms in the second line describes the deterministic change of the frequency of allele B due to mutation and migration. As well as the previous section, I use the effective migration rate (Bengtsson 1985):

$$m_{e,2\to1} = \frac{(1+\tilde{s}_1)r}{1-(1+\tilde{s}_1)(1-r)}m_1, \tag{2.20}$$

where $\tilde{s}_1 = 1/(1+s_1) - 1$ is the relative selection coefficient of maladapted individuals in subpopulation I. $m_{e,1\to2}$ is defined by Equation 2.15. I consider the dynamics of the first and second order moments, and put $\boldsymbol{y} = (E(y_{A1}), E(y_{a2}), E(y_{A1}^2), E(y_{A1}y_{a2}), E(y_{a2}^2))^T$. By using Equation 2.18, I derive a differential equation for $\boldsymbol{y}$ as follows:

$$\frac{d\boldsymbol{y}}{dt} = \boldsymbol{Q}\boldsymbol{y} + \boldsymbol{e}, \tag{2.21}$$

where $\boldsymbol{Q}$ is the 5×5 matrix given by

$$\boldsymbol{Q} = \begin{pmatrix} -(u+v+m_{e,2\to1}) & m_{e,2\to1} & 0 & 0 & 0 \\ m_{e,1\to2} & -(u+v+m_{e,1\to2}) & 0 & 0 & 0 \\ 2v+\frac{1}{2N_1} & 0 & -2(u+v+m_{e,2\to1}+\frac{1}{4N_1}) & 2m_{e,2\to1} & 0 \\ v & v & m_{e,1\to2} & -(2u+2v+m_{e,2\to1}+m_{e,1\to2}) & m_{e,2\to1} \\ 0 & 2v+\frac{1}{2N_2} & 0 & 2m_{e,1\to2} & -2(u+v+m_{e,1\to2}+\frac{1}{4N_2}) \end{pmatrix} \tag{2.22}$$

and $\boldsymbol{e} = (v, v, 0, 0, 0)^T$. See Appendix C for details. By solving Equation 2.21, $\boldsymbol{y}$ is given by

$$\boldsymbol{y}(t) = \exp(t\boldsymbol{Q})\boldsymbol{y}(0) + \boldsymbol{Q}^{-1}(\exp(t\boldsymbol{Q}) - \boldsymbol{I})\boldsymbol{e} \tag{2.23}$$

where $\boldsymbol{I}$ is the identity matrix of size 5 (Appendix C). $\boldsymbol{y}$ at equilibrium is given by $\tilde{\boldsymbol{y}} = -\boldsymbol{Q}^{-1}\boldsymbol{e}$. My solution at equilibrium is well consistent with previous studies (Charlesworth *et al.* 1997, Yeaman *et al.* 2016) that used the coalescent approach (see Appendix D for a proof).

Figure 2.5 compares my theoretical results from Equation 2.23 (broken lines) with simu-

lation results (closed circles). $N_1 = N_2 = 1000, s_1 = -s_2 = 0.05, u = v = 2.5 \times 10^{-6}, m_1 = m_2 = 1.25 \times 10^{-3}$ are assumed to represent a strong selection case. As the initial condition ($t = 0$), I set $h_{w1} = 0$, $h_{w2} = 0.18$ and $h_b = 0.1$, representing a situation after a local sweep in subpopulation I. Equation 2.23 describes how a sharp peak of divergence grows along time. As time goes, h_{w1} and h_{w2} become closer to each other, and eventually reaches their equilibrium values ($t \gg 10,000$). h_b also decreases except for a short region surrounding the selected site. The rate of erosion (decrease of h_b) increases moving away from the selected site. At the selected site, h_b gradually increases and eventually develops a sharp peak, and simultaneously h_{w1} and h_{w2} also exhibit a small peak that can be created by migration between two subpopulations. It reaches an equilibrium after a significant amount of time, where the selection-migration balance holds so that the shape of the peak does not change much.

Figure 2.5 shows that Equation 2.23 (broken lines) is consistent with the simulation results, but the agreement could be further improved if we account for the presence of locally maladapted allele, i.e. allele A (a) in subpopulation I (II). At migration-selection equilibrium, alleles A and a are present in subpopulation I and II at an expected frequency of $1 - x_1 \approx -m_1/\tilde{s}_1$ and $x_2 \approx -m_2/s_2$, respectively. Even though these frequencies are small under my assumption of weak migration relative to selection, I show in the following that the approximation in Equation 2.23 can be improved by accounting for them. Let us focus on the fate of a single neutral allele at the neutral locus linked to an immigrant locally maladaptive allele. I ask how long such a neutral immigrant allele survives on the locally maladaptive background. The linked neutral allele will either be eliminated by selection against the locally maladapted allele in its background, or it recombines off its deleterious background onto a locally beneficial background. The expected time until elimination by selection or recombination in subpopulations I and II are, respectively, given by

$$\begin{aligned} t_{2\to1} &= \sum_{i=0}^{\infty} \{(1+\tilde{s}_1)(1-r)\}^i = \frac{1}{1-(1+\tilde{s}_1)(1-r)}, \\ t_{1\to2} &= \sum_{i=0}^{\infty} \{(1+s_2)(1-r)\}^i = \frac{1}{1-(1+s_2)(1-r)}. \end{aligned} \tag{2.24}$$

Therefore, the expected numbers of neutral alleles from the other subpopulation with the maladapted allele is $N_1 m_1 t_{2\to1}$ and $N_2 m_2 t_{1\to2}$ in subpopulations I and II, respectively.

Let the frequencies of B in subpopulations I and II including those on the locally maladapted background $\tilde{y}_1$ and $\tilde{y}_2$. Accounting for the presence of locally maladaptive alleles, the first and second-order moments of $\tilde{y}_i$ are,

$$\begin{aligned} E(\tilde{y}_1) =& (1-m_1t_{2\to1})E(y_{A1}) + m_1t_{2\to1}E(y_{a2}) \\ E(\tilde{y}_2) =& m_2t_{1\to2}E(y_{A1}) + (1-m_2t_{1\to2})E(y_{a2}) \\ E(\tilde{y}_1^2) =& (1-m_1t_{2\to1})^2E(y_{A1}^2) + m_1^2t_{2\to1}^2E(y_{a2}^2) + 2m_1t_{2\to1}(1-m_1t_{2\to1})E(y_{A1}y_{a2}) \\ E(\tilde{y}_1\tilde{y}_2) =& (1-m_1t_{2\to1})m_2t_{1\to2}E(y_{A1}^2) + m_1t_{2\to1}(1-m_2t_{1\to2})E(y_{a2}^2) \\ &+ \Big\{(1-m_1t_{2\to1})(1-m_2t_{1\to2}) + m_1t_{2\to1}m_2t_{1\to2}\Big\}E(y_{A1}y_{a2}) \\ E(\tilde{y}_2^2) =& m_2^2t_{1\to2}^2E(y_{A1}^2) + (1-m_2t_{1\to2})^2E(y_{a2}^2) + 2m_2t_{1\to2}(1-m_2t_{1\to2})E(y_{A1}y_{a2}). \end{aligned} \tag{2.25}$$

See Appendix C for details. Figure 2.5 shows that Equation 2.25 fits to the simulation

results better than Equation 2.23. A notable improvement is seen in h_{w1} for a narrow region around the selected site. Because Equation 2.23 ignores the presence of maladaptive alleles (assuming their immediate death), Equation 2.23 predicts a small dip, but rather my simulation demonstrated that a small peak arises. This small peak of h_{w1} is well described by the improved Equation 2.25.

2.3 Discussion

In the early stages of ecological speciation with gene flow, divergent selection is required to maintain phenotypes that are adaptive to each niche (Wu 2001, Turner *et al.* 2005, Nosil 2012). Each target locus of divergent selection works as a barrier locus to migration, because maladaptive migrants should be selected out in a short time. Such a barrier locus can be formed if a locally adaptive mutation arises and established in subpopulations where it is adaptive. This quasi-fixation of a locally adaptive mutation causes a local partial sweep, thereby creating a block of region with elevated F_{ST}. Then, during when divergent selection maintains the mutation, recombination shuffles genetic variation in the linked regions while mutations accumulate around the barrier locus. Through this process, a sharp peak of divergence develops in a narrow region around the barrier locus.

This article theoretically considers the evolutionary behavior of a barrier locus, from its initial establishment to stable preservation. The process was divided into three phases, the establishment, consolidation and equilibrium phases (Figure 2.1). I obtained (i) the establishment probability of a locally adaptive mutation, (ii) the expected reduction of genetic variation within subpopulations I and II after a partial local sweep, (iii) the evolutionary dynamics at both the barrier locus and the linked neutral sites since the sweep, and (iv) the expected shape of the peak of divergence around the barrier locus at equilibrium.

For (i), I have derived a closed-form formula of the establishment probability along the formulation of Barton (1987). My simulations showed that my theoretical results for $F(1/2N_1, 0)$ and $F(0, 1/2N_2)$ outperform the previous approximations, although Yeaman and Otto (2011)'s heuristic approach is almost as good as the presented one. Because I focused on divergent selection so that allele A is quasi-fixed in subpopulation I whereas allele a is quasi-fixed in subpopulation II, I assumed $s_1 > 0$ and $s_2 < 0$. However, as shown in Figure 2.3, it is possible that either allele A or a could fix in the entire population even if $s_1 > 0$ and $s_2 < 0$ hold, although it might take an extremely long time. In contrast, Gavrilets and Gibson (2002) and Whitlock and Gomulkiewicz (2005) obtained the probability of such eventual fixation in the entire population. These studies and my result can be understood in a single framework as follows. Assuming $s_1 > 0$ and $s_2 < 0$, the establishment of allele A first occurs and is maintained quite stably for a long time, but with time going towards infinity, allele A could fix in the entire population most likely when the average selection coefficient $\bar{s}$ is positive, while allele a could likely fix when $\bar{s}$ is negative. This is why my formula of the establishment probability (Equation 2.2) is the same as the numerator of the fixation probability when $\bar{s}$ is positive (Equations 7 and 8 in Gavrilets and Gibson 2002 and Equation 6 in Whitlock and Gomulkiewicz 2005). On the other hand, the establishment probability significantly differs from the fixation probability of Gavrilets and Gibson (2002) and Whitlock and Gomulkiewicz (2005) when $\bar{s}$ is negative because such a mutation hardly goes to eventual fixation, although it can be maintained as a quasi-fixed state for a sufficiently long time.

For (ii), I extended the diffusion method of Stephan *et al.* (1992) to the two-population model. Because the beneficial allele A quasi-fixes only in one subpopulation, the process is very similar to that of a single population model (Stephan *et al.* 1992), except that migration between two subpopulations has some effect. My theoretical result (see Figure 2.4) demonstrated a relatively minor effect of migration; with an increasing migration rate, the level of polymorphism in subpopulation I increases because migration brings genetic variation from subpopulation II.

For (iii) and (iv), I considered the evolutionary dynamics at both the barrier locus and the linked neutral sites since the quasi-fixation, followed by the development of a stable peak of divergence around the barrier locus. This process to equilibrium can be described by a single formula 2.25. Furthermore, Equation 2.25 is flexible enough to plug in any initial state, such as a secondary contact of already diverged subpopulation. To demonstrate this, in Figure 2.6, I compare the pattern after a local sweep (left panels) and that after a secondary contact (right panels) (see also Appendix E for details). After a secondary contact, h_b is already high across the genome, and h_b gradually decreases but selection works to keep divergence around the selected site, thereby creating a peak of divergence. After a very long time (i.e., in equilibrium), the shape of the peak becomes identical to that after a sweep, as pointed out by Yeaman *et al.* (2016). I further performed simulations to investigate how robust my derivation is when the selection intensity is reduced (although I assumed strong selection). The results with 10 times lower selection intensity are shown in Figure 2.7. This selection intensity is fairly weak, and close to the lower limit to maintain the quasi-fixation state of the two alleles. Yet, Equation 2.25 is in fairly good agreement with the simulation results, although the performance of Equation 2.23 is not very good. This is because the frequency of maladaptive alleles is not negligible with a reduced selection intensity.

I have thus developed analytical expressions for the evolutionary behavior of a barrier locus, from its emergence to development of a peak of divergence. In the early stages of ecological speciation, it is possible that multiple barrier loci are developed and genomic islands of divergence arise, but it does not necessarily mean that the emergence of genomic islands of divergence always results in speciation. It is possible that genomic islands of divergence could disappear by environmental changes or by chance, and no speciation occurs. To achieve speciation, there would be many other forces necessary, including emergence of additional islands (Feder *et al.* 2012a, Via 2012, Feder *et al.* 2012b, Aeschbacher and Bürger 2014, Yeaman *et al.* 2016), further divergence on a genomic-scale possible due to a reduction in migration rate, and environmental changes. More theoretical works are needed to fully understand the process to ecological speciation.

2.4 Appendices

Appendix A: Forward simulation

I here describe the setting and assumptions of my forward simulations. A model with two subpopulations (I and II) is used. Subpopulations I and II consist of $2N_1$ and $2N_2$ haploids. I am interested in how DNA sequence evolves at the population level around a selected locus. I considered a genomic region encompassing a selected locus at the center, and assumed the infinite-site model for simulating patterns of nucleotide polymorphisms (e.g., Figure 1). For

other simulations, I consider a two-locus model with the selected locus and a linked neutral locus. The recombination rate between the two loci is r. The fitness of an individual is determined by the allelic state at the selected locus: The fitness of an individual with allele A and a are, respectively, $1+s_1$ and 1 in subpopulation I, and $1+s_2$ and 1 in subpopulation I. Every generation, migration is allowed such that $2Nm$ individuals are swapped between the two subpopulations, Then, to construct a new population in the next generation, $2N_1$ and $2N_2$ individuals are randomly chosen from the current subpopulations I and II, respectively, where their fitness is taken into account. No recurrent mutation is allowed at this site in order to trace the fate of the mutation (unless otherwise mentioned). In contrast, at the linked neutral locus, recurrent mutation is allowed at rate μ per generation. Heterozygosities within and between (h_w and h_b) subpopulations can be scored at any arbitrary time point.

Appendix B: The solution of Equations 2.4 and 2.5

First, I present a proof that there is at most one solution which fulfills $p_1 > 0$ and $p_2 > 0$, and the condition on which such a solution exists is $a + d > 0$ or $ad - bc < 0$. Then, I give a closed expression of the solution.

For ψ_1 and ψ_2 to satisfy $p_1 > 0$ and $p_2 > 0$, $\psi_1 > 0$ and $\psi_2 > 0$ are needed. Notice that $b, c > 0$ because the migration rate and population size are always positive. Although in this work I consider only the case of $d < 0$, Equations 2.4 and 2.5 may also work in the case of $d \geq 0$. Therefore, I here present the proof which allows $d \geq 0$. I set $f(x) = x^3 - 2ax^2 + (a^2 - bd)x + (abd - b^2c)$ and note that the first derivative of $f(x)$ is $f'(x) = 3x^2 - 4ax + (a^2 - bd)$. I discuss for the complementary following three cases.

1. $a \geq 0$

   From Equation 2.5, $\psi_1 > a$, then $x > a$ is needed. Because the x-cordinate of the vertex of $f'(x)$,$\frac{2}{3}a$, is not greater than a, $f'(x)$ monotonically increases when $x > a$. Noting that $f(a) = -b^2c < 0$, there is only one solution to $f(x) = 0$.

2. $a < 0$ and $d \leq 0$

   From Equation 2.5, $\psi_1 > 0$, then $x > 0$ is needed. Because $f'(0) = a^2 - bd > 0$ and the x-coodinate of the vertex of $f'(x)$,$\frac{2}{3}a$, is smaller than 0, $f'(x) > 0$ when $x > 0$. Therefore, whether $f(x) = 0$ has a solution or not in $(0, \infty)$ depends on the sign of $f(0)$. If $f(0) \geq 0$, i.e. $b(ad - bc) \geq 0$, there is no solution. Otherwise, there is only one solution.

3. $a < 0$ and $d > 0$

   From Equation 2.5, $\psi_1 > 0$, then $x > 0$ is needed. Because the x-coodinate of the vertex of $f'(x)$,$\frac{2}{3}a$, is smaller than 0, $f'(x)$ monotonically increases when $x > 0$. Noting that $f(0) = b(ad - bc) < 0$, there is only one solution.

Noting that $b, c > 0$ and $ad - bc$ is negative when $ad \leq 0$, the condition on which one solution exists is rearranged to $a + d > 0$ or $ad - bc < 0$. This is the same as the condition where a deterministic model,

$$\frac{d}{dt}\begin{pmatrix} x_1 \\ x_2 \end{pmatrix} = \frac{1}{2}\begin{pmatrix} a & b \\ c & d \end{pmatrix}\begin{pmatrix} x_1 \\ x_2 \end{pmatrix}, \tag{2.26}$$

has a positive growth rate, in other words, the matrix in Equation 2.26 has at least one positive eigenvalue.

Next, I present a closed form of ψ_1. From the above proof, if there is a nonzero real root of $f(\psi_1) = 0$ which fulfills $p_1 > 0$ and $p_2 > 0$, the root is the largest real root of $f(\psi_1) = 0$. Therefore, by using the solution of cubic equation, ψ_1 can be expressed as

$$\psi_1 = \begin{cases} 0 & \text{when } a+d \leq 0 \text{ and } ad-bc \geq 0 \\ \sqrt[3]{-\frac{Q}{2}+\sqrt{R}} + \sqrt[3]{-\frac{Q}{2}-\sqrt{R}} - \frac{A_2}{3} & \text{when } R > 0 \text{ and } (a+d > 0 \text{ or } ad-bc < 0) \\ 2S\cos(\frac{1}{3}\arccos(\frac{T}{2S})) - \frac{A_2}{3} & \text{when } R \leq 0 \text{ and } (a+d > 0 \text{ or } ad-bc < 0) \end{cases}, \tag{2.27}$$

where $A_0 = abd - b^2c, A_1 = a^2 - bd, A_2 = -2a, P = A_1 - \frac{A_2^2}{3}, Q = A_0 - \frac{A_1 A_2}{3} + \frac{2}{27}A_2^3, R = (\frac{P}{3})^3 + (\frac{Q}{2})^2, S = \sqrt{-\frac{P}{3}}, T = -\frac{Q}{S^2}$. In the above expression, I assume the range of principal value of $y = \arccos(x)$ as $0 \leq y \leq \pi$.

Appendix C: Derivation of Equation 2.21, 2.23 and 2.25

I here describe the derivation of Equation 2.21, 2.23 and 2.25 in more detail. By applying Equation 2.18 to $f = y_{A1}, y_{a2}, y_{A1}^2, y_{A1}y_{a2}$ and y_{a2}^2, we can derive the time derivative of moments of y_{A1} and y_{a2} as follows:

$$\begin{aligned} \frac{dE(y_{A1})}{dt} &= v - (u+v+m_{e,2\to1})E(y_{A1}) + m_{e,2\to1}E(y_{a2}) \\ \frac{dE(y_{a2})}{dt} &= v - (u+v+m_{e,1\to2})E(y_{a2}) + m_{e,1\to2}E(y_{A1}) \\ \frac{dE(y_{A1}^2)}{dt} &= (2v + \frac{1}{2N_1})E(y_{A1}) - 2(u+v+m_{e,2\to1}+\frac{1}{4N_1})E(y_{A1}^2) + 2m_{e,2\to1}E(y_{A1}y_{a2}) \\ \frac{dE(y_{A1}y_{a2})}{dt} &= vE(y_{A1}) + vE(y_{a2}) \\ &\quad + m_{e,1\to2}E(y_{A1}^2) - (2u+2v+m_{e,2\to1}+m_{e,1\to2})E(y_{A1}y_{a2}) + m_{e,2\to1}E(y_{a2}^2) \\ \frac{dE(y_{a2}^2)}{dt} &= (2v + \frac{1}{2N_2})E(y_{a2}) - 2(u+v+m_{e,1\to2}+\frac{1}{4N_2})E(y_{a2}^2) + 2m_{e,1\to2}E(y_{A1}y_{a2}). \end{aligned} \tag{2.28}$$

By setting $\boldsymbol{y} = (E(y_{A1}), E(y_{a2}), E(y_{A1}^2), E(y_{A1}y_{a2}), E(y_{a2}^2))^T$, $\boldsymbol{e} = (v, v, 0, 0, 0)^T$ and defining $\boldsymbol{Q}$ as Equation 2.22, Equation 2.28 can be rearranged in a matrix form (Equation 2.21). Then, by using the solution of a linear differential equation with constant coefficients, the solution of Equation 2.21 is given by

$$\begin{aligned} \boldsymbol{y}(t) &= \exp(t\boldsymbol{Q})\boldsymbol{y}(0) + \int_0^t \exp((t-s)\boldsymbol{Q})\boldsymbol{e}ds \\ &= \exp(t\boldsymbol{Q})\boldsymbol{y}(0) + \boldsymbol{Q}^{-1}(\exp(t\boldsymbol{Q}) - \boldsymbol{I})\boldsymbol{e}. \end{aligned} \tag{2.29}$$

The solution 2.23 is further improved by accounting for neutral immigrant alleles linked to maladaptive alleles. To do so, we derive the expected time of a neutral immigrant allele until its elimination by selection or recombination as Equation 2.24. The expected frequencies of such an allele are $m_1 t_{2\to1}$ and $m_2 t_{1\to2}$ in subpopulations I and II, respectively. $\tilde{y}_1$ and $\tilde{y}_2$, denote the frequencies of B in subpopulations I and II including those on the locally

maladapted background. Then, $\tilde{y}_1$ and $\tilde{y}_2$ can be approximated by

$$\begin{aligned}\tilde{y}_1 &= (1 - m_1 t_{2\to 1}) y_{A1} + m_1 t_{2\to 1} y_{a2}, \\ \tilde{y}_2 &= (1 - m_2 t_{1\to 2}) y_{a2} + m_2 t_{1\to 2} y_{A1}.\end{aligned} \tag{2.30}$$

By using Equation 2.30 and taking expectations, the first and second-order moments of $\tilde{y}_1$ and $\tilde{y}_2$ are given by Equation 2.25.

Appendix D: Comparison between diffusion and coalescent at equilibrium phase

In the main text, I show that replacing the migration rate in the neutral diffusion equation by the effective migration rate well approximates the effect of linkage with the locus under divergent selection. In a neutral model, heterozygosity at equilibrium in a structured population is already well studied by the coalescent theory under the infinite-site model (reviewed in Wakeley 2009). In this work, I alternatively used the forward diffusion approach because the diffusion approach can be applied to more general conditions. In this Appendix, I show my diffusion result at equilibrium is consistent with that of the coalescent theory.

I attempt to derive the expected heterozygosity under the infinite-site setting along my diffusion-based derivation. In practice, I first consider a K-allele model, and then the results will be transformed to the infinite-site model. Let B allele be one of the alleles at the locus. I put y_1 and y_2 as frequency of allele B in subpopulation I and II, respectively. In the following derivation, I assume $N_1 = N_2 = N$ and $m_1 = m_2 = m$. The differential operator of the Kolmogorov backward equation is as follows,

$$\begin{aligned}L =& \frac{y_1(1-y_1)}{4N}\frac{\partial^2}{\partial y_1^2} + \frac{y_2(1-y_2)}{4N}\frac{\partial^2}{\partial y_2^2} \\ &+ [v - (u+v)y_1 + m(y_2 - y_1)]\frac{\partial}{\partial y_1} + [v - (u+v)y_2 + m(y_1 - y_2)]\frac{\partial}{\partial y_2},\end{aligned} \tag{2.31}$$

At the equilibrium, I derive the moments up to the second order as

$$\begin{aligned}E(y_1) = E(y_2) &= \frac{V}{U+V}, \\ E(y_1^2) = E(y_2^2) &= \frac{V(V+1)(U+V+M) + V^2 M}{(U+V)(U+V+M+1)(U+V+M) - M^2(U+V)}, \\ E(y_1 y_2) &= \frac{MV(V+1) + V^2(U+V+M+1)}{(U+V)(U+V+M+1)(U+V+M) - M^2(U+V)},\end{aligned} \tag{2.32}$$

where $U = 4Nu$, $V = 4Nv$ and $M = 4Nm$. In the limit to the infinite-allele model, that is, $v = \frac{u}{K-1}$ and $K \to \infty$, the expected heterozygosity within and between subpopulation goes to

$$\begin{aligned}h_w = 1 - KE(y_1^2) &\to \frac{U^2 + 2UM}{(U+M+1)(U+M) - M^2}, \\ h_b = 1 - KE(y_1 y_2) &\to \frac{U(U+2M+1)}{(U+M+1)(U+M) - M^2}.\end{aligned} \tag{2.33}$$

This result under the infinite-allele setting can be transformed to the infinite-site mode: If

we put $U = \frac{\theta}{n}$ and n goes to ∞, π_w and π_b are described as

$$\begin{aligned} \pi_w &= nh_w \to 2\theta \\ \pi_b &= nh_b \to \theta(2 + \frac{1}{M}), \end{aligned} \tag{2.34}$$

which is identical with the result from the coalescent theory (Charlesworth *et al.* 1997, Yeaman *et al.* 2016).

Appendix E: Comparing the scenarios of local partial sweep and secondary contact

I compute Equation 2.23 for a scenario of secondary contact, and compared with the results of a local partial sweep shown in Figure 2.5. For a secondary-contact scenario, I assume that already diverged two subpopulation have merged so that there are a number of fixed sites between the two subpopulations. To make a realization of this situation, I set $y_1(0) = 0.1$ and $y_2(0) = 0.9$, and the other parameters are identical to those used for Figure 2.5 (i.e., $4N_1s_1 = -4N_2s_2 = 200$ and $4N_1m_1 = 4N_2m_2 = 5$). Figure 2.6 compares the patterns after a local sweep (left panels) and after a secondary contact (right panels). After a secondary contact, h_b is already high across the genome, and h_b gradually decreases but selection works to keep divergence around the selected site, thereby creating a peak of divergence. In equilibrium, the shape of the peak becomes identical to that after a sweep, in agreement with Yeaman *et al.* (2016).

Figure 2.7 shows the results with identical parameter sets to those for Figure 2.5 except for the selection intensity. The purpose is to check how robust my derivation is when the selection intensity is reduced. I here set $4N_1s_1 = -4N_2s_2 = 20$ and $4N_1m_1 = 4N_2m_2 = 5$. The results with 10 times lower selection intensity are shown in Figure 2.6. This selection intensity is fairly weak, and it is close to the lower limit to maintain the quasi-fixation state of the two alleles.

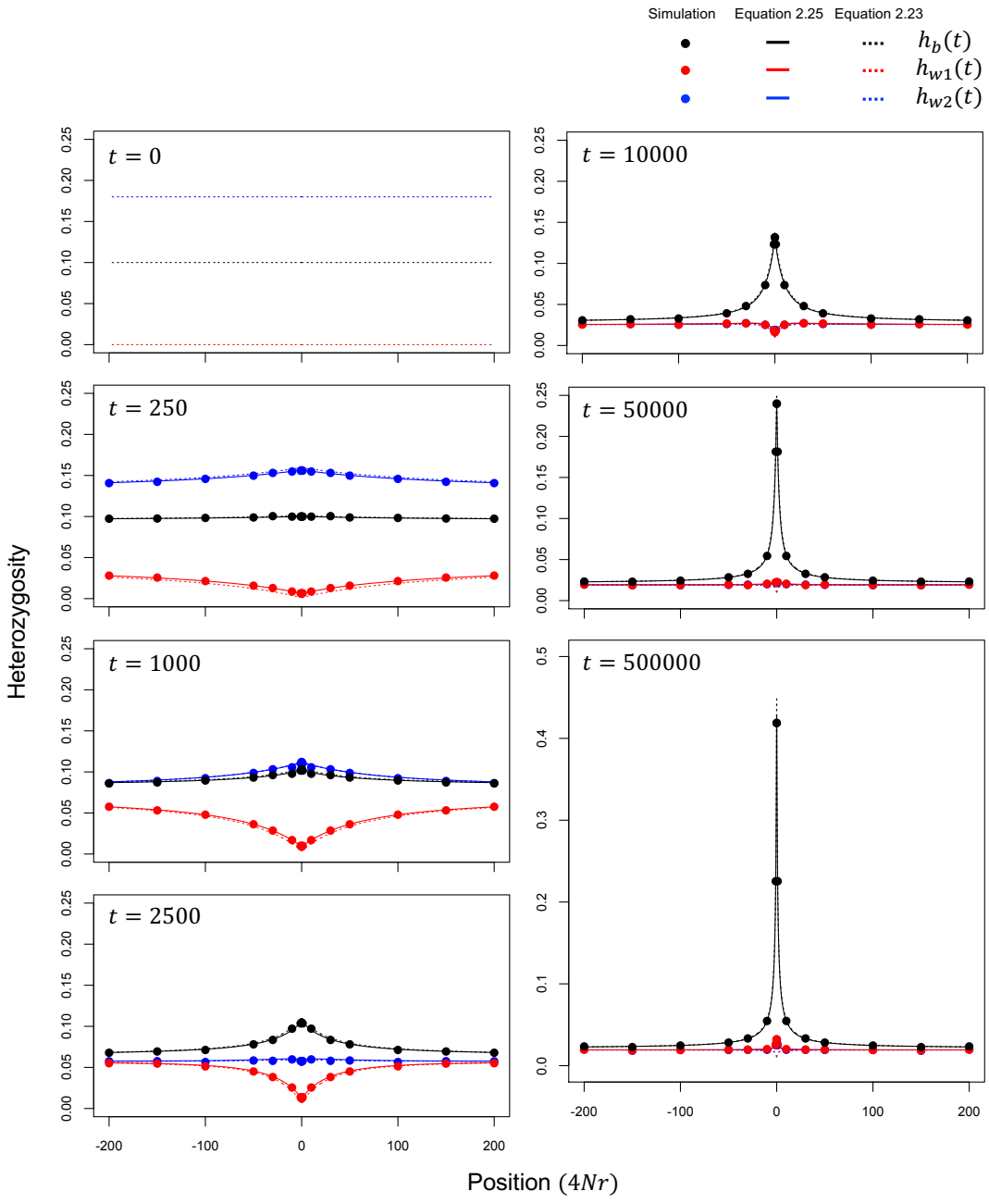

Figure 2.5: Temporal change of heterozygosity (h_{w1}, h_{w2}, h_b) after a local sweep in subpopulation I. The spacial distributions of h_{w1}, h_{w2} and h_b are shown for seven time points (t=0, 250, 1000, 2500, 10000, 50000, and 500000 generations after a sweep). Position in the simulated regions is shown in $4Nr$ from the selected site. $N_1 = N_2 = 1000, s_1 = -s_2 = 0.05, u = v = 2.5 \times 10^{-6}, m_1 = m_2 = 1.25 \times 10^{-3}$, $y_1(0) = 0.0$ and $y_2(0) = 0.1$ are assumed. Theoretical results from Equations 2.23 and 2.25 are shown by broken and solid lines, respectively. Simulation results (closed circles) are the averages over 50,000 replications of forward simulations.

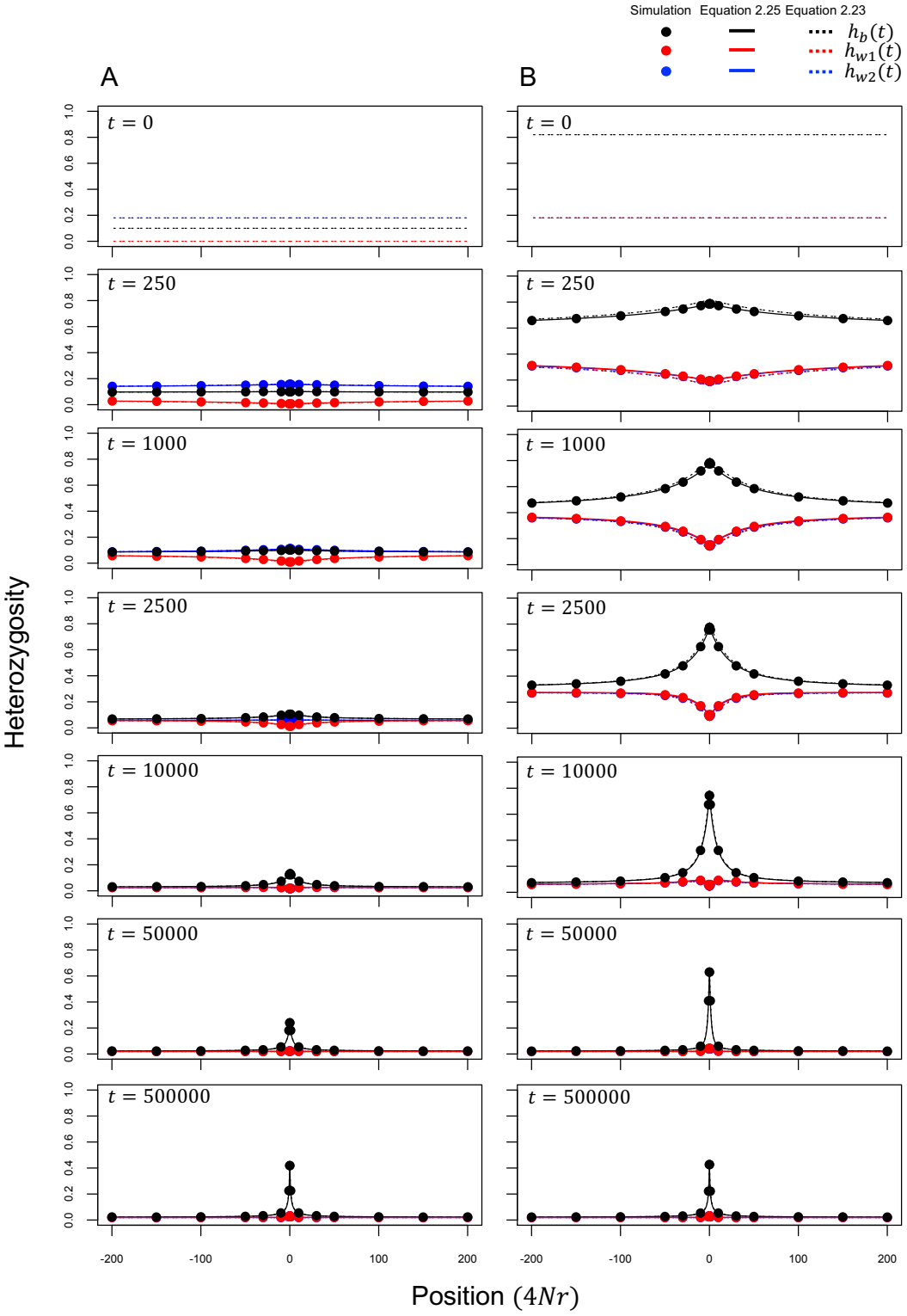

Figure 2.6: Temporal change of heterozygosity (h_{w1}, h_{w2}, h_b) as a function of recombination rate (A) after a local sweep in subpopulation I and (B) after a secondary contact. $y_1(0) = 0.0$ and $y_2(0) = 0.1$ are assumed in (A), whereas $y_1(0) = 0.1$ and $y_2(0) = 0.9$ in (B). Theoretical results from Equations 2.23 and 2.25 are shown by broken and solid lines, respectively. Simulation results (closed circles) are the averages over 50,000 replications of forward simulation. The left panel is identical to Figure 2.5.

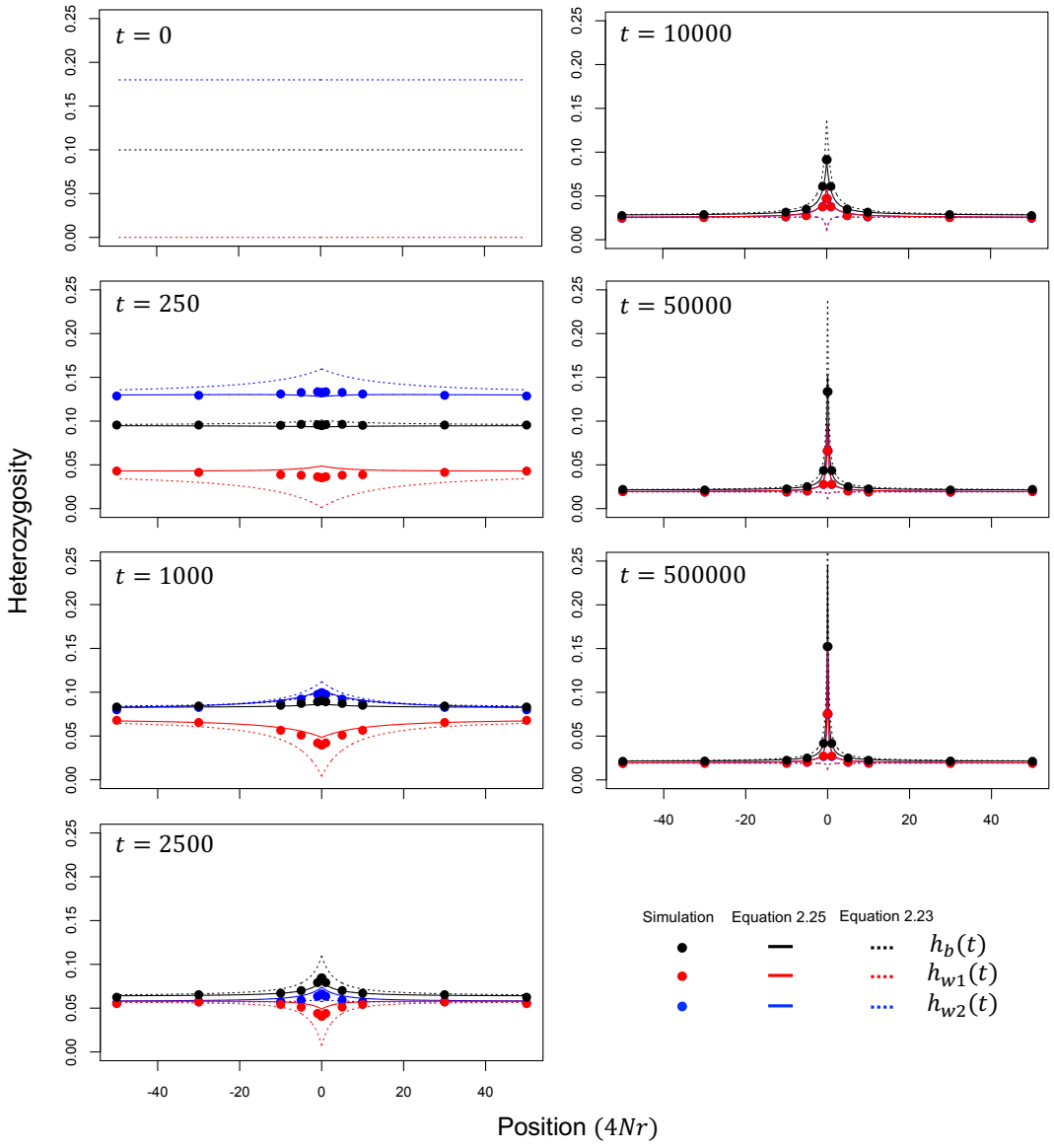

Figure 2.7: Temporal change of heterozygosity (h_{w1}, h_{w2}, h_b) as a function of recombination rate (A) after a local sweep in subpopulation I and (B) after a secondary contact. I here set $4N_1s_1 = -4N_2s_2 = 20$, while all other parameters are the same as those for Figure 2.6. The theoretical results from Equations 2.23 and 2.25 are shown by broken and solid lines, respectively. Simulation results (closed circles) are the averages over 50,000 replications of forward simulations.

Chapter 3

Establishment Process of a Magic Trait Allele subject to Both Divergent Selection and Assortative Mating

3.1 Introduction

Speciation occurs when reproductive isolation establishes between different populations. One of the major forces driving reproductive isolation is sexual selection (Coyne and Orr 2004). Speciation driven by sexual selection could occur when phenotypic difference is involved in mate choice. Several theoretical models indicated that sexual selection alone can lead to speciation even in the face of gene flow (Wu 1985, Turner and Burrows 1995, Higashi *et al.* 1999, Takimoto *et al.* 2000), but these results largely rely on their assumptions such as ample genetic variation, symmetric distribution of female preference or strong female choice (Arnegard and Kondrashov 2004, Gavrilets 2004), and are empirically not well supported yet, as reviewed in Ritchie (2007). At the moment, it is considered that speciation by sexual selection alone is difficult to occur (Gavrilets 2004). This is largely because diversity in female preference is difficult to maintain in the presence of genetic drift, as female preference is not directly subject to selection (i.e., selection works through male phenotype). Ritchie (2007) pointed out that sexual selection should work efficiently together with niche specialization or local adaptation.

Synergy between local adaptation and assortative mating can be a powerful driver of speciation (Gavrilets 2004). Establishment of a locally adaptive mutation could lead to stable genetic divergence between local populations in different environments, even in the face of gene flow between them. If there is another locus that is involved in sexual selection, it also reduces gene flow between populations. This effect is particularly strong when the locus is genetically linked to the target locus of local adaptation, and an extreme case is that a single locus is pleiotropically subject to both divergent selection and sexual selection. Models that handle sexual selection at a locus under divergent selection are called "magic trait" models (Gavrilets 2004, Servedio *et al.* 2011). Previous theoretical studies revealed that the magic trait models are one of the easiest scenarios of speciation with gene flow (see Gavrilets 2004, Kopp *et al.* 2018, for reviews). There are many potential examples of a magic trait in nature (Maan and Seehausen 2011, Servedio *et al.* 2011), suggesting the importance of the establishment process of a magic trait for speciation. In the present article, I specifically focus on a case of a single magic trait locus, which produces a phenotype difference and

undergoes similarity-based mating (i.e., females prefer males with similar phenotypes).

Many theoretical models have considered a magic trait that is subject to both natural selection and similarity-based assortative mating (Dieckmann and Doebeli 1999, Matessi *et al.* 2001, Doebeli and Dieckmann 2003, Kirkpatrick and Nuismer 2004, Bürger and Schneider 2006, Otto *et al.* 2008, Pennings *et al.* 2008, Thibert-Plante and Gavrilets 2013, Rettelbach *et al.* 2013, Servedio and Bürger 2015, Cotto and Servedio 2017) (see Kirkpatrick and Ravigné 2002, Gavrilets 2004, Weissing *et al.* 2011, Servedio and Boughman 2017, Kopp *et al.* 2018, for review). However, these models often consider complicated scenarios, for example, that a magic trait contributes to speciation in interaction with other traits or other selective forces, making it difficult to understand the relative contribution of the magic trait.

So far, theoretical arguments on the evolutionary dynamics of a magic trait have been only based on limited studies in an infinite population (Slatkin 1982, Kisdi and Priklopil 2011, Servedio 2011). Slatkin (1982) considered a haploid infinite-size island population connected to a stable continent population, between which migration is allowed. The model involves a single magic trait locus, at which two alternative alleles are considered: One allele is preferred in the island subpopulation, and the other allele is fixed in the continent subpopulation. In addition, assortative mating is incorporated by assuming that mating pairs of haploid individuals with different alleles produce fewer offspring than pairs with the same alleles. Although this is a form of fecundity selection, it is mathematically identical to assortative mating, where females dislike to mate with males having different alleles. Slatkin (1982) analytically showed that successful invasion of a new allele requires a larger selection coefficient of adaptive selection than the sum of the migration rate and strength of assortative mating, both of which have an effect against the invasion of new alleles. Additionally, the author derived the critical migration rate, above which a polymorphic state is unstable so that new alleles likely become extinct. Recently, Kisdi and Priklopil (2011) explored the evolutionary branching of a magic trait in an infinite population, although this model is not very relevant to my interest because the magic trait is a quantitative trait determined by multiple genes. Servedio (2011) investigated the evolution of the strength of assortment after the stable maintenance of magic trait is established (i.e., secondary contact), which is also not very relevant to this work because my interest is in the establishment process of a magic trait before its stable maintenance. While the analysis assuming an infinite population gives a great deal of insight, it is also very important to consider this process in a finite population with the stochasticity of random genetic drift. However, to the best of my knowledge, there has been no research which explored analytically the establishment process of a magic trait in stochastic two-population models, while some theoretical results are available only in one-population models (Yamamichi and Sasaki 2013, Newberry *et al.* 2016).

The aim of this work is to theoretically describe the behavior of allele frequency along the establishment of a magic trait allele in a finite population. One of the advantage of my theory over deterministic theory under an infinite population is that my theory can be applied to any size of population, while deterministic theory works only for a sufficiently large population. Local adaptation often occurs in a small niche with a limited number of individuals, in which the behavior of a magic trait allele should be quite different from that in a large population. By exploring this process stochastically, I can probabilistically argue the fate of a magic trait allele, whereas deterministic theory simply tells which of the counteracting forces (selection

vs. assortative mating) is dominant. Another advantage is that stochastic theory allows us to theoretically understand how the allele frequency behaves along time.

To take these advantages of stochastic theory, I here consider a two-population model with bidirectional migration and derive the establishment probability of an allele that is pleiotropically subject to both divergent selection and assortative mating. My model can arbitrarily set the sizes of the two populations, so that Slatkin's situation (with the assumption of infinite population size) can be a special case of my model. I consider haploid and diploid models, and obtain theoretical expressions of the establishment probability and the trajectory of allele frequency along the establishment. My derivation of the establishment probability bases on the approximation method developed by Yeaman and Otto (2011). Yeaman and Otto (2011) considered divergent selection alone in a two-population model and derived an approximate formula for the establishment probability of a locally adaptive allele (for theoretical works on this model of selection, see also Pollak 1966, Barton 1987, Tomasini and Peischl 2018, Sakamoto and Innan 2019). The authors developed a heuristic method, which essentially focuses on the process in the subpopulation where a new allele is beneficial, rather than considering the dual process in both subpopulations. This is because the establishment probability is largely determined by how the focal allele increases in frequency when it invades into the subpopulation it is favored in, and the process in the other subpopulation does not play a crucial role. The authors showed that Kimura's formula (Kimura 1962) well approximates the establishment probability when a new allele arises in the subpopulation where it is beneficial if the selection coefficient is replaced by the leading eigenvalue of transition matrix of deterministic dynamics. However, their method considered only frequency-independent selection and cannot be directly apply to frequency-dependent selection such as sexual selection. In addition, they did not provide the establishment probability when a new allele arises in the subpopulation where it is deleterious. In this work, by extending the idea of Yeaman and Otto (2011) to my model with sexual selection, I derive the establishment probability and time in both of the two cases, when a new allele arises in the subpopulation where it is beneficial and deleterious. My result describes the stochastic process on how a magic trait allele behaves in a finite population.

3.2 Model

I use a discrete-generation model with two populations, between which bidirectional migration is allowed, and I consider both haploid and diploid cases. The assumptions and model settings shared by the haploid and diploid models are described here. The sizes of subpopulations I and II are assumed to be N_1 and N_2, respectively. On average, $N_1 m_1 = N_2 m_2$ individuals are exchanged per generation where m_1 and m_2 are backward migration rates of subpopulation I and II, respectively. There are two alleles, A and a, on which selection works. Allele A is favored in subpopulation I, and disfavored in subpopulation II. Assuming no recurrent mutation between the two alleles, I focus on the behavior of allele frequencies to obtain the establishment probability of allele A forward in time. The life cycle is assumed to be in the order of (natural) selection, mating (inducing sexual selection), reproduction (including random genetic drift) and migration in each generation. The major difference between the haploid and diploid models is in how selection and assortative mating work. I assume that the fitness of allele a is 1 in both subpopulations, and the fitness of allele A is given depending

on the model, as will be explained below.

3.2.1 Haploid model

In the haploid model, I simply assume that the fitness of allele A is $1+s_1 > 1$ in subpopulation I, but $0 < 1+s_2 < 1$ in subpopulation II (summarized in Table 3.1). Let p_i be the frequency of allele A in subpopulation i. Then, the expected frequency after selection is

$$p_i' = \frac{(1+s_i)p_i}{1+s_i p_i}. \tag{3.1}$$

For females, the reproductive opportunity (i.e., expected number of offspring) is independent of genotype. Assortative mating occurs such that a female avoids mating with males carrying an allele different from hers with probability α, whereas if she meets a male with the same allele as hers, she accepts him with probability 1 (see also Table 3.1). Since males can be chosen by more than one female (or none at all), this results in sexual selection against males carrying the locally rare allele. Then, the expected frequency of allele A after mating and sexual selection is given by

$$p_i'' = \underbrace{p_i' \frac{p_i'}{1-\alpha(1-p_i')}}_{\text{A (female)}\times\text{A (male)}} + \underbrace{\frac{p_i'}{2}\frac{(1-\alpha)(1-p_i')}{1-\alpha(1-p_i')}}_{\text{A (female)}\times\text{a (male)}} + \underbrace{\frac{1-p_i'}{2}\frac{(1-\alpha)p_i'}{1-\alpha p_i'}}_{\text{a (female)}\times\text{A (male)}}. \tag{3.2}$$

Reproduction and the formation of the next generation occurs by binomial sampling (i.e., offsprings are drawn from a binomial distribution with parameters N_i and p_i'', as in the Wright-Fisher model of random genetic drift. Finally, $N_1 m_1 = N_2 m_2$ individuals are exchanged between subpopulations in the migration step.

Genotype	A	a
Fitness in subpopulation I	$1+s_1$	1
Fitness in subpopulation II	$1+s_2$	1

Female genotype	Male genotype	
	A	a
A	1	$1-\alpha$
a	$1-\alpha$	1

Table 3.1: Relative fitness (left) and relative female preference (right) in the haploid model.

3.2.2 Diploid model

In the diploid model, we need to consider the effect of dominance. I assume allele A has a dominance coefficient, h, which means that if genotype AA and genotype aa have trait values P_{AA} and P_{aa}, respectively, the trait value of genotype Aa is given by $hP_{AA} + (1-h)P_{aa}$. Both selection and assortative mating will be proportional to this phenotype. I denote by p_i, q_i and r_i the frequencies of genotypes AA, Aa and aa, respectively, in subpopulation i.

During selection, I assume the fitness of genotype AA, Aa and aa to be $1+s_1$, $1+hs_1$ and 1, respectively, in subpopulation I, and $1+s_2$, $1+hs_2$ and 1 in subpopulation II ($s_1 > 0$ and $s_2 < 0$) (summarized in Table 3.2). Then, the expected frequencies of AA, Aa after selection

are given by

$$\begin{aligned} p_i' &= \frac{(1+s_i)p_i}{1+s_i(p_i+hq_i)} \\ q_i' &= \frac{(1+hs_i)q_i}{1+s_i(p_i+hq_i)}, \end{aligned} \tag{3.3}$$

and the expected frequency of aa is given by $r_i' = 1 - p_i' - q_i'$.

In the mating step, females avoid mating with males whose phenotype differs from their own. To incorporate the effect of dominance, I assume that mate discrimination is proportional to the trait difference, and that AA females reject aa males with probability α (see Table 3.2). Then, the expected frequencies of genotype AA and aa after mating are

$$\begin{aligned} p_i'' = {} & \underbrace{p_i' \frac{p_i'}{1-(1-h)\alpha q_i' - \alpha r_i'}}_{\text{AA (female)}\times\text{AA (male)}} + \underbrace{\frac{p_i'}{2}\frac{(1-(1-h)\alpha)q_i'}{1-(1-h)\alpha q_i' - \alpha r_i'}}_{\text{AA (female)}\times\text{Aa (male)}} \\ & + \underbrace{\frac{q_i'}{2}\frac{(1-(1-h)\alpha)p_i'}{1-(1-h)\alpha p_i' - h\alpha r_i'}}_{\text{Aa (female)}\times\text{AA (male)}} + \underbrace{\frac{q_i'}{4}\frac{q_i'}{1-(1-h)\alpha p_i' - h\alpha r_i'}}_{\text{Aa (female)}\times\text{Aa (male)}} \\ r_i'' = {} & \underbrace{r_i' \frac{r_i'}{1-\alpha p_i' - h\alpha q_i'}}_{\text{aa (female)}\times\text{aa (male)}} + \underbrace{\frac{r_i'}{2}\frac{(1-h\alpha)q_i'}{1-\alpha p_i' - h\alpha q_i'}}_{\text{aa (female)}\times\text{Aa (male)}} \\ & + \underbrace{\frac{q_i'}{2}\frac{(1-h\alpha)r_i'}{1-(1-h)\alpha p_i' - h\alpha r_i'}}_{\text{Aa (female)}\times\text{aa (male)}} + \underbrace{\frac{q_i'}{4}\frac{q_i'}{1-(1-h)\alpha p_i' - h\alpha r_i'}}_{\text{Aa (female)}\times\text{Aa (male)}}, \end{aligned} \tag{3.4}$$

and the expected frequency of Aa is given by $q_i'' = 1 - p_i'' - r_i''$. Individuals for the next generation are produced by multinomial sampling according to these probabilities. Following reproduction, $N_1 m_1 = N_2 m_2$ individuals are exchanged between subpopulations.

Genotype	AA	Aa	aa
Fitness in subpopulation I	$1+s_1$	$1+hs_1$	1
Fitness in subpopulation II	$1+s_2$	$1+hs_2$	1

Female genotype	Male genotype		
	AA	Aa	aa
AA	1	$1-(1-h)\alpha$	$1-\alpha$
Aa	$1-(1-h)\alpha$	1	$1-h\alpha$
aa	$1-\alpha$	$1-h\alpha$	1

Table 3.2: Relative fitness (left) and relative female preference (right) in the diploid model.

3.3 Results

3.3.1 Establishment probability in the haploid model

The initial state is that all individuals have allele a in both subpopulations. First, I derive the establishment probability of allele A if it arises in subpopulation I with initial frequency $\frac{1}{N_1}$. I assume $m_i \ll |s_i|, \alpha$ to ensure the stable maintenance of divergence (see below). By assuming that $|s_i|, \alpha, m_i \ll 1$ and ignoring second-order terms in these parameters, the

expected changes in allele frequency in one generation are given by

$$\begin{aligned} M_{p_1} &= (s_1 - \frac{\alpha}{2} + \alpha p_1)p_1(1-p_1) + m_1(p_2 - p_1) \\ M_{p_2} &= (s_2 - \frac{\alpha}{2} + \alpha p_2)p_2(1-p_2) + m_2(p_1 - p_2). \end{aligned} \tag{3.5}$$

The first term in each equation represents the total effect of natural and sexual selection and the second term is for migration. I note that, from the first terms of the above equations, the direction of sexual selection is negative when $p < \frac{1}{2}$ and positive when $p > \frac{1}{2}$.

The change of allele frequencies, p_1 and p_2, can be well described by a two-dimensional diffusion equation, which unfortunately is very difficult to solve. Alternatively, I use the heuristic approach developed by Yeaman and Otto (2011), which is based on their demonstration that the establishment probability of an allele that arises in subpopulation where it is beneficial can be approximated by the establishment probability of an allele under directional selection (in a homogeneous environment) if the selection intensity is replaced by the leading eigenvalue of the transition matrix of the deterministic process. This means that the leading eigenvalue is considered to represent the 'effective' strength of natural selection on allele A in subpopulation I.

The deterministic process considering divergent selection and migration (but not assortative mating) is described as

$$\frac{d}{dt}\begin{pmatrix} p_1 \\ p_2 \end{pmatrix} = \begin{pmatrix} s_1 - m_1 & m_1 \\ m_2 & s_2 - m_2 \end{pmatrix}\begin{pmatrix} p_1 \\ p_2 \end{pmatrix}. \tag{3.6}$$

The leading eigenvalue of the transition matrix in Equation 3.6, λ, is given by

$$\lambda = \frac{1}{2}\left[(s_1 + s_2 - m_1 - m_2) + \sqrt{(s_1 - s_2 - m_1 + m_2)^2 + 4m_1m_2}\right]. \tag{3.7}$$

By incorporating λ and the term of assortative mating, the expected change in allele frequency in one generation is approximated in the one-population system by:

$$M_p = (\lambda - \frac{\alpha}{2} + \alpha p)p(1-p). \tag{3.8}$$

Then, the establishment probability of allele A which newly arises in subpopulation I, u_1, is given along Kimura's formula (Kimura 1962) as

$$u_1 = \frac{\int_0^{1/N_1} G(x)dx}{\int_0^1 G(x)dx}, \tag{3.9}$$

where $G(x) = e^{-2N_1(\lambda - \frac{\alpha}{2})x - N_1\alpha x^2}$.

Next, I derive the establishment probability of allele A if it newly arises in subpopulation II with initial frequency $\frac{1}{N_2}$. Because allele A is maladaptive in subpopulation II, we can assume that its frequency in this subpopulation should remain low and can be described by a branching process. Since p_2 is small, the selection coefficient against allele A is $s_2 - \frac{\alpha}{2}$ in

subpopulation II. Then, the establishment probability is approximated by

$$u_2 \approx u_1 \frac{c}{1-b} - \frac{u_1^2}{2} \frac{c^2}{(1-b)^3}, \tag{3.10}$$

where $b = (1 + s_2 - \frac{\alpha}{2})(1 - m_2), c = (1 + s_2 - \frac{\alpha}{2})m_2$. For the details of the derivation, see Appendix A.

The accuracy of my derivation was checked by simulations (Figure 3.1). Forward simulations were carried out under the haploid model to obtain u_1 and u_2, with initial frequency of allele A $(p_1, p_2) = (1/N_1, 0)$ and $(0, 1/N_2)$, respectively. For each parameter set, I ran $\geq$100,000 replications and counted the number of replications in which A established in the simulated population. "Establishment" in my simulation is defined such that the newly introduced mutation is still present after $T_E = 5N_1$ generations (I confirm that the effect of this arbitral choice of T_E on the establishment probability is very small as long as T_E is sufficiently large). It should be noted that, according to my definition, the established replications include two cases; case C, where alleles A and a coexist, namely, allele A is nearly fixed in subpopulation I while allele a is nearly fixed in subpopulation II, typical for strong divergent selection, and case F, where allele A is fixed in both subpopulations (swamping). Let Pc be the relative proportion of case C in established replications. In Figure 3.1, a gray region is shown such that $Pc > 0.9$ on its left (corresponding to low migration rates), while $Pc < 0.1$ on the right (high migration). According to my derivation, u_1 and u_2 from Equations 3.9 and 3.10 evaluate the sum of these two cases, so that they are comparable to the simulation results, even though my interest is mostly in case C where divergent selection is strong relative to migration and both alleles are maintained in the population (i.e., on the left of the gray region).

Figure 3.1 shows the establishment probability derived from Equations 3.9 and 3.10 as a function of migration rate, together with the simulation results. I fix $s_1 = 0.02$ and $s_2 = -0.01$, and the strength of assortative mating varies between subplots. In addition, three pairs of population sizes N_1 and N_2 were considered; (A): $N_1 = N_2 = 2000$; (B): $N_1 = 2000, N_2 = 10000$; (C): $N_1 = 10000, N_2 = 2000$. It is found that Equations 3.9 and 3.10 generally agree well with the simulation result as long as the selection intensities s_i and α are small enough so that their second-order terms are ignorable.

When the effect of assortative mating is very weak (i.e., $\alpha = 0.01$, the top left panel in Figures 3.1A, B, C), my results are overall similar to the model that considers only divergent selection (Sakamoto and Innan 2019): when the migration rate is very low, the two subpopulations can be treated as independent, so that $u_1 \sim 2\lambda$ where $\lambda = s_1$ if I ignore assortative mating, while $u_2 \sim 0$. As the migration rate increases, u_1 decreases and u_2 increases, and they become similar to each other for large migration rates. Because allele A is advantageous only in subpopulation I, this beneficial effect is reduced with increasing the migration rate, and vise versa for allele a. When the migration rate is very large ($m \sim 0.5$), the two subpopulations can be considered as a single randomly-mating population, and the fixation probability of a single mutation is mainly determined by the average selection coefficient,

$$u_1 = u_2 = \frac{\int_0^{1/N_T} G(x)dx}{\int_0^1 G(x)dx}, \tag{3.11}$$

where $G(x) = e^{-2N_T(\bar{s}-\frac{\alpha}{2})x-N_T\alpha x^2}$, $\bar{s} = \frac{N_1 s_1 + N_2 s_2}{N_T}$ and $N_T = N_1 + N_2$ (presented by a triangle in Figure 3.1). The gray region for $0.1 \leq Pc \leq 0.9$ occupies a narrow window of the migration rate, indicating that a fairly small difference in the migration rate around the gray region could change the typical outcome dramatically (maintenance or loss of polymorphism). In the cases of asymmetric subpopulations (Figures 3.1B, C), the larger subpopulation affects the establishment probability more because individuals tend to stay for a longer time in the larger subpopulation. For example, in Figure 3.1B, u_2 is over smaller than that in the symmetric case (Figure 3.1A) because allele A is more strongly selected against in population II. u_1 quickly drops as the migration rate increases with the same reason. In contrast, when population I is larger (Figure 3.1C), the opposite pattern is observed.

In the following, I explain the effect of α on u_i by focusing on the symmetric case ($N_1 = N_2 = 2000$) shown in Figure 3.1A. Allele A is favored in subpopulation I through divergent selection, which is a positive force for its establishment, although this positive effect is weakened by migration. Mathematically, λ in Equation 3.7 can be considered as the effective intensity of divergent selection, when migration is taken into account. In contrast, assortative mating is a negative force when allele A is rare, which makes it difficult for allele A to increase in frequency. This is because males carrying allele A almost exclusively encounter females with allele a, by which they are rejected with probability α. Thus, the relative contributions of divergent selection and assortative mating largely determines the fate of allele A, in agreement with the results of the deterministic models (Slatkin 1982, Kirkpatrick and Nuismer 2004).

Let us first assume a very small migration rate (see the left end at $m_1 = 5 \times 10^{-5}$ in each panel in Figure 3.1A). If we ignore migration, λ is simply given by s_i and the total strength of selection (divergent selection and assortative mating) on allele A is roughly given by $s_i - \frac{\alpha}{2}$ in subpopulation i. As expected, the establishment probabilities u_1 and u_2 decrease with increasing α. When assortative mating is weak ($\alpha = 0.01 \sim 0.03$ in Figure 3.1A), u_1 can be roughly approximated by $u_1 = 2s_1 - \alpha$. When $\alpha = 0.04$, I have $2s_1 - \alpha = 0$, where the two selective forces should roughly cancel each other, but it seems that u_1 exceeds the neutral expectation ($1/N_1$) because the negative effect of assortative mating is relaxed once p_1 increases. The establishment probability u_1 is very low for $\alpha > 0.04$, where selection in total works against allele A due to strong assortative mating. It is interesting to point out that, even with strong assortative mating, allele A can establish if it happens to initially increase in frequency by random genetic drift. Once it becomes common, the negative effect of assortative mating is reduced, and the allele could successfully go to establishment by the positive effect of divergent selection.

As the migration rate increases, the intensity of divergent selection is effectively weakened, so that u_1 decreases and I have u_1 as given by Equation 3.11 in the limit of free migration (yellow triangle). The behavior of u_2 is more complex: u_2 decreases to the level presented by the yellow triangle with increasing the migration rate due to the same reason as u_1 when the migration rate is high (roughly in the right of the gray region), whereas u_2 increases as the migration rate increases when migration rate is low (roughly in the left of the gray region) because migration helps allele A in subpopulation II to move to subpopulation I.

Focusing on u_1, Figure 3.2 explores a wider parametric space for s_1 and α, while the other parameters are fixed ($m_1 = m_2 = 0.005$ and $s_2 = -0.02$). To demonstrate the effect

of the population size, three population sizes are considered, assuming the same sizes for the two subpopulations ($N = N_1 = N_2 = 2000, 6000, 20000$). In each panel, analytical and simulation results are shown: Analytical results from Equation 3.9 are presented by the color of the background, while colors inside the circles represent simulation results.

Again, the overall agreement of colors in the circle and those in the background suggest excellent performance of Equation 3.9 for a wide range of the parameter set. It seems that my analytical result slightly overestimates the establishment probability when s_i and α are so large that the establishment probability is sensitive to the second order of s_i, α, which were ignored in my derivation. The blue dashed line represents $2\lambda = \alpha$, where the two selective forces roughly cancel each other so that it can be considered as a threshold for establishment in an infinite population. When the population size is very large, u_1 drops quickly above this line, whereas allele A may still establish when the population size is small, because of random genetic drift.

3.3.2 Establishment probability in the diploid model

In the diploid case, the initial state is that all individuals are aa homozygotes in both subpopulations. I first consider the establishment probability of an allele A that newly arises in subpopulation I with initial frequency $\frac{1}{2N_1}$. As in my derivation for the haploid model, I approximate the two-population process by a one-population system by focusing on the establishment process in subpopulation I alone (Yeaman and Otto 2011). To do so, the fitnesses of genotypes AA, Aa and aa are given by $1 + \lambda$, $1 + h\lambda$ and 1, respectively, where λ is the effective strength of natural selection as defined above. Allele A can be considered dominant over allele a when $h = 1$, and recessive when $h = 0$. Following Yeaman and Otto (2011), I assume that the leading eigenvalue of the transition matrix approximates the growth rate of allele A in a hypothetical one-population system (when allele A is rare). Then, λ is given by

$$h\lambda = \frac{1}{2}\left[(hs_1 + hs_2 - m_1 - m_2) + \sqrt{(hs_1 - hs_2 - m_1 + m_2)^2 + 4m_1m_2}\right], \tag{3.12}$$

where I assume fairly strong selection, say $hs_i \gg \frac{1}{N_i}$.

Given Equation 3.12, M_p and M_q, the expected changes in the genotype frequencies of AA and Aa in one generation, are obtained by assuming that $\lambda, \alpha \ll 1$ and ignoring second-order terms in these parameters, and the Kolmogorov forward equation is given by

$$\frac{\partial\phi}{\partial t} = -\frac{\partial[M_p\phi]}{\partial p} - \frac{\partial[M_q\phi]}{\partial q} + \frac{1}{2}\frac{\partial^2[V_p\phi]}{\partial p^2} + \frac{\partial^2[V_{pq}\phi]}{\partial p\partial q} + \frac{1}{2}\frac{\partial^2[V_q\phi]}{\partial q^2}, \tag{3.13}$$

where $V_p = \frac{p(1-p)}{N_1}, V_{pq} = -\frac{pq}{N_1}, V_q = \frac{q(1-q)}{N_1}$ and $\phi(p, q)$ is a transition density (see Appendix B for the expressions of M_p and M_q). By changing the variables, Equation 3.13 is rewritten as a function of the allele frequency of A, x, and the frequency of heterozygotes q as

$$\frac{\partial\tilde{\phi}}{\partial t} = -\frac{\partial[M_x(x,q)\tilde{\phi}]}{\partial x} - \frac{\partial[M_q(x,q)\tilde{\phi}]}{\partial q} + \frac{1}{2}\frac{\partial^2[V_x(x,q)\tilde{\phi}]}{\partial x^2} + \frac{\partial^2[V_{xq}(x,q)\tilde{\phi}]}{\partial x\partial q} + \frac{1}{2}\frac{\partial^2[V_q(x,q)\tilde{\phi}]}{\partial q^2}, \tag{3.14}$$

where $\tilde{\phi}(x, q)$ is a transition density after changing the variables (for the expression of each term, see Appendix B).

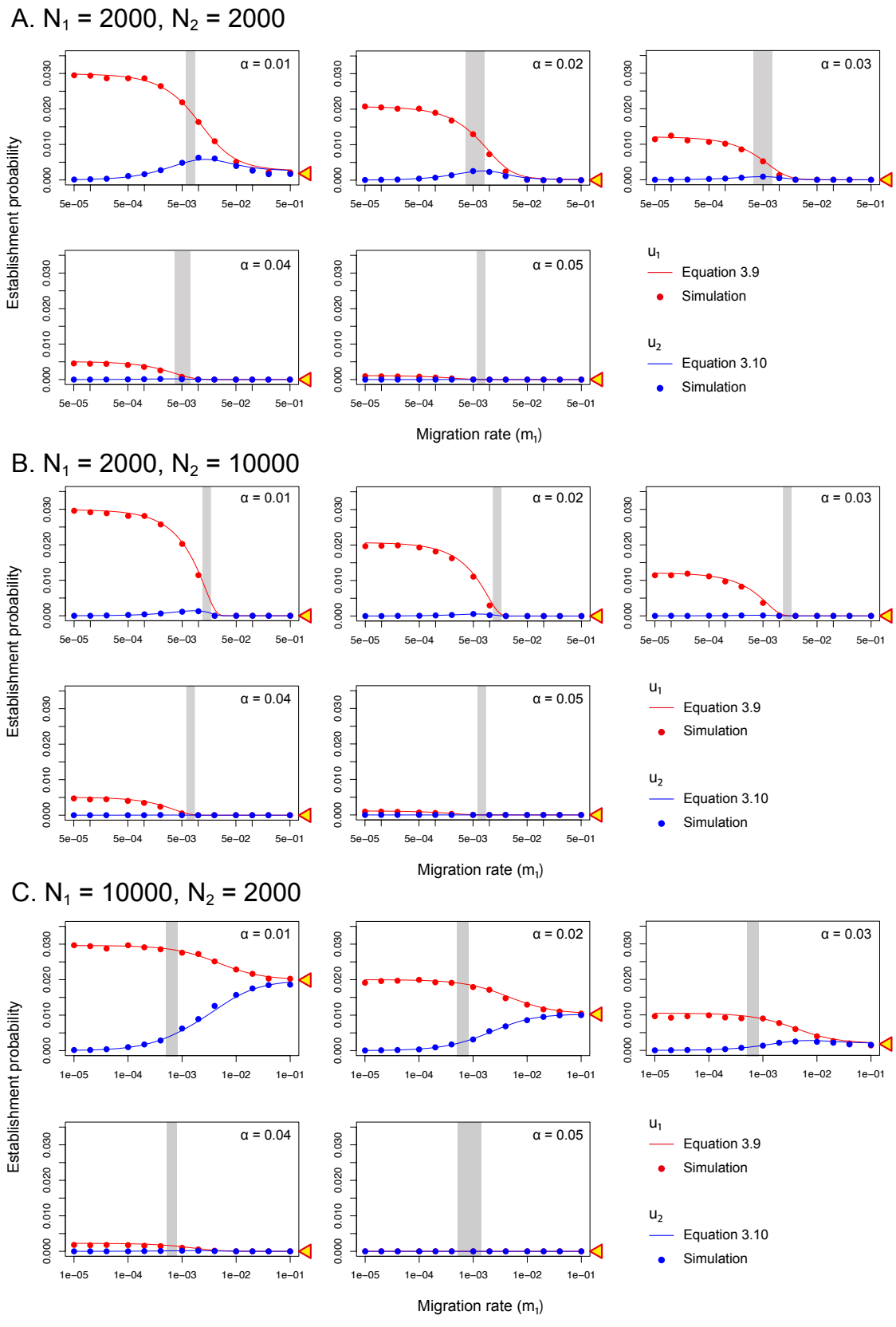

Figure 3.1: Establishment probability of a magic trait allele in the haploid model, plotted against the migration rate. $s_1 = 0.02$ and $s_2 = -0.01$ are fixed, and three pairs of the population sizes are assumed: (A) $N_1 = N_2 = 2000$, (B) $N_1 = 2000$ and $N_2 = 10000$, (C) $N_1 = 10000$ and $N_2 = 2000$. For each pair of population sizes, the strength of assortative mating is changed from $\alpha = 0.01$ to 0.05. In each panel, a gray region is presented such that the proportion of the replications where two alleles (A and a) coexisted (Pc) > 0.9 in the left, while $Pc < 0.1$ in the right. The yellow triangle on the right vertical axis indicates the establishment probability assuming a very large migration rate.

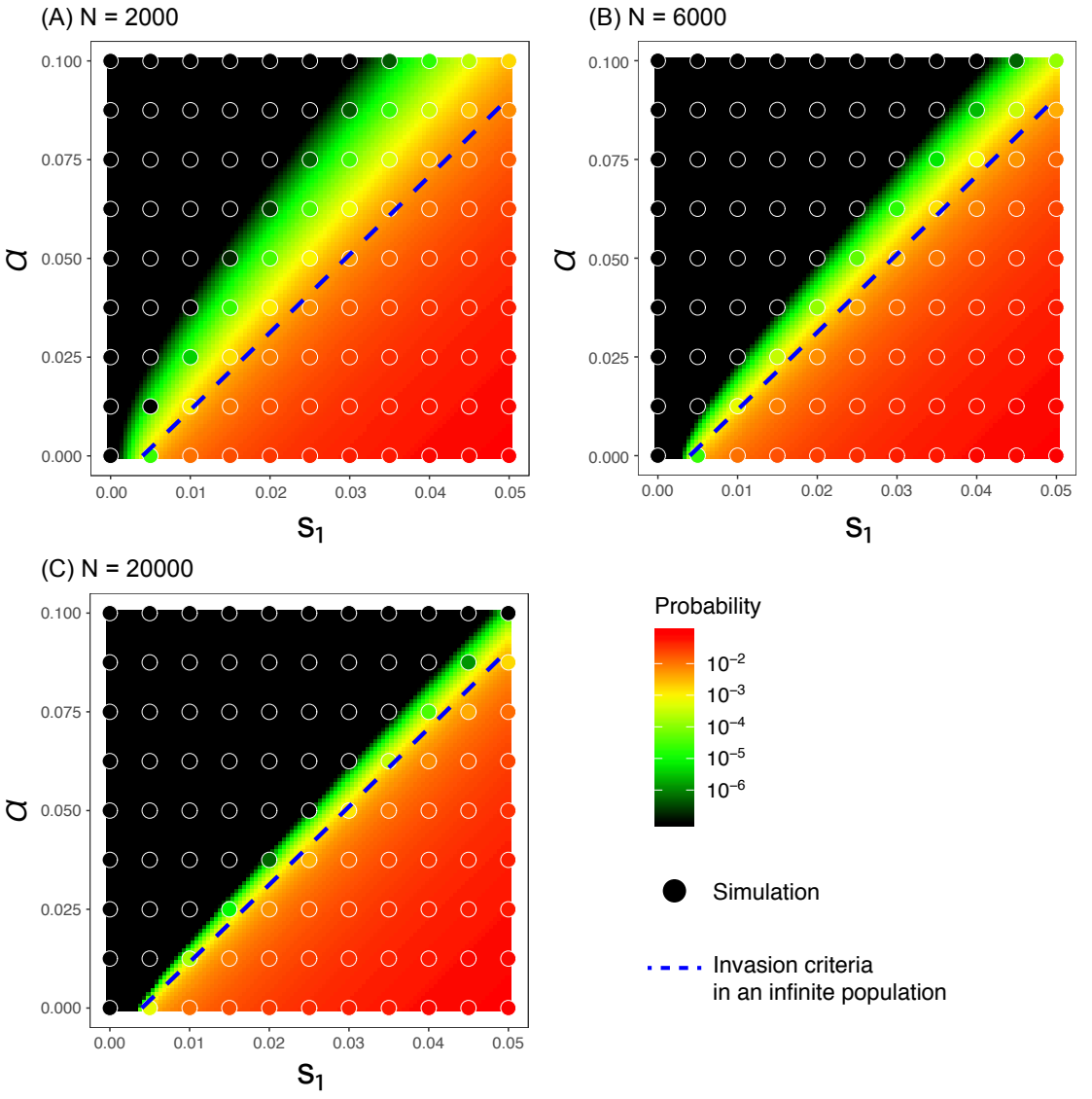

Figure 3.2: Establishment probability of a magic trait allele in the haploid model with different population sizes ($N_1 = N_2 = 2000, 6000, 20000$). $m_1 = m_2 = 0.005$ and $s_2 = -0.02$ are fixed. The background color presents the theoretical approximation (Equation 3.9) while circle's color presents the simulation result. The blue dashed line presents the invasion criteria assuming an infinite population (see text for details).

This forward equation with two variables, x and q, is still difficult to solve, so that I attempt to reduce the dimension by approximation, that is, the frequency of heterozygotes, q, is approximated by a function of x. If I ignore assortative mating so that the Hardy-Weinberg equilibrium holds, we can simply assume $q(x) = 2x(1-x)$. Even with assortative mating, Yamamichi and Sasaki (2013) demonstrated that the assumption of the Hardy-Weinberg equilibrium (i.e., $q(x) = 2x(1-x)$) works fairly well. Recently, Newberry *et al.* (2016) proposed that $q(x)$ can be given by the solution of the differential equation $\frac{dq}{dx} = \frac{M_q(x,q)}{M_x(x,q)}$ which satisfies the condition $\lim_{x\to 0} q(x) = 0$. I here employ the method of Newberry *et al.* (2016) and obtain $q(x) \approx 2x(1-x) - 4x^2(1-x)^2(x^2 - 2hx + h)\alpha$ by a perturbation approach (for details see Appendix C). With this approximation of $q(x)$ and by ignoring the stochastic deviation of the frequency of heterozygotes from $q(x)$, Equation 3.14 can be reduced to a one-dimensional diffusion equation:

$$\frac{\partial \tilde{\phi}}{\partial t} = -\frac{\partial [M_x(x, q(x))\tilde{\phi}]}{\partial x} + \frac{1}{2}\frac{\partial^2 [V_x(x, q(x))\tilde{\phi}]}{\partial x^2}. \tag{3.15}$$

Then, by using Kimura's formula (Kimura 1962), the establishment probability of an allele A that newly arises in subpopulation I, u_1, is given by

$$u_1 = \frac{\int_0^{1/2N_1} G(x)dx}{\int_0^1 G(x)dx}, \tag{3.16}$$

where $G(x) = \exp\Big(-\int \frac{2M_x(x,q(x))}{V_x(x,q(x))}dx\Big)$.

The establishment probability of an allele A that newly arises in subpopulation II, u_2 can be derived as in the haploid case, and is given by

$$u_2 \approx u_1\frac{c}{1-b} - \frac{u_1^2}{2}\frac{c^2}{(1-b)^3}, \tag{3.17}$$

where $b = \big(1 + h(s_2 - \frac{\alpha}{2})\big)(1-m_2), c = \big(1 + h(s_2 - \frac{\alpha}{2})\big)m_2$.

The establishment probability derived from Equations 3.16 and 3.17 is compared with simulation in Figure 3.3. Simulations were performed by assuming $N = N_1 = N_2 = 1000, s_1 = 0.02, s_2 = -0.01$, and α was changed from 0.01 to 0.05. Three different degrees of dominance were considered; complete dominance ($h = 1$), additivity ($h = 0.5$), and near recessivity ($h = 0.05$). Overall, my analytical results again agree well with the simulation results when $\frac{1}{N} \ll hs_i, h\alpha \ll 1$. I obtain almost the same results as in the haploid model when $h = 1$ (Figure 3.3A), and u_1 and u_2 decrease as h decreases (Figures 3.3B and C). This trend can be explained if I consider how selection works on allele A in the very early phases, namely, when the allele frequency is very low. When $h = 1$, a newly arisen allele A causes a full phenotypic difference, which is immediately subject to selection. This is a similar situation to the haploid model. For $h < 1$, the phenotypic effect of allele A is reduced to some extent (i.e., by a factor of h), therefore the selective pressure is relaxed. Thus, the selective pressure on allele A in the diploid model can be summarized by hs_i and $h\alpha$ in the early phases. As expected, if I plot u_1 for different h where the horizontal and vertical axises are adjusted by hs_i and $h\alpha$, respectively, the establishment probabilities are very similar (Figure 3.4).

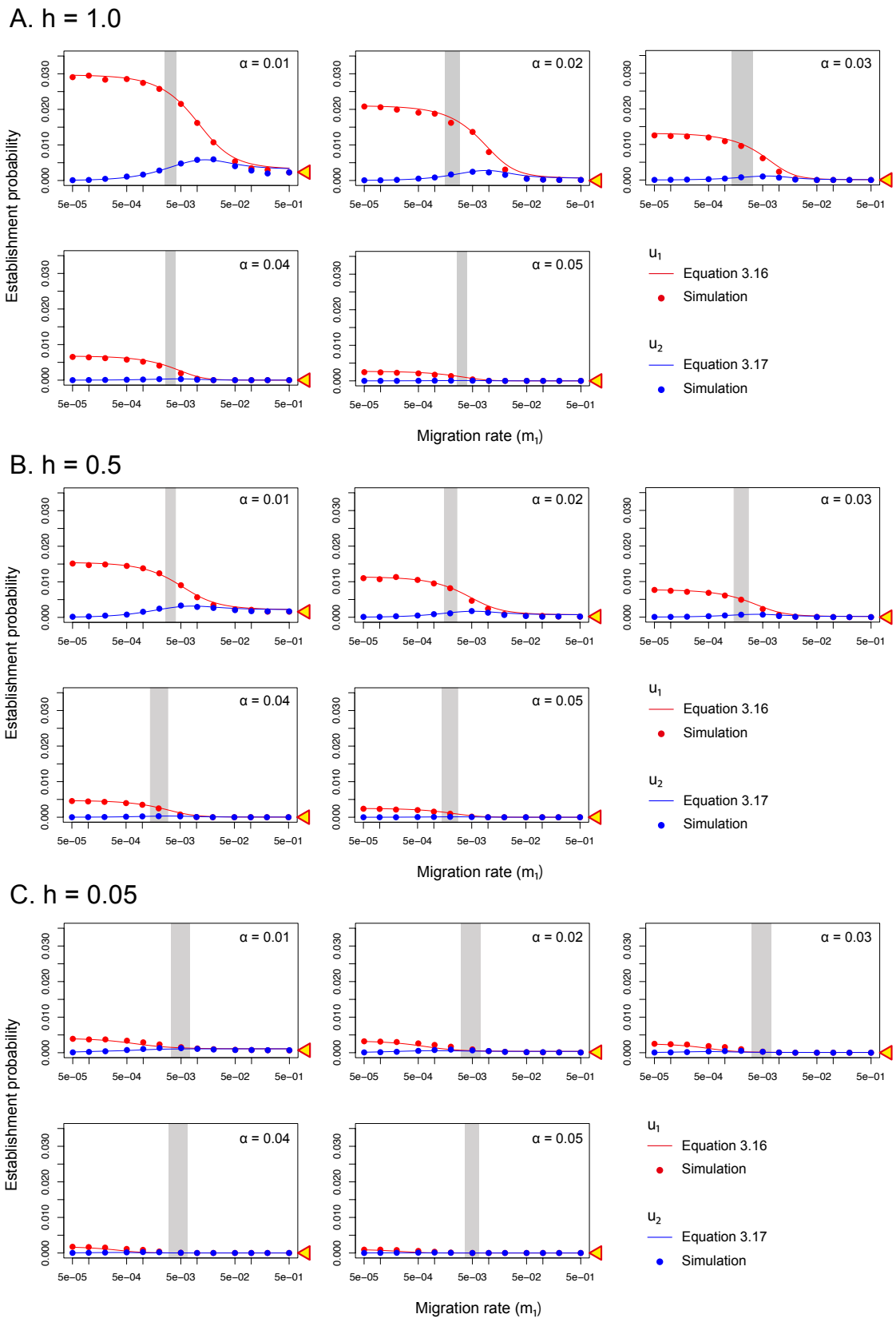

Figure 3.3: Establishment probability of a magic trait allele in the diploid model, plotted against the migration rate. $s_1 = 0.02$, $s_2 = -0.01$ and $N_1 = N_2 = 1000$ are fixed, and three dominance coefficients are assumed: (A) $h = 1.0$, (B) $h = 0.5$, (C) $h = 0.05$. For each dominance coefficient, the strength of assortative mating is changed from $\alpha = 0.01$ to 0.05. In each panel, a gray region is presented such that the proportion of the replications where two alleles (A and a) coexisted (Pc) > 0.9 in the left, while $Pc < 0.1$ in the right. The yellow triangle on the right vertical axis indicates the establishment probability assuming a very large migration rate.

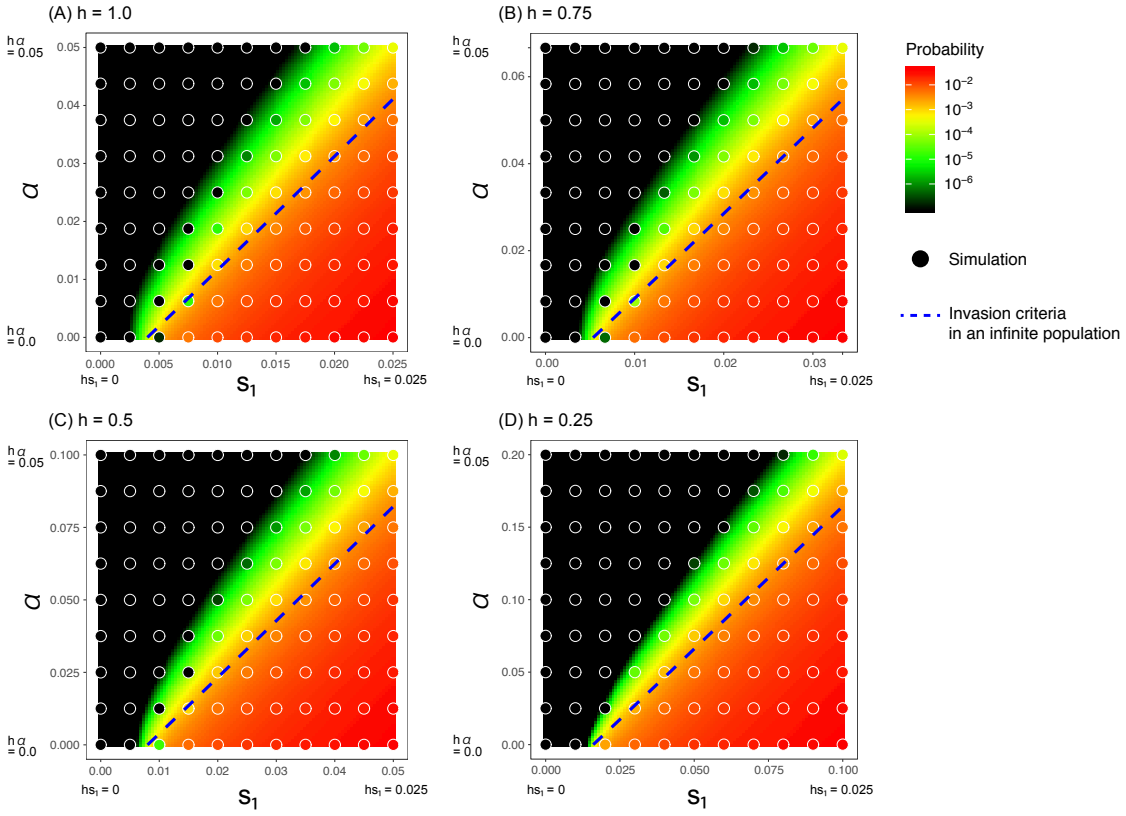

Figure 3.4: Establishment probability of a magic trait allele in the diploid model in different level of dominance ($h = 1.0, 0.75, 0.5, 0.25$). $N_1 = N_2 = 3000$, $m_1 = m_2 = 0.005$ and $hs_2 = -0.02$ are fixed. The background color presents the theoretical approximation (Equation 3.16) while circle's color presents the simulation result. The blue dashed line presents the invasion criteria assuming an infinite population (see text for details). The results are plotted such that the horizontal and vertical axises are scaled by hs_1 and $h\alpha$, respectively, therefore the blue dashed lines show up at the same position in each panel.

3.3.3 Establishment trajectory of allele frequency

When allele A establishes, it rapidly spreads in subpopulation I and is stably maintained at frequencies around the migration-selection balance, p_1^*. I now consider the frequency trajectory of allele A under the condition that it establishes. In practice, I obtain the mean sojourn time of allele A until it reaches frequency p_1^* for the first time under the condition that it reaches frequency p_1^*.

In the haploid model, assuming a low migration rate and strong selection, p_1^* is given by $p_1^* \approx 1 - \frac{m_1}{s_1 + \frac{\alpha}{2}}$. Following Ewens (1973), I can derive the conditional mean sojourn time at frequency x, $T^*(x)$ as

$$T^*(x) = \frac{2}{V_x G(x)} \frac{\int_x^{p^*} G(p)dp}{\int_0^{p^*} G(p)dp} \int_0^x G(p)dp, \tag{3.18}$$

where $V_x = \frac{x(1-x)}{N_1}$, $G(x) = e^{-2N_1(\lambda - \frac{\alpha}{2})x - N_1 \alpha x^2}$. I then obtain the time required for a newly arisen allele A to reach allele frequency x:

$$t(x) = \int_0^x T^*(p)dp, \tag{3.19}$$

so that $t(p_1^*)$ provides the establishment time. Note that although this argument holds for a new allele arisen in subpopulation I, it can also be applied to an allele arisen in subpopulation II after it has migrated into subpopulation I.

In the diploid model, I can approximate $p_1^* = 1 - \sqrt{\frac{m_1}{(s + \frac{\alpha}{2})}}$ for $h \sim 1$ and $p_1^* = 1 - \frac{m_1}{(1-h)(s+\frac{\alpha}{2})}$ for other cases where h is relatively smaller than 1. I then obtain the conditional mean sojourn time at frequency x by using Equation 3.18 while replacing $V_x = V_x(x, q(x))$ and $G(x) = \exp(-\int \frac{2M_x(x,q(x))}{V_x(x,q(x))} dx)$. My derivation works well when h is not small.

The theoretical result is quite simple, and there is no marked difference between the haploid and diploid models. Therefore, I demonstrate the point by using the haploid model. Figure 3.5A shows the theoretical trajectory of $t(x)$ by the red line when assortative mating is strong ($\alpha = 0.04$), compared with the case with no assortative mating ($\alpha = 0$, Figure 3.5B). For each panel, I also show ten independent established runs by black lines. The major difference is that the allele frequency tends to stay a long time at low frequency with assortative mating (Figure 3.5A), in comparison with the symmetric function in Figure 3.5B. This difference is easy to understand: As mentioned above, the negative effect of sexual selection on the newly arisen allele is strong only when its allele frequency is low, and the effect is relaxed once it increases. This pattern is globally observed both in the haploid and diploid models.

3.4 Discussion

I am interested in how a newly arisen allele for a magic trait (allele A) behaves and contributes to ecological speciation. A magic trait is defined such that a single trait is subject to both divergent selection and assortative mating. Divergent selection simply favors the new allele to fix where it is beneficial, thereby creating a genetic difference between subpopulations. Assortative mating works in a more tricky way: it also favors difference between subpopulations but a new allele is not always advantageous. This is because, when allele A is still rare after it arises, it is disadvantageous because male carriers encounter females with allele

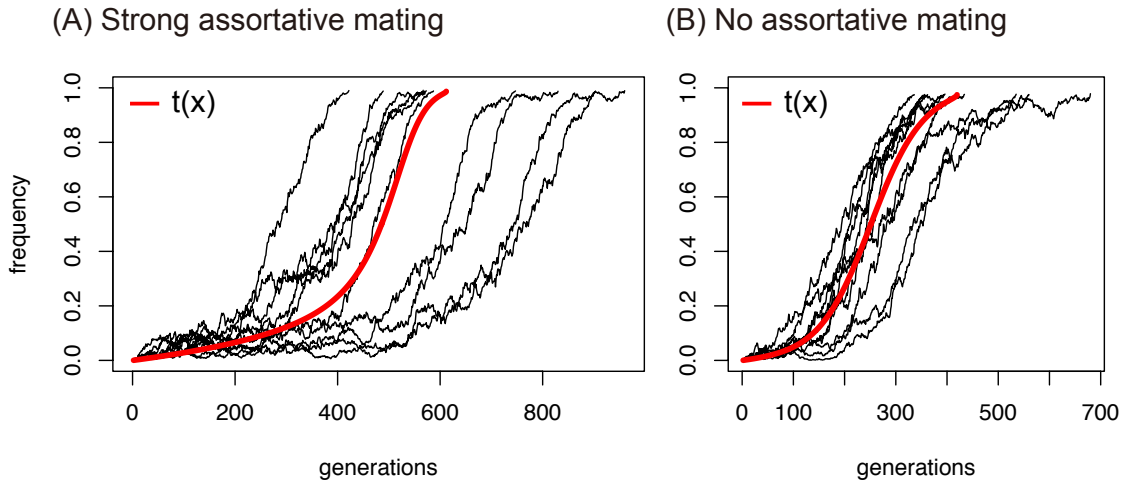

Figure 3.5: Trajectory of the frequency of allele A in the haploid model. $s_1 = 0.02, s_2 = -0.01, m_1 = m_2 = 0.0005$ and $N_1 = N_2 = 2000$ are assumed. (A) with strong assortative mating $\alpha = 0.04$ and (B) with no assortative mating $\alpha = 0$. The black lines shows 10 independent paths from simulations and the red line is the theoretical prediction.

a in most cases with a risk of being rejected. Once allele A becomes common so that A-A encounters are frequent, the allele A loses this disadvantage and can fix in the subpopulation it is adapted to, thereby contributing to genetic divergence.

Many theoretical studies have focused on the evolution of magic traits and demonstrated that assortative mating impedes the invasion of a new magic trait (Slatkin 1982, Kirkpatrick and Nuismer 2004). However, because most of them used deterministic treatments, it has not been known how much the establishment probability of a new magic trait is reduced by assortative mating. In order to understand the quantitative effect of random genetic drift, this work investigated the establishment probability of a magic trait allele for both haploid and diploid models. I successfully obtained the establishment probability by using the approximation method of Yeaman and Otto (2011). I confirmed that my derivation agreed well with my simulation results. My theory mainly focuses on the early phases, that is, when allele A is still rare so that divergent selection and assortative mating counteract. It is theoretically demonstrated that the relative contributions of divergent selection and assortative mating largely determine the fate of allele A.

In the haploid model, λ in Equation 3.7 explains the effective intensity of divergent selection with migration taken into account, and the intensity of assortative mating is parameterized by α. Theoretically, $2\lambda - \alpha$ is the key quantity to determine the fate of allele A when its frequency (p_1) is rare. If $2\lambda - \alpha > 0$, allele A is on average selected for, and selected against if $2\lambda - \alpha < 0$, at least in an infinite population. In a finite population, I show that allele A can establish even when $2\lambda - \alpha < 0$. This is especially true for small populations (Figures 3.2, 3.6-3.8), because random genetic drift occasionally increases p_1, and the negative effect of assortative mating is relaxed once allele A becomes common. Then, it is likely that allele A goes to establishment.

The results for the diploid model are similar to those for the haploid model. The major difference is due to dominance. I show that the establishment process can be well described if both s_i and α are scaled by h.

I also explore how the allele frequency behaves over the course of establishment. I theoretically obtained the trajectory of allele frequency, which clearly demonstrated that the

negative effect of assortative mating retards establishment while this effect is relaxed once the allele frequency increases.

In summary, my theory well demonstrates the behavior of a magic trait allele that is subject to divergent selection and assortative mating. My result is qualitatively in agreement with those based on deterministic models; the establishment of a magic trait allele is quite likely under the invasion criteria ($2\lambda > \alpha$). It is indicated that a magic trait allele could contribute to ecological speciation when assortative mating is weak. In such a case, strong assortment may evolve after the magic trait diverges (Servedio 2011), leading to solid speciation.

The main focus of this work is the effect of random genetic drift on the establishment process. The establishment of a magic trait allele is largely affected by the population size, because the fate of a newly arisen allele is mainly determined when it is rare, where random genetic drift plays a central role. Considering that local adaptation (potentially followed by ecological speciation) often occurs in a small niche with a limited number of individuals, a magic trait allele with a fairly strong assortative mating might happen to increase in frequency by random genetic drift and establish. My result provides fundamental understandings on the stochastic process of a magic trait allele in a finite population.

3.5 Appendices

Appendix A: Establishment probability of allele A that arises in subpopulation II

I here derive the establishment probability of a single allele A which arises in the subpopulation II where it is deleterious. First, I use a branching process approximation to derive the probability distribution of the number of A alleles originating from a single mutant allele in subpopulation II that migrate into subpopulation I. Then, by assuming that migrant alleles behave independently, I derive an approximate formula for the establishment probability. The derivation works for both haploid and diploid models.

I define the random variable X_t as the number of A alleles in subpopulation II in generation t and Y_t as the number of A alleles that have migrated to subpopulation I by generation t. Because I consider the case where selection on allele A in subpopulation II is negative, we can assume that its frequency stays low and the allele mostly exist in heterozygotes in the diploid case. Therefore, X_t is almost identical to the number of heterozygotes in the diploid model. I define a probability generating function in generation t as $f_t(x, y) = E[x^{X_t} y^{Y_t}]$. I also define the generating function of the joint distribution of the number of A alleles in subpopulation II and the number of A alleles that have just migrated to subpopulation I while originating from one allele A in subpopulation II in generation $t-1$ as $h(x, y)$. If we assume the number of offspring follows a Poisson distribution with mean $1 + s_2 - \frac{\alpha}{2}$, $h(x, y) = e^{-(1+s_2-\frac{\alpha}{2})(1-(1-m_2)x-m_2 y)}$ in the haploid case. Then, we have

$$f_{t+1}(x, y) = f_t(h(x, y), y). \tag{3.20}$$

I put $\boldsymbol{v}_t = \left(\frac{\partial f_t(1,1)}{\partial x}, \frac{\partial f_t(1,1)}{\partial y}, \frac{\partial^2 f_t(1,1)}{\partial x^2}, \frac{\partial^2 f_t(1,1)}{\partial x \partial y}, \frac{\partial^2 f_t(1,1)}{\partial y^2}\right)^T$. By using Equation 3.20, we obtain

$$\boldsymbol{v}_{t+1} = \boldsymbol{Q}\boldsymbol{v}_t, \tag{3.21}$$

where

$$\boldsymbol{Q} = \begin{pmatrix} b & 0 & 0 & 0 & 0 \\ c & 1 & 0 & 0 & 0 \\ b^2 & 0 & b^2 & 0 & 0 \\ bc & 0 & bc & b & 0 \\ c^2 & 0 & c^2 & 2c & 1 \end{pmatrix}, b = (1 + s_2 - \frac{\alpha}{2})(1 - m_2), c = (1 + s_2 - \frac{\alpha}{2})m_2.$$

When t goes to infinity, $\boldsymbol{v}_\infty = (0, \frac{c}{1-b}, 0, 0, \frac{c^2}{(1-b)^3})^T$.

Then, the establishment probability of a single allele A that arises in the subpopulation II, u_2, is approximately given by

$$\begin{aligned} u_2 &\approx 1 - f_\infty(1, 1 - u_1) \\ &\approx u_1 \frac{c}{1-b} - \frac{u_1^2}{2}\frac{c^2}{(1-b)^3}. \end{aligned} \tag{3.22}$$

For the diploid case, we should substitute s_2 and α by hs_2 and $h\alpha$ in the above equations.

Appendix B: Coefficients of diffusion equations 3.13 and 3.14

I here describe the coefficients of the diffusion process in Equations 3.13 and 3.14. Following Equations 3.3 and 3.4, $M_p(p,q)$ and $M_q(p,q)$ in Equation 3.13 are given by

$$\begin{aligned} M_p &= \left(p^2 + pq + \frac{q^2}{4} - p\right) \\ &\quad - \frac{hq^3 + \{(4h+1)p - h\}q^2 + \{(4h+4)p^2 - (2h+2)p\}q + 4p^3 - 4p^2}{2}\lambda \\ &\quad - \frac{hq^3 + \{(6h-1)p - h\}q^2 + \{8hp^2 + (2-6h)p\}q + 4p^3 - 4p^2}{4}\alpha \\ M_q &= \left\{pq + \frac{q^2}{2} + 2p(1-p-q) + q(1-p-q) - q\right\} \\ &\quad + \left[hq^3 + \{(4h+1)p - 2h\}q^2 + \{(4h+4)p^2 - (4h+3)p + h\}q + 4p^3 - 6p^2 + 2p\right]\lambda \\ &\quad + \frac{-hq^3 + \{-(2h+1)p + 2h\}q^2 + \{-2p^2 + (2h+3)p - h\}q + 2p^2 - 2p}{2}\alpha, \end{aligned} \tag{3.23}$$

and $V_p = \frac{p(1-p)}{N_1}, V_{pq} = -\frac{pq}{N_1}, V_q = \frac{q(1-q)}{N_1}$. By changing the variables, the coefficients in Equation 3.14 are given by

$$\begin{aligned}
M_x &= -\frac{2\alpha x^3 + \{2s + (4\alpha h - 2\alpha)q - 3\alpha\}x^2}{2} \\
&\quad - \frac{[\{(4h-2)q - 4\}s + \alpha q^2 + (5\alpha - 8\alpha h)q + 2\alpha]x + (2-2h)qs + (\alpha h - \alpha)q^2 + (\alpha h - \alpha)q}{4} \\
M_q &= 4sx^3 + [\{(4h-2)q - 6\}s - \alpha q + \alpha - 2]x^2 \\
&\quad + \frac{[\{(6-8h)q + 4\}s + (\alpha - 2\alpha h)q^2 + (2\alpha h + \alpha)q - 2\alpha + 4]x + (2h-2)qs + (\alpha h - \alpha)q^2 + (-\alpha h + \alpha - 2)q}{2} \\
V_x &= \frac{4x(1-x) - q}{4N_1} \\
V_{xq} &= \frac{q(1-2x)}{2N_1} \\
V_q &= \frac{q(1-q)}{N_1}.
\end{aligned} \tag{3.24}$$

Appendix C: Approximation of the frequency of heterozygotes

I derive an approximate formula which describes the frequency of heterozygotes in the diploid model. I assume that the strength of assortment mating, α, is small and the frequency of heterozygote $q(x)$ can be expanded as

$$q(x) = 2x(1-x) + q_1(x)\alpha + \mathcal{O}(\alpha^2), \tag{3.25}$$

where x is the frequency of allele A. Following Newberry *et al.* (2016), I assume that $q(x)$ is the solution of the differential equation, $\frac{dq}{dx} = \frac{M_q(x,q)}{M_x(x,q)}$. By substituting Equation 3.25, I have

$$sq_1'(x) = -\frac{4x^2(1-x)^2(x^2 - 2hx + h) + q_1(x)}{(2h-1)x^3 + (-3h+1)x^2 + hx} \tag{3.26}$$

Because I assume $s \ll 1$, I can derive $q_1(x) \approx -4x^2(1-x)^2(x^2 - 2hx + h)$ by ignoring the left side of Equation 3.26.

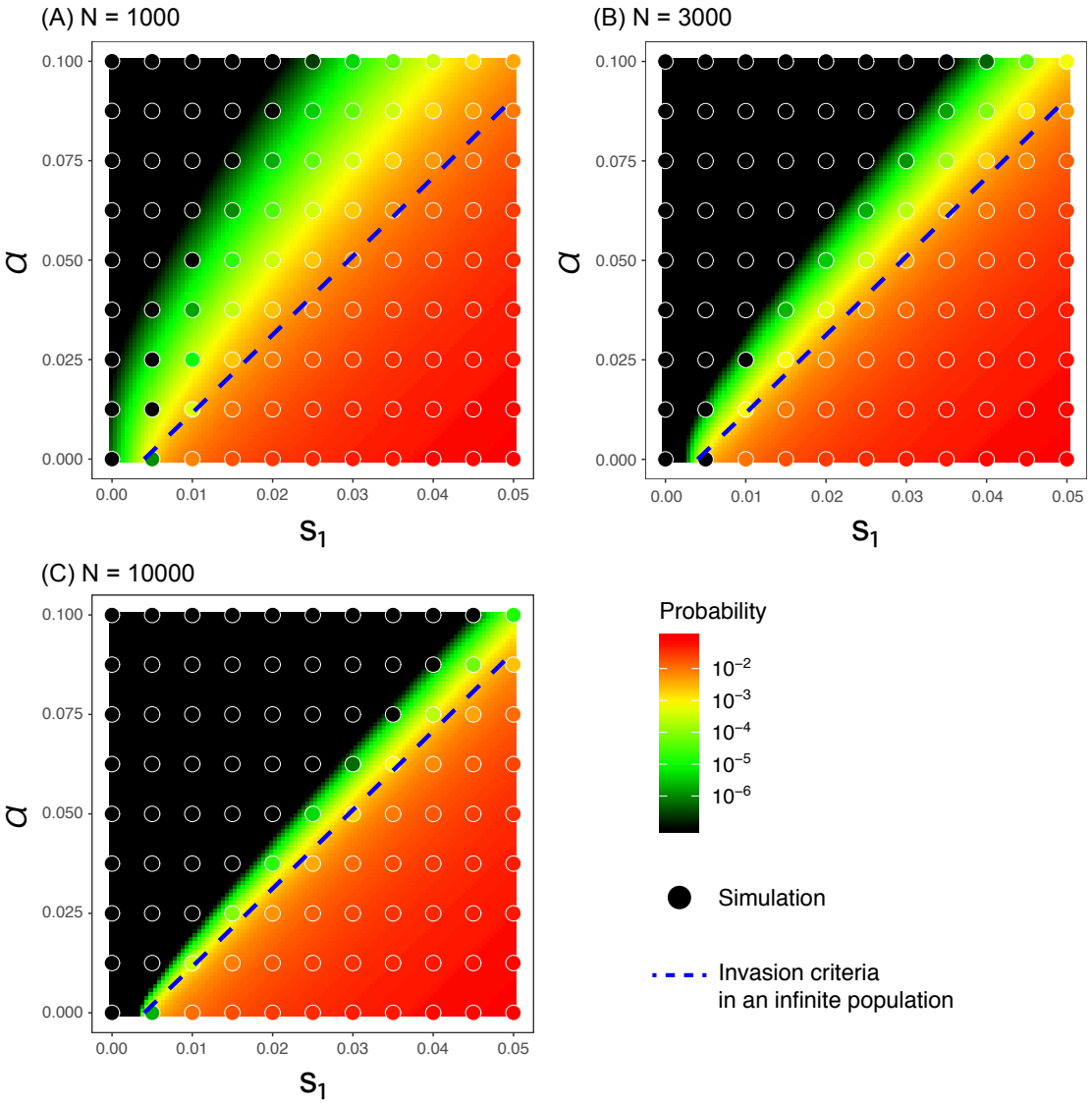

Figure 3.6: Establishment probability of a magic trait allele in the complete dominant case ($h = 1.0$) for different population size ($N_1 = N_2 = 1000, 3000, 10000$). $m_1 = m_2 = 0.005$ and $s_2 = -0.02$ are assumed. The background color presents the theoretical approximation (Equation 3.16) while circle's color presents the simulation result.

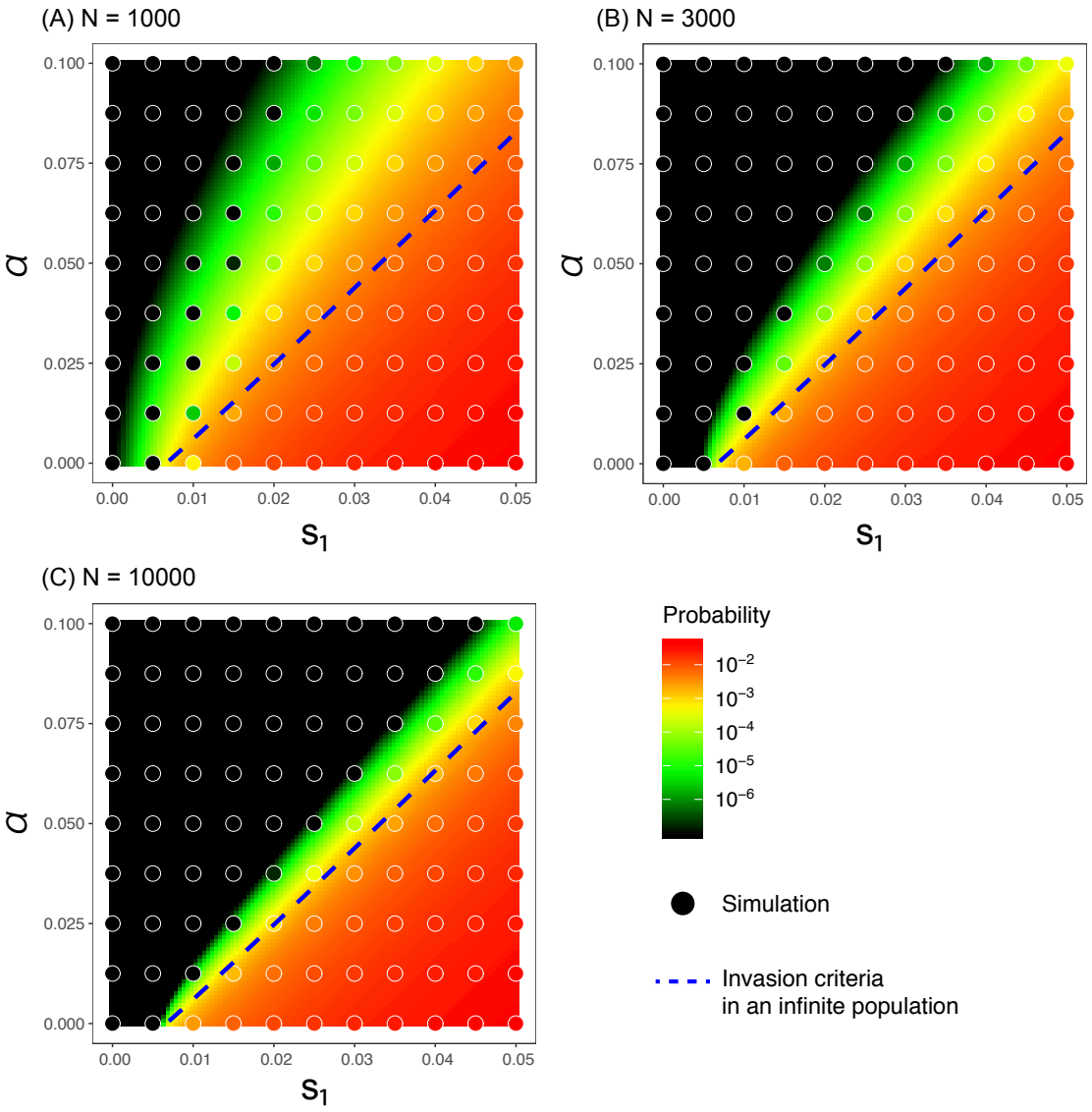

Figure 3.7: Establishment probability of a magic trait allele in the additive case ($h = 0.5$) for different population sizes ($N_1 = N_2 = 1000, 3000, 10000$). Other parameters are the same as Figure 3.6.

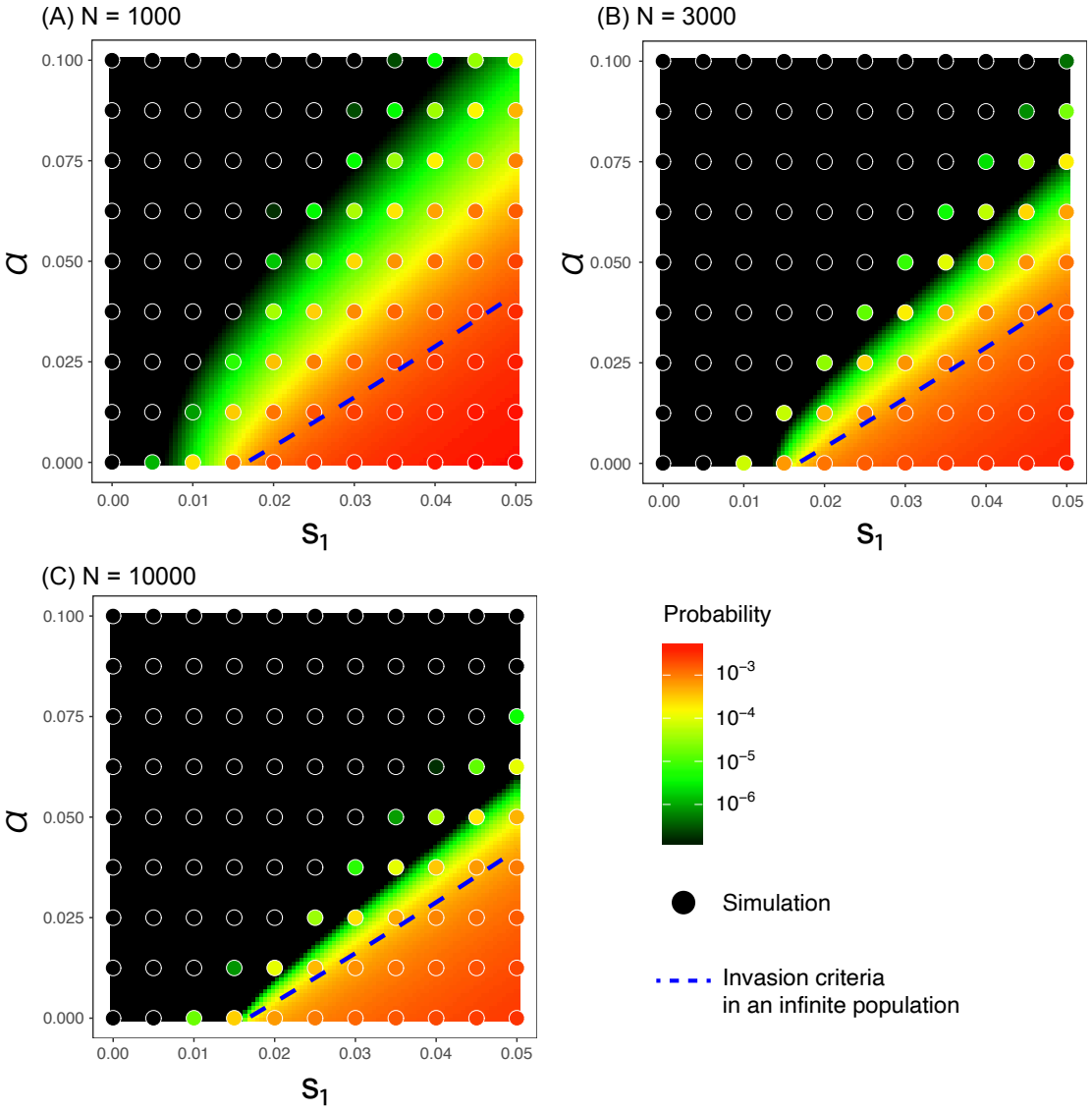

Figure 3.8: Establishment probability of a magic trait allele in a nearly recessive case ($h = 0.05$) for different population sizes ($N_1 = N_2 = 1000, 3000, 10000$). Other parameters are the same as Figure 3.6.

Chapter 4

Establishment of a new sex-determining allele driven by sexually antagonistic selection

4.1 Introduction

Recent genome analyses have demonstrated that genetic systems that determine sex are more labile than previously thought and that the turnover of sex-determining loci has repeatedly occurred. In some clades such as teleost fish and amphibians, sex-determining loci differ among closely related species or even within a species (Bachtrog *et al.* 2014, Beukeboom and Perrin 2014). Frequent turnover should occur in species especially when sex is determined by a single sex-determining locus, rather than a pair of highly diverged sex chromosomes. Turnover should be initiated by mutation at another potentially sex-determining locus, which could become a new sex-determining locus while the polymorphism at the original sex-determining locus disappears.

Many theoretical studies have investigated the evolutionary process of such turnover (Bull and Charnov 1977, van Doorn and Kirkpatrick 2007, 2010, Kozielska *et al.* 2010, Blaser *et al.* 2013, 2014, Veller *et al.* 2017, Scott *et al.* 2018, Saunders *et al.* 2018, 2019). A consensus has been established that, if a new sex-determination system has higher fitness than the old one, the new system could potentially override the old one. This explains why turnover hardly occurs in species with a diverged pair of sex chromosomes, such as the X/Y system in mammals and the W/Z system in birds. Theoretical examinations of turnover usually involves a two-locus system, under which turnover has to pass through a phase in which dimorphic sex-determining alleles segregate at both of the two sex-determining loci. A deterministic theory assuming a population with an infinite size (Bull and Charnov 1977) demonstrated that the system with higher fitness can be stably maintained by selection. It is indicated that the fitness advantage of the new locus over the existing one would be an important factor for the turnover of sex-determining loci.

A possible scenario that a new sex-determining locus confers a fitness advantage is that the new locus arises in close linkage to a locus under sexually antagonistic selection (van Doorn and Kirkpatrick 2007, 2010). This process is explained in Figure 4.1A. Initially, sex is determined by the original X/Y locus, while the A/a locus is another potential sex-determining locus on a different chromosome (autosome). That is, the A/a locus is monomorphic (fixed for allele a) so that it does not play a role in sex determination, but when allele A arises from allele a by mutation, it creates a new sex-determination system. I refer to allele A as a sex-determining allele. There is another polymorphic locus (B/b) that is located close to

the A/a locus. The B/b locus is assumed to be subject to sexually antagonistic selection; for example, allele B is beneficial in males and allele b is beneficial in females. At this point, the B/b locus does not confer any advantage or disadvantage because there is no physical linkage to the sex-determining locus X/Y. If a sex-determining allele (A) arises by mutation at the A/a locus, then one of the possible outcomes is that this new dimorphic locus takes over the role of sex determination and the original X/Y locus becomes monomorphic.

I am here interested in how often such turnover of sex-determining loci occurs. To understand this, it is crucial to theoretically describe the entire process, from the birth of a new sex-determining allele to its stable establishment. However, previous studies on this topic mainly by van Doorn and Kirkpatrick (2007, 2010) focused on the second half of the process (as explained below). The purpose of this work is to provide an analytical description for the first half, which largely determines how often turnover occurs under what conditions.

The entire process may be divided into two phases, which are referred to as the stochastic and deterministic phases. The stochastic phase starts when a new sex-determining allele A arises, and continues until the frequency becomes high enough to escape from extinction due to random genetic drift. Then, the deterministic phase follows, in which allele A further increases in frequency by positive selection and genotype Aa becomes fixed in the heterogametic sex; in this way, the new A/a locus takes over the role in sex determination. The theoretical results currently available are for the deterministic phase, in which analytical treatment is quite straightforward because random genetic drift may be ignored. van Doorn and Kirkpatrick (2007, 2010) used a deterministic approach to describe the rate of increase in the frequency of allele A during the early stages of the deterministic phase. In contrast, the behavior of allele A in the initial stochastic phase is much more complicated and many factors are involved in it, which is the scope of this work. One such factor is the effect of random genetic drift, which is the major evolutionary force acting when the allele frequency is low. The linkage to B/b is also a very important factor. If allele A arises in linkage with allele B, allele A immediately benefits from positive selection because the haplotype A-B confers a selective advantage. On the other hand, if allele A arises in linkage with allele b, selection works against allele A because the haplotype A-b is deleterious. Recombination plays a crucial role in determining the rate at which the advantageous haplotype A-B is created and broken up. Another important factor is how selection works on the B/b locus. Depending on the parameter setting for the effect of the B/b locus on fitness, selection operates in various modes (see Figure 4.2): Selection works for or against allele B, or even in some parameter space, balancing selection works to maintain the two alleles at intermediate frequencies. It is easy to imagine that this parameter setting largely affects the fate of the sex-determining mutation.

The purpose of this work is to theoretically understand how often turnover of a new sex-determining A/a locus occurs. I here mathematically describe the probability that a newly arisen sex-determining locus turns over the old one, which is referred to as the establishment probability. I found that the establishment probability is markedly high in the case of balancing selection, while it is very low in other modes of selection. It is indicated that the mode of selection at the B/b locus is critical in determining the fate of a newly arisen sex-determining allele. Therefore, to understand the rate of turnover, it is necessary to know how many sexually antagonistic loci are under balancing selection. My simulations provide insight

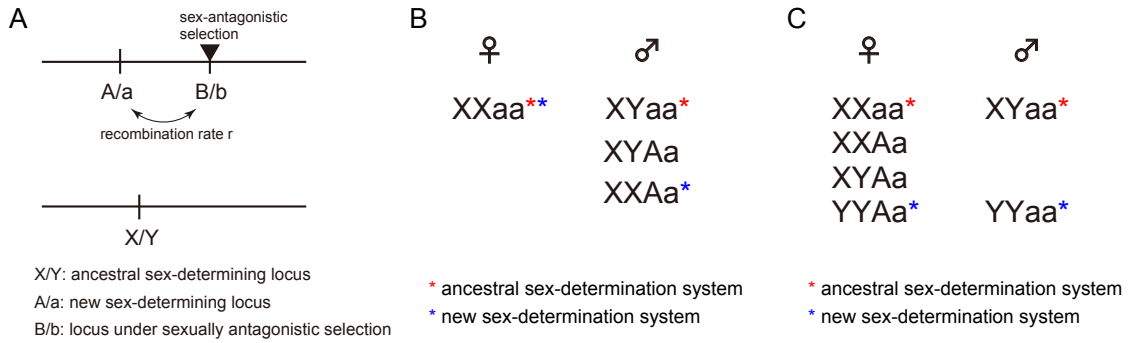

Figure 4.1: (A) The three loci model used in this work. (B) Relationship between sexes and genotypes when allele A has a masculinizing effect. (C) Relationship between sexes and genotypes when allele A has a feminizing effect. The red and blue stars are given to the genotypes that determine sex under the ancestral and new systems, respectively. The genotypes with no stars arise in the phase of transition from the ancestral to the new system.

into how to distinguish the mode of selection from the pattern of polymorphism around the sex-determining locus.

4.2 Model

I use a discrete-generation model of a diploid species with population size N. Three loci are considered in the model (Figure 4.1A). One is the ancestral sex-determining locus, which is located on the sex chromosome where males have genotype XY and females have genotype XX. Although male heterogamety (XY system) is assumed here, my model can also handle female heterogamety (ZW system) by swapping males and females. The model includes another sex-determining locus A/a on the autosome, at which the initial state is that allele a is fixed, so that the locus does not play a role in sex determination. Then, I consider that masculinizing or feminizing allele A just arises by mutation at locus A/a. I am interested in how this new sex-determining allele A behaves in a finite population and how often it spreads and eventually enables the A/a system to override the old X/Y system.

In my model, if allele A has a masculinizing effect, its turnover does not change the heterogamety sex and involves four genotypes (Case 1, Figure 4.1B). If allele A has a *strongly* feminizing effect (i.e., strong enough to make XYAa a female) (van Doorn and Kirkpatrick 2010), the turnover changes the heterogamety system and involves six genotypes (Case 2, Figure 4.1C). In either case, to evaluate the effect of the B/b locus, I assume that the levels of fitness of the new and old systems are identical. Therefore, the fate of allele A is mainly determined by the selection effect of another linked locus B/b. It is assumed that the recombination rate is r between the A/a and the B/b loci. I ignore mutation at the A/a locus to trace the fate of a single mutation, whereas at the B/b locus, recurrent mutation is allowed between alleles B and b such that this locus should be under selection-mutation balance. The mutation rate from allele B to allele b is denoted by u and v denotes the reverse mutation rate from allele b to allele B. The frequency of allele B is denoted by p. The fitness of genotypes BB, Bb, and bb is given by $1+s_m$, $1+h_m s_m$, and 1 in males and $1+s_f$, $1+h_f s_f$, and 1 in females, respectively. As I assume allele B is beneficial for allele A, I set $s_m > 0$ and $s_f < 0$ when allele A has a masculinizing effect (Case 1), and $s_m < 0$ and $s_f > 0$ is set when allele A has a feminizing effect (Case 2).

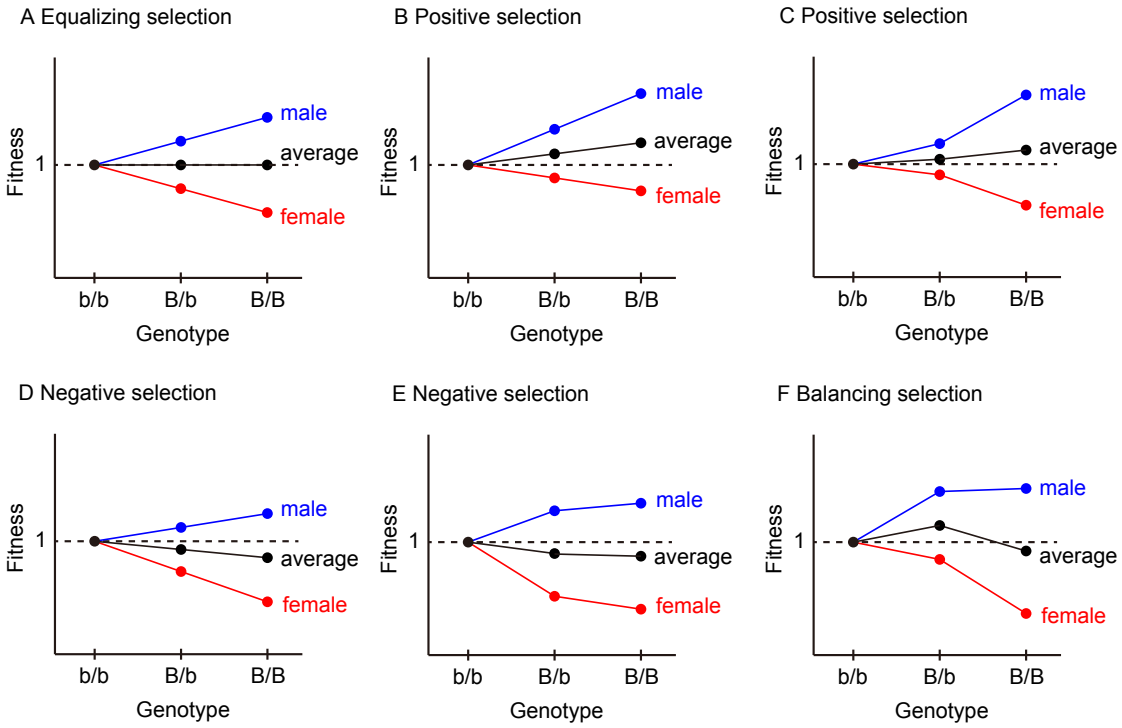

Figure 4.2: Various modes of selection depending on dominance and selection coefficient at the B/b locus when locus X/Y determines sex. The net effect of selection at locus B/b is given by the average of the two sexes. If the dominance and strength of selection are similar in males and females but the directions of selection are opposite, the fitness of allele B equals the fitness of allele b (A). Positive selection works when the average fitness of the three genotypes genotype (shown in black) is in the order of b/b $<$ B/b $<$ B/B (B, C), while negative selection works when the order is b/b $>$ B/b $>$ B/B (D, E). Balancing selection works such that the average fitness is in the following order: b/b $<$ B/b $>$ B/B (F).

4.3 Results

I derive the probability that a single sex-determining mutation at the A/a locus spreads in the population so that the A/a locus becomes the new sex-determining locus and the old X/Y locus becomes monomorphic under the three-locus model illustrated in Figure 4.1A. This probability is essentially identical to the probability that the new sex-determining mutation successfully increases in frequency by avoiding extinction immediately after its introduction, as pointed out by van Doorn and Kirkpatrick (2007, 2010). Once the frequency of the new sex-determining mutation increases, it is very likely that it further increases to an intermediate frequency so that the sex-determining locus transitions from the X/Y locus to the A/a locus. This is because my model assumes that the presence of the B/b sex antagonistic locus provides a benefit only for the new A/a system. In the following, I derive this probability of the successful spread of allele A, which is referred to as the "establishment probability." The "establishment" means that the new system is used by all individuals in the population (i.e., the new system is fixed but alleles A and a coexist stably), rather than the old and new systems coexisting in the population. The establishment probability is derived separately for the two cases (Cases 1 and 2).

4.3.1 Case 1: Turnover without changing the heterogametic sex

I first consider Case 1, where allele A has a masculinizing effect (Figure 4.1B). For allele B to be beneficial for allele A, I assume $s_m > 0$ and $s_f < 0$ in this section. I derive the probability of allele A escaping immediate extinction by using the branching process. Let $\varphi_i(p_0)$ $(i \in \{B, b\})$ be the establishment probability of allele A that arises in linkage with allele i at the B/b locus when the frequency of allele B is p_0. If allele A links with male-beneficial allele B, allele A is favored by linked selection. On the other hand, if allele A links with female-beneficial allele b, allele A is disfavored by linked selection. By denoting the frequencies of haplotypes A-B and A-b by x_B and x_b, respectively, and ignoring second-order terms in s_m, r, u and v, the expected changes of the frequencies of A-B and A-b in one generation are given by

$$\begin{pmatrix} E[\Delta x_B] \\ E[\Delta x_b] \end{pmatrix} = \begin{pmatrix} \alpha(p) - (1-p)r - u & pr + v \\ (1-p)r + u & \beta(p) - pr - v \end{pmatrix} \begin{pmatrix} x_B \\ x_b \end{pmatrix}, \tag{4.1}$$

where $\alpha(p)$ and $\beta(p)$ are functions defined such as $\alpha(p) = h_m s_m + (s_m - 3h_m s_m)p + (2h_m s_m - s_m)p^2$ and $\beta(p) = -h_m s_m p + (2h_m s_m - s_m)p^2$ (for details, see Appendix B). It is interesting to point out that Equation 4.1 involves only selection parameters in males, not those in females. This means that $E[\Delta x_i]$ directly depends on selection among males, but does not necessarily mean that selection does not work in females. Selection in females is involved because it affects p, the frequency of allele B.

In the following, I first derive the establishment probability for a special case where selection at the B/b locus does not provide any systematic pressure on p. In this case, p does not change rapidly, so we can treat it as a constant, at least in the timescale of a newly arisen allele escaping from initial extinction (see Appendix C). With this assumption, we can obtain the establishment probability as a solution of a cubic equation, which is given by a function of p_0, the frequency of allele B when allele A arises. Next, I consider a more general

case where p changes, from the initial value p_0 to the equilibrium value p^*. In this case, by contrast, I show that the establishment probability is given by a function of both p_0 and p^*, of which the effect of p^* is quite large. In either case, I first obtain the establishment probability conditional on p_0, and then I derive the unconditional establishment probability by incorporating the stationary distribution of p_0.

Establishment probability when a constant p can be assumed

I consider a case where we can assume p does not change significantly in the timescale in which I am interested in. In other words, the expected change of p in one generation, $M_p \equiv E[\Delta p]$, is assumed to be as small as $\sim \frac{1}{N}$, where M_p is given by:

$$\begin{aligned} M_p &= \frac{1}{2}\sum_{i\in\{m,f\}} s_i p(1-p)\{h_i + (1-2h_i)p\} - up + v(1-p) \\ &= \Big[\frac{h_f s_f + h_m s_m}{2} + \frac{(1-2h_f)s_f + (1-2h_m)s_m}{2}p\Big]p(1-p) - up + v(1-p), \end{aligned} \tag{4.2}$$

if the second-order terms of s_m, s_f, u, and v are ignored. This assumption holds when $h_m \approx h_f$ and $s_m \approx -s_f$, so that the levels of selection in the two sexes are of the same strength, but work in opposite directions. This mode of selection is referred to as "equalizing selection". I assume that s_m, s_f, u, v, and r are so small that their second-order terms can be ignored. Then, following the branching process approximation (Barton 1987), it is straightforward to show that the two establishment probabilities satisfy:

$$\begin{cases} [\alpha(p) - (1-p)r - u]\varphi_B(p) + [(1-p)r + u]\varphi_b(p) - \dfrac{\varphi_B(p)^2}{2} = 0 \\ [pr + v]\varphi_B(p) + [\beta(p) - pr - v]\varphi_b(p) - \dfrac{\varphi_b(p)^2}{2} = 0 \end{cases} \tag{4.3}$$

(for details, see Appendix C). Notably, similar models were used to analyze the effect of a linked allele on the establishment of locally beneficial alleles (Aeschbacher and Bürger 2014) or the effect of population structure on the establishment of a beneficial mutation (Pollak 1966, Barton 1987, Tomasini and Peischl 2018, Sakamoto and Innan 2019). Equations 4.3 can be reduced to a cubic equation and be solved analytically (for details, see Appendix D). It is important to note that establishment is promoted by selection if $\varphi_B(p)$ is positive; otherwise, allele A is likely selected against and goes extinct. Whether $\varphi_B(p) > 0$ depends on the leading eigenvalue of the matrix in Equation 4.1. When the leading eigenvalue is positive, $\varphi_B(p)$ and $\varphi_b(p)$ are given by:

$$\varphi_B(p) = \begin{cases} \sqrt[3]{-\frac{Q}{2} + \sqrt{R}} + \sqrt[3]{-\frac{Q}{2} - \sqrt{R}} - \frac{A_2}{3} & \text{when } R > 0 \\ 2\sqrt{-\frac{P}{3}}\cos(\frac{1}{3}\arccos(\frac{3Q}{2P}\sqrt{\frac{-3}{P}})) - \frac{A_2}{3} & \text{when } R \le 0 \end{cases}, \tag{4.4}$$

and

$$\varphi_b(p) = \frac{\varphi_B(p)^2 - 2[\alpha(p) - (1-p)r - u]\varphi_B(p)}{2[(1-p)r + u]} \tag{4.5}$$

where

$$
\begin{aligned}
A_0 &= 8[(1-p)r+u][\alpha(p)\beta(p) - (pr+v)\alpha(p) - ((1-p)r+u)\beta(p)] \\
A_1 &= 4[\alpha(p) - (1-p)r - u]^2 - 4((1-p)r+u)[\beta(p) - pr - v] \\
A_2 &= -4[\alpha(p) - (1-p)r - u] \\
P &= A_1 - \frac{A_2^2}{3} \\
Q &= A_0 - \frac{A_1 A_2}{3} + \frac{2}{27}A_2^3 \\
R &= (\frac{P}{3})^3 + (\frac{Q}{2})^2.
\end{aligned}
$$

When r is small, they can be approximated in quite simple equations:

$$
\begin{cases}
\varphi_B \approx 2[\alpha(p) - (1-p)r] \\
\varphi_b \approx 0.
\end{cases}
\tag{4.6}
$$

I performed simple forward simulations in a Wright–Fisher population to check the accuracy of my derivation (for details of the simulations, see Appendix A). I confirmed that Equation 4.3 is in excellent agreement with the simulations for a wide range of the parameters. Some of the results are shown in Figure 4.3, where the two establishment probabilities, $\varphi_B(p_0)$ and $\varphi_b(p_0)$, are plotted by assuming $s_m = -s_f = 0.02, N = 10,000$. Through this work, the mutation rates at locus B/b are fixed to be quite small values, $u = v = 1.0 \times 10^{-6}$, unless otherwise mentioned. Note that the effect of mutation rate is small in the establishment process unless the mutation rate is very large (but the mutation matters when the stationary distribution of allele B is considered, as demonstrated below).

I first focus on the case of $r = 0$, that is, the A/a and B/b loci are completely linked, in order to investigate the effect of dominance (h). Suppose that allele B is recessive ($h = 0$, left panel in Figure 4.3A). Then, a newly arisen allele A can benefit from the B/b locus only when it arises in a BB homozygote. In such a case, φ_B increases as p_0 increases to $p_0 = 0.5$ (plotted in red), where the effect of sexually antagonistic selection is maximized. φ_B decreases as p_0 decreases from 0.5 to 1, making a symmetric function. With the assumption of no recombination, it is obvious that $\varphi_b \approx 0$ for any p_0 (plotted in blue). The weighted average of φ_B and φ_b (i.e., $p_0\varphi_B + (1-p_0)\varphi_b$) is plotted in black.

In contrast, in the dominant case ($h = 1$, left panel in Figure 4.3C), φ_B for a small p_0 is quite high because a newly arisen allele A in linkage with allele B is immediately selected for, regardless of the genotype at the B/b locus. This selection works particularly efficiently when B is so rare that the selective advantage of A-B haplotypes is large in comparison with the population fitness. Therefore, φ_B is given by a monotonically increasing function with decreasing p_0, but as p_0 decreases the probability that allele A arises in linkage with allele B decreases; therefore, the weighted average has a peak in the middle. An intermediate pattern is observed in a case of partial dominance ($h = 0.5$, left panel in Figure 4.3B). Similar results were obtained for other values of selection intensity as long as $s_m = -s_f$ (not shown).

I next consider the effect of recombination. The approximations given by Equation 4.6 agree overall with the simulation results as long as r is small. As the recombination rate increases, φ_B decreases because the association with allele B becomes weaker. When r is

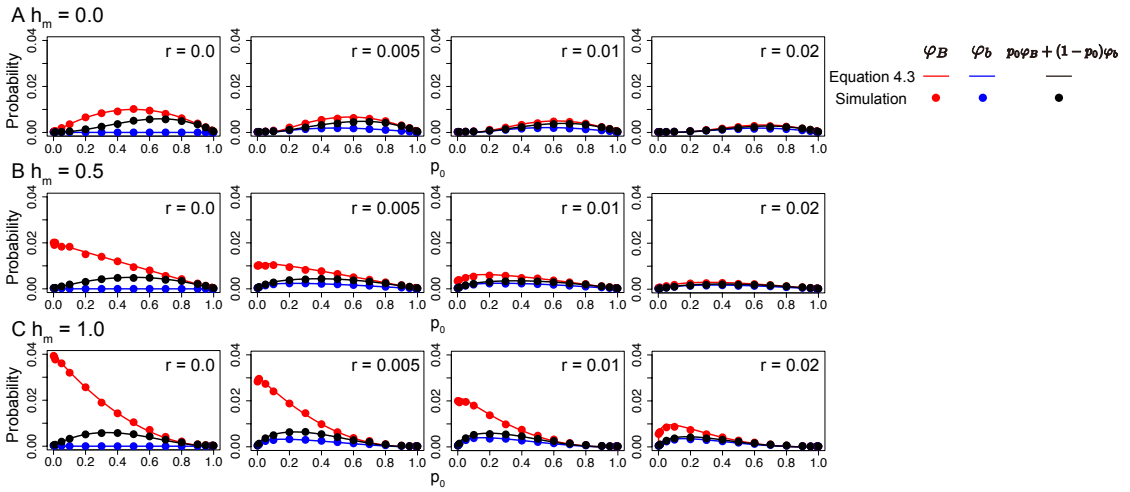

Figure 4.3: Establishment probability of allele A for different dominance and recombination rates. Three dominance coefficients are assumed: (A) $h_m = 0.0$, (B) $h_m = 0.5$ and (C) $h_m = 1.0$. The other parameters are as follows: $s_m = -s_f = 0.02, h_f = h_m, N = 10,000, u = v = 1.0 \times 10^{-6}$. Error bars on the red and blue circles represent the 95 % confidence interval, but they are too small to be seen.

relatively small, φ_b increases as the recombination rate increases because recombination gives a chance to link with allele B and the A-B association may be preserved if further frequent recombination does not break the association. However, this benefit does not hold for a large r, and φ_b decreases as the recombination rate increases because further recombination prevents the stable linkage of allele A and allele B and reduces the benefit of linkage.

Establishment probability when p changes

I next consider the case where p can change during the establishment process due to selection and mutation (i.e., $M_p \gg \frac{1}{N}$). To derive $\varphi_B(p_0)$ and $\varphi_b(p_0)$, I use a continuous time approximation of the branching process (Barton 1995). With a deterministic approximation for M_p ($M_p \neq 0$), the two establishment probabilities satisfy:

$$\begin{cases} [\alpha(p) - (1-p)r - u]\varphi_B(p) + [(1-p)r + u]\varphi_b(p) + M_p \frac{d\varphi_B(p)}{dp} - \frac{\varphi_B(p)^2}{2} = 0 \\ [pr + v]\varphi_B(p) + [\beta(p) - pr - v]\varphi_b(p) + M_p \frac{d\varphi_b(p)}{dp} - \frac{\varphi_b(p)^2}{2} = 0, \end{cases} \tag{4.7}$$

(for details, see Appendix C). This differential equation can be solved numerically by setting an initial condition, for which I use the establishment probability of allele A that arises when p is at stable equilibrium p^*. $\varphi_B(p^*)$ and $\varphi_b(p^*)$ can be numerically computed by Equation 4.3 because we can assume p does not change significantly around p^*. Technically, we cannot use the exact values of $\varphi_B(p^*)$ and $\varphi_b(p^*)$ as an initial condition because they violate the assumption of $M_p \neq 0$. To avoid this problem, assuming a very small ε, I use $\varphi_B(p^* \pm \varepsilon) \approx \varphi_B(p^*)$ and $\varphi_b(p^* \pm \varepsilon) \approx \varphi_b(p^*)$ as an initial condition, which does not markedly affect the numerical solutions as long as ε is small.

When p is not constant, both p_0 and p^* play an important role in determining $\varphi_B(p_0)$ and $\varphi_b(p_0)$. The relative contribution of p^* can be large when selection is strong and p_0 is not far from p^*, so that p quickly approaches p^*. In such a case, $\varphi_B(p_0)$ and $\varphi_b(p_0)$ cannot be large when $\varphi_B(p^*)$ and $\varphi_b(p^*)$ are very small. This argument can be explained as follows. Let us consider the fate of the descendants of an allele A that arises. After the mutation

arises, p changes and finally reaches around p^*. Denote the numbers of haplotypes A-B and A-b when p reaches p^* as X_B and X_b, respectively. Then, the establishment probability is approximately given by:

$$1-\{1-\varphi_B(p^*)\}^{X_B}\{1-\varphi_b(p^*)\}^{X_b} \approx \varphi_B(p^*)X_B+\varphi_b(p^*)X_b, \tag{4.8}$$

unless the population is very small.

Because p^* largely depends on the mode of selection on the B/b locus (see Figure 4.2), I here consider $\varphi_B(p_0)$ and $\varphi_b(p_0)$ under three modes of selection separately (i.e., balancing, negative, and positive selection on allele B). For each mode of selection, I performed extensive forward simulations to check the performance of Equation 4.7. It was found that $\varphi_B(p_0)$ and $\varphi_b(p_0)$ computed by Equation 4.7 well agreed with the simulation results for a wide range of parameter space, and representative cases are shown in Figures 4.4, 4.5 and 4.6 (see also Figures 4.14 and 4.15).

First, I consider the case of balancing selection. To make a realization of balancing selection, it is necessary to set h_m large enough to secure the average fitness of B/b heterozygote higher than 1. When h_m is large, a newly arisen allele A would be immediately selected for together with allele B. Therefore, the overall behavior of $\varphi_B(p_0)$ and $\varphi_b(p_0)$ could be quite similar to that in the case of a high h when p does not change (e.g., Figure 4.3C where $h_m = 1$ is assumed). This is demonstrated in Figure 4.4, where I assume $s_m = 0.02, s_f = -0.02, h_m = 1.0, h_f = 0.0$ (as a consequence, $p^* = 0.5$), while all other parameters are the same as those used in Figure 4.3. To emphasize the difference from the case of a constant p, this figure also shows $\varphi_B(p_0)$ and $\varphi_b(p_0)$ computed by Equation 4.3 for comparison. The major difference from Equation 4.3 is that, when $p_0 < p^*$, $\varphi_B(p_0)$ is lower than that in the case of constant p (the red broken lines in Figure 4.4), because the selective advantage of haplotype A-B would be reduced by the rapid increase in the frequency of allele B by selection (i.e., both haplotypes A-B and a-B increase). $\varphi_b(p_0)$ is overall very low, similar to the case of a constant p (Figure 4.3C). On the other hand, when $p_0 > p^*$, $\varphi_B(p_0)$ is larger than that in the case of constant p because the number of males having allele B decreases, with which haplotype A-B has to compete. Figures 4.14B and C are for weaker selection coefficients ($s_m = -s_f = 0.008$ and 0.002), where $\varphi_B(p_0)$ and $\varphi_b(p_0)$ are overall reduced and the difference from Equation 4.3 is small perhaps because p does not change rapidly with weak selection.

I next consider the case of negative selection, where p would move from p_0 to p^*, which is usually very low. If a very low p^* is assumed, from Equation 4.3, I can approximate $\varphi_B(p^*)$ and $\varphi_b(p^*)$ as:

$$\begin{aligned}\varphi_B(p^*) &\approx \begin{cases} 2(h_m s_m - r) & \text{when } r < h_m s_m \\ 0 & \text{when } r > h_m s_m \end{cases} \\ \varphi_b(p^*) &\approx 0.\end{aligned} \tag{4.9}$$

These equations mean that the establishment of allele A is very unlikely when $r > h_m s_m$. Thus, the major difference from the case of a constant p is that, as the recombination rate increases, the establishment rate decreases to ~ 0 around the threshold $r > h_m s_m$ (see Appendix E for the behavior for large r). This is demonstrated in Figure 4.5, where

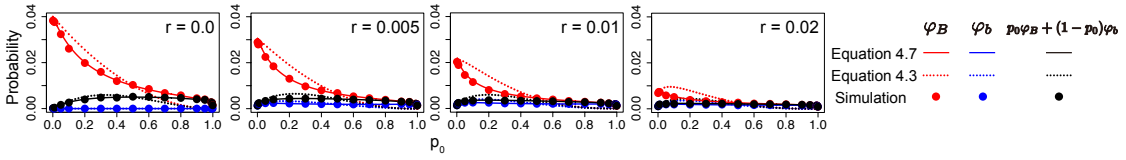

Figure 4.4: Establishment probability for the case of balancing selection on allele B. Parameters are assumed to be $s_m = -s_f = 0.02, h_m = 1.0, h_f = 0.0, N = 10,000, u = v = 1.0 \times 10^{-6}$. Error bars on the red and blue circles represent the 95 % confidence interval, but they are too small to be seen. For full version, see Figure 4.14.

$s_m = 0.02, s_f = -0.04, h_m = h_f = 0.5$ are assumed such that the comparable result for the case of a constant p is Figure 4.3B with the same selection parameters for males (all other parameters are identical). In Figure 4.5, $r = h_m s_m$ holds at $r = 0.01$, which works as the threshold. When r is smaller than this threshold ($r = 0.0$ and 0.005 in Figure 4.5), $\varphi_B(p_0)$ and $\varphi_b(p_0)$ are roughly in agreement with those in Figure 4.3B, although $\varphi_B(p_0)$ and $\varphi_b(p_0)$ are slightly higher than the case of a constant p, especially when p_0 is not small. The situation changes dramatically as the recombination rate exceeds the threshold (i.e., $r = 0.02$ in Figure 4.5): $\varphi_B(p_0)$ and $\varphi_b(p_0)$ decrease to as low as $\sim 2/N$ (i.e., the neutral expectation for a sex-determining allele), where there is no benefit of linked selection and only drift-driven establishment occurs in a nearly neutral fashion. In contrast, in Figure 4.3B, $\varphi_B(p_0), \varphi_b(p_0) \gg 2/N$ unless p_0 is close to 0 or 1. Such strong reduction of $\varphi_B(p_0)$ when r exceeds $h_m s_m$ (Figure 4.5) can be explained as follows. A newly arisen allele A benefits from linked selection when it arises in association with allele B. Once the linkage is broken by recombination, allele A has almost no chance to recombine back to link to allele B because the frequency of allele B is very low. Therefore, after allele A loses linkage with allele B, there would be no selection for allele A so that the establishment of allele A has to rely on random genetic drift. Figures 4.15B and C show the results for weaker selection ($s_m = 0.015$ and 0.008), where the general pattern is similar to that in Figure 4.5, while $\varphi_B(p_0)$ and $\varphi_b(p_0)$ are overall reduced.

I finally consider the case of positive selection, where p^* is generally very large (i.e., ≈ 1). Unless p_0 is small, p increases very quickly to $p^* \approx 1$, that is, the B/b locus is almost fixed for allele B. Therefore, even when allele A arises in association with allele B, allele A does not benefit from linked selection on locus B, resulting in a very low $\varphi_B(p_0)$. Particularly when allele A at $p \approx p^*$, random genetic drift plays a role in the establishment process. The theoretical treatment for this situation is shown in Appendix E. Figure 4.6 shows $\varphi_B(p_0)$ and $\varphi_b(p_0)$ for the case of positive selection assuming $s_m = 0.02, s_f = -0.01, h_m = h_f = 0.5$. It is demonstrated that allele A can spread efficiently with the help of linked selection for allele B only when p_0 is small and r is so small that the initial association between A and B can be maintained for a while. The performance of Equation 4.7 is not as good as that in the cases of balancing selection and negative selection. It appears that Equation 4.7 underestimates the establishment probability because my derivation based on the branching process ignores establishment events occurring in a nearly neutral fashion.

Unconditional establishment probability

In the above, I consider the establishment probability as a function of the initial frequency of allele B, p_0. I am here interested in the unconditional establishment probability, which is the

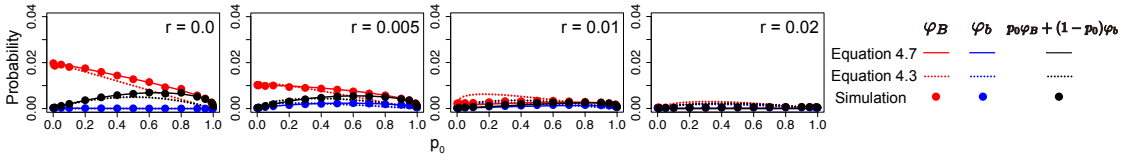

Figure 4.5: Establishment probability for the case of negative selection against allele B. Parameters are assumed to be $s_m = 0.02, s_f = -0.04, h_m = h_f = 0.5$, $N = 10,000$, and $u = v = 1.0 \times 10^{-6}$. Error bars on the red and blue circles represent the 95 % confidence interval, but they are too small to be seen. For full version, see Figure 4.15.

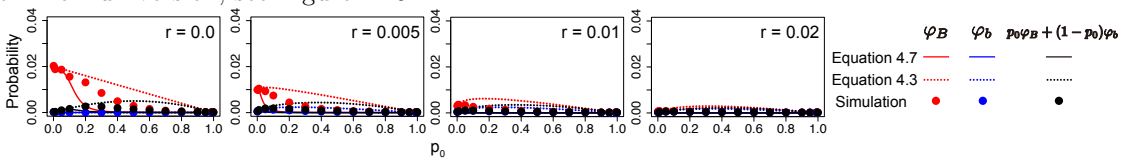

Figure 4.6: Establishment probability for the case of positive selection for allele B. Parameters are assumed to be $s_m = 0.02, s_f = -0.01, h_m = h_f = 0.5$, $N = 10,000$, and $u = v = 1.0 \times 10^{-6}$. Error bars on the red and blue circles represent the 95 % confidence interval, but they are too small to be seen.

weighed average over the stationary distribution of p_0. Following Wright's formula (Wright 1931), the stationary distribution of p_0, $g(p)$, is given by:

$$\begin{aligned} g(p) &= \frac{C}{V_p} \exp\Big(\int \frac{2M_p}{V_p} dp \Big) \\ &= C(1-p)^{4Nu-1} p^{4Nv-1} \exp\big(2N(h_f s_f + h_m s_m)p + N((1-2h_f)s_f + (1-2h_m)s_m)p^2\big). \end{aligned} \tag{4.10}$$

where $V_p = \frac{p(1-p)}{2N}$ and C is determined such that $\int_0^1 g(p) = 1$ (Connallon and Clark 2012). It is well recognized that this formula works very well when the selection intensities, s_f and s_m, are relatively small so that their second-order terms are negligible (Crow and Kimura 1970, Ewens 2004). An intriguing exceptional case is when selection is weak but the absolute values of the selection intensities are not small. In the previous section, I considered a case where selection in males and that in females are well balanced when $h_f \approx h_m$ and $s_f \approx -s_m$, irrespective of the absolute values of s_f and s_m. In such a special case of equalizing selection, the stationary distribution may be better given by:

$$g(p) = C(1-p)^{4Nu-1} p^{4Nv-1} \exp\Big(\big(-(1-2h_f)^2 p^4 - 4h_f(1-2h_f)p^3 - 4h_f^2 p^2\big) N s_f^2 \Big). \tag{4.11}$$

Then, the unconditional establishment probability of allele A, φ, is given by:

$$\varphi = \int_0^1 g(p)[p\varphi_B(p) + (1-p)\varphi_b(p)]dp, \tag{4.12}$$

where $\varphi_B(p)$ and $\varphi_b(p)$ are given by Equation 4.3 for $h_f \approx h_m$ and $s_f \approx -s_m$, and otherwise by Equation 4.7.

We can obtain an approximation of the establishment probability in a simple form for several special cases of $r = 0$. When sexually antagonistic selection works as balancing

selection, the establishment probability for $r = 0$ is approximated by:

$$\begin{aligned}\varphi &\approx 2p^*\alpha(p^*) \\ &\approx 2p^*[h_m s_m + (s_m - 3h_m s_m)p^* + (2h_m s_m - s_m){p^*}^2].\end{aligned} \tag{4.13}$$

It is implied that φ is on the same order of magnitude as s_m.

In the case of negative selection, assuming that selection is much stronger than mutation (u and v) and h_m is not very small, we have $p^* \approx 0$ and $\varphi \sim \varphi_b(0)$. Furthermore, because $\varphi_B(p) \gg \varphi_b(p)$ and $M_p \approx 0$, Equation 4.7 for $r = 0$ is roughly simplified:

$$\begin{aligned}\alpha(0)\varphi_B(0) &= \frac{\varphi_B(0)^2}{2} \\ v\varphi_B(0) &= \frac{\varphi_b(0)^2}{2}.\end{aligned}$$

Under these approximations, φ is given by

$$\varphi \approx \sqrt{4vh_m s_m}, \tag{4.14}$$

indicating that φ is on the order of $\sqrt{vh_m s_m}$. For selection to be dominant over random genetic drift, $N^2 vh_m s_m \gg 1$ is required.

If sexually antagonistic selection works as positive selection and the mutation rate is low, linked selection no longer works and establishment is driven by random genetic drift, as discussed above. Then, the establishment probability is roughly given by $\frac{2}{N}$. In such cases, sexually antagonistic selection does not markedly increase the establishment probability.

The unconditional establishment probability computed by Equation 4.12 is plotted for the four modes of sexually antagonistic selection in Figure 4.7. The approximations for $r = 0$ (Equations 4.13, 4.14) are also presented by triangles on the y-axis, which show excellent agreement with the exact formula and simulation results. Three different values of the mutation rate are considered ($u = v = 10^{-5}, 10^{-6}, 10^{-7}$).

The establishment probability is in general highest when balancing selection works (Figure 4.7A). This is because an intermediate p provides both the benefit of linkage and a higher chance to link with allele B to allele A. Because the mutation rate at locus B/b does not markedly influence the stationary distribution of p, the establishment probability does not depend on the mutation rate either.

When negative selection works at locus B, the establishment probability is quite low (Figure 4.7B) because negative selection keeps allele B very rare. Mutation from allele b to B contributes to the establishment of allele A in two ways. First, it increases the frequency of beneficial allele B, resulting in a higher chance that allele A acquires linkage with allele B by recombination. Second, it increases the probability that haplotype A-b mutates to A-B. As a consequence, as the mutation rate v increases, the establishment probability becomes larger.

When positive selection works, the establishment probability is very low for all three mutation rates (Figure 4.7C). This is because allele B is already fixed and linkage with allele B is no longer beneficial. Allele A may benefit from linked selection only when u is extremely high.

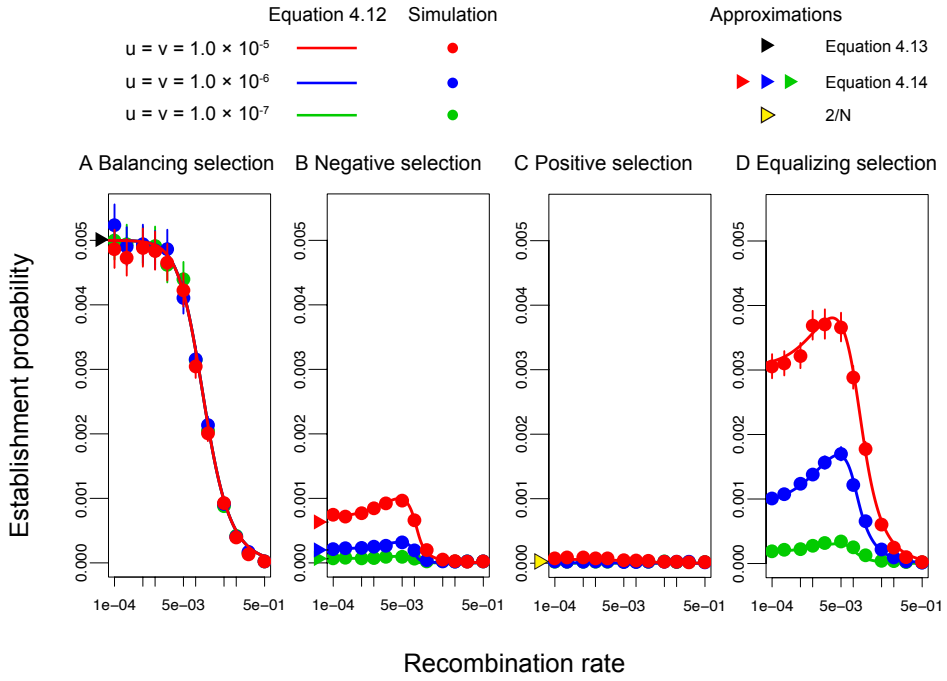

Figure 4.7: Establishment probability of a masculinizing allele for different modes of sexually antagonistic selection. $N = 100,000$ and $u = v$ are assumed. Other parameters are (A) $s_m = 0.02, s_f = -0.02, h_m = 1.0, h_f = 0.0$, (B) $s_m = 0.02, s_f = -0.025, h_m = h_f = 0.5$, (C) $s_m = 0.02, s_f = -0.01, h_m = h_f = 0.5$ and (D) $s_m = 0.02, s_f = -0.02, h_m = h_f = 0.5$. Similar results were obtained for $N = 10,000$. Error bars for circles represent the 95 % confidence interval.

Thus, if selection is directional, p^* is very low or high (under negative or positive selection, respectively), which does not markedly help the establishment of allele A. On the other hand, if balancing selection maintains alleles B and b in an intermediate frequency, allele A can take advantage of it. An intermediate situation is when equalizing selection works ((Figure 4.7D), where the process is nearly neutral because $s_f \approx -s_m$ and $h_f \approx h_m$). Because p fluctuates between 0 and 1 by random genetic drift, allele A can likely benefit from locus B/b if it arises when p is intermediate. This is why the establishment probability is largely affected by the mutation rate at locus B/b, which determines how often mutation is produced.

It is interesting to note that very tight linkage does not necessarily increase the unconditional establishment probability (e.g., Figures 4.7B, D). With an increasing the recombination rate, in general, φ_b increases while φ_B decreases because recombination enhances exchange between haplotype A-B and haplotype A-b. Because the unconditional probability is given by the weighted average of φ_B and φ_b, there appears to be an optimal recombination rate to maximize φ.

The pattern of neutral polymorphism after turnover

To investigate the effect of the mode of selection at locus B/b on the pattern of neutral polymorphism in a surrounding region, I performed forward simulations under the infinite-sites model. The spatial distributions of the nucleotide diversity after turnover in a typical run are plotted for each of the four modes of selection in Figure 4.8. The amount of nucleotide variation is measured by the average pairwise differences (π) standardized by the neutral expectation ($\theta = 4N\mu$ where μ is the neutral mutation rate). Haplotype i ($i \in$ {A, a}) is denoted as the haplotype with allele i, and Figure 4.8 plots three π values: π_{A-A} for π within haplotype A (red line); π_{a-a} for π within haplotype a (blue line); and π_{A-a} for π

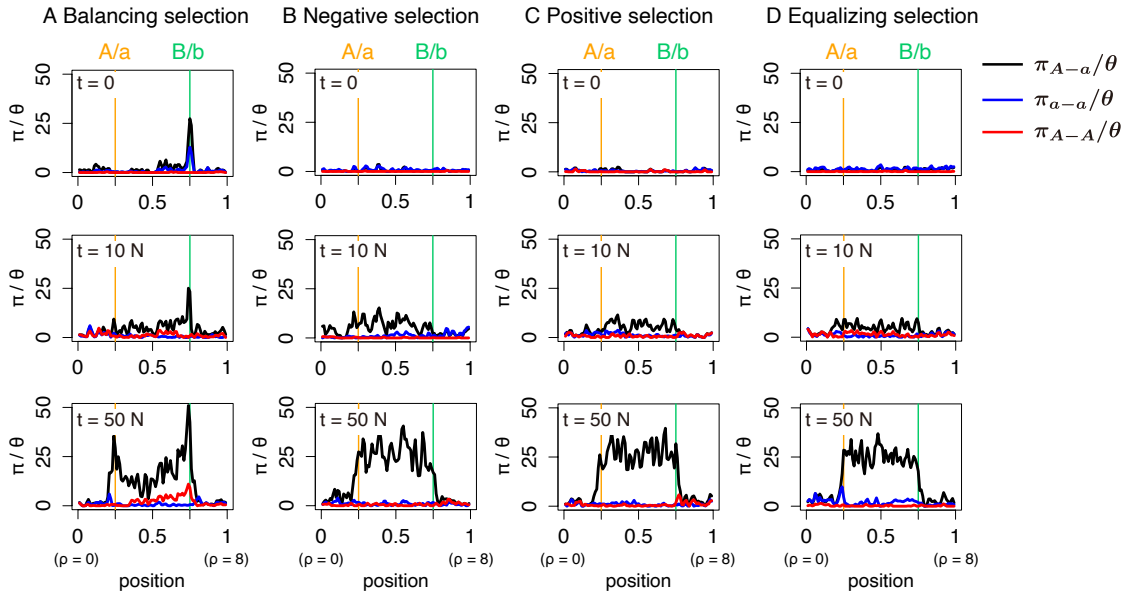

Figure 4.8: The temporal dynamics of nucleotide diversity after turnover of the sex-determining locus. Results for a single simulation run with $N = 10,000$ are shown for each mode of selection. The spacial distributions of the normalized π_{A-A}, π_{a-a} and π_{A-a} are shown in red, blue, and black, respectively, along the relative position in the (0,1) interval (also rescaled in units of $4Nr$ in parentheses). In the simulation, locus A/a is located at relative position 0.25 (vertical orange lines) in the (0,1) simulated region, while locus B/b is located at relative position 0.75 (vertical green lines). t is denoted as the number of generations since the new sex-determination system was fixed (i.e., since the old sex-determining locus X/Y became monomorphic). The recombination rate of the entire region was assumed to be 0.0002 such that the recombination rate between loci A/a and B/b = 0.0001. The selection parameters used for each mode of selection were (A) $s_m = -s_f = 0.02, h_m = 1.0, h_f = 0.0$, (B) $s_m = 0.02, s_f = -0.04, h_m = h_f = 0.5$, (C) $s_m = 0.025, s_f = -0.02, h_m = h_f = 0.5$ and (D) $s_m = -s_f = 0.02, h_m = h_f = 0.5$.

between haplotypes A and a (black line). Let us first focus on the case of $t = 0$ (i.e., just after the turnover has completed). When balancing selection works, π_{A-a} has a striking peak around the locus B/b (Figure 4.8A), and a weaker peak is observed for π_{A-A} and π_{a-a} due to recombination between the two loci. This is because the B/b polymorphism had been maintained for a very long time by balancing selection before the turnover occurred, which is not observed in the other modes of selection (Figures 4.8B-D).

As time passes, in all four cases, neutral mutations start to accumulate around the A/a locus, making a novel peak of divergence between haplotypes A and a (i.e., π_{A-a}). The growth of the peak at the A/a locus proceeds while maintaining the peak at the B/b locus in the case of balancing selection (Figure 4.8A). The pattern is as predicted by Kirkpatrick and Guerrero (2014). In contrast, in the other three cases (Figures 4.8B-D), a peak newly arises at the B/b locus and grows along with the peak at the A/a locus. Thus, the patterns are similar in the cases of negative, positive and equalizing selection, whereas balancing selection is unique in that the peak at the B/b locus already exists, which is much higher than that at the A/a locus shortly after the turnover.

4.3.2 Case 2: Turnover with changing heterogametic sex

I next consider Case 2, where allele A has a feminizing effect so that the heterogametic sex changes from male to female. That is, Case 2 assumes $s_f > 0$ for allele B to be beneficial for allele A. As in Case 1, allele A can spread if allele A successfully avoids extinction shortly

after it arises (van Doorn and Kirkpatrick 2010). Therefore, I again use the approximation of the branching process, following Case 1. By ignoring the second-order terms in s_f, r, u, and v, the expected change of the frequency in one generation is given by:

$$\begin{pmatrix} E[\Delta x_B] \\ E[\Delta x_b] \end{pmatrix} = \begin{pmatrix} \alpha(p) - (1-p)r - u & pr + v \\ (1-p)r + u & \beta(p) - pr - v \end{pmatrix} \begin{pmatrix} x_B \\ x_b \end{pmatrix}, \tag{4.15}$$

where $\alpha(p) = h_f s_f + (s_f - 3h_f s_f)p + (2h_f s_f - s_f)p^2$ and $\beta(p) = -h_f s_f p + (2h_f s_f - s_f)p^2$ (see Appendix B for details).

By comparing Equation 4.15 with Equation 4.1, I notice that the two equations are identical if we replace h_f by h_m and s_f by s_m. It is indicated that the above arguments for Case 1 are also applicable to Case 2 by changing these variables. When equalizing selection works and p does not change rapidly (i.e., $h_m \approx h_f$ and $s_m \approx -s_f$), the establishment probability is given by Equation 4.3. On the other hand, when p changes when allele A is rare, the establishment probability depends on both p_0 and stable equilibrium p^*. If balancing selection works, the establishment probability is given by Equation 4.7. When allele B is subject to negative selection, the establishment probability depends on whether r is larger or smaller than the threshold that is given by $h_f s_f$. When $h_f s_f > r$, the establishment probability is given by Equation 4.7. Whereas, when $h_f s_f < r$, $\varphi_B(p^*) \approx 0$ so that the establishment of allele A would be drift-driven once p reaches p^*: therefore, $\varphi_B(p_0)$ could be as small as $\sim 1/N$. When allele B is subject to positive selection, we have $\varphi_B(p^*) \approx 0$. Consequently, the establishment process is driven by random genetic drift after p reaches p^*. Therefore, as long as p_0 is near p^* and positive selection is strong, the establishment probability is as low as $\sim 1/N$ (for more details, see Appendix E). Thus, the process in Case 2 can be well described by the equations developed for Case 1, as is demonstrated in Figures 4.16-4.19. The unconditional establishment probability is also given by Equation 4.12 (see Figure 4.20).

4.4 Discussion

In some clades such as teleost fish and amphibians, sex is often determined by a single locus rather than heteromorphic sex chromosomes. In such species, turnover of the sex-determining locus occurs so frequently that genetic divergence around the locus does not proceed. There are many factors that potentially promote the turnover of sex-determining loci, such as random genetic drift (Bull and Charnov 1977, Veller *et al.* 2017, Saunders *et al.* 2018), deleterious mutation load (Blaser *et al.* 2013, 2014), sexually antagonistic selection (van Doorn and Kirkpatrick 2007, 2010), sex ratio bias (Kozielska *et al.* 2010) and haploid selection (Scott *et al.* 2018). Recently, van Doorn and Kirkpatrick (2007, 2010) pointed out that turnover of sex-determining loci could be enhanced by linked selection. That is, a new sex-determining allele (allele A in my model) can be beneficial when it arises near a locus under sexually antagonistic selection (locus B/b). This study is aimed at understanding how often turnover of sex-determining loci occurs with the help of linked selection at a nearby locus. Previous studies mainly by van Doorn and Kirkpatrick (2007, 2010) focused on the deterministic phase to obtain the rate of increase in the frequency of allele A, which is not sufficient to address the question on the rate of turnover, as mentioned in the Introduction. I

here provide a full theoretical description of the behavior of allele A from when it newly arises to its establishment, where both the initial stochastic and following deterministic phases are taken into account. I provide some technical comments in Appendix F to provide intuitive insights on how to understand the results of van Doorn and Kirkpatrick (2007, 2010) in my framework.

My theory shows that the establishment probability is given by a function of the initial frequency of allele B, p_0, and the equilibrium frequency, p^*. It is demonstrated that the establishment probability largely depends on the mode of selection on allele B, which determines p^* (Figure 4.7). The establishment probability is relatively high when balancing or equalizing selection works because polymorphism at locus B/b increases the benefit of linkage. In contrast, when directional selection works (either positive or negative), linked selection does not significantly help establishment. When negative selection works, the establishment probability is low because the frequency of allele B is so low that allele A has difficulty linking with it. When positive selection works, the establishment probability is also low because beneficial allele B should be almost fixed. The effect of p_0 appears to be smaller unless p_0 is very different from p^*.

My results demonstrate that the fate of newly arisen sex-determining mutation is mainly determined in the early phases (i.e., stochastic phase), where random genetic drift is the major evolutionary force. It is indicated that the stochastic phase plays an important role in understanding the evolutionary process of turnover of sex-determining loci. In the stochastic phase, p_0 is a very important factor affecting the initial behavior of the new mutation, and the density distribution of p_0 largely depends on the mode of selection at the B/b locus. The establishment probability of allele A is very low when directional selection works at the B/b locus, indicating that the presence of loci under sexually antagonistic selection could significantly enhance turnover of sex-determining loci only when sexually antagonistic selection works in the form of balancing selection.

My theory has great implications for the rate of turnover of sex-determining loci in natural populations. An important biological question is how sexually antagonistic loci help the turnover of sex-determining loci on the genomic scale. One might think that most turnover occurs with the help of sexually antagonistic loci under balancing selection, because the establishment probability is markedly high when balancing selection works at the B/b locus (see also van Doorn and Kirkpatrick 2007, 2010). On one hand, one might consider that there may not be a large number of sexually antagonistic loci under balancing selection in a genome, so that their relative contribution might be small. Alternatively, there might be a negligible contribution of sexually antagonistic loci under other modes of selection (i.e., equalizing and directional selection). Even if the establishment probability is not high for each, on a genomic scale, their cumulative effect may not be small. To answer the question on the relative contribution of linked selection, we need to know how many sexually antagonistic loci exist in the genome, and what mode of selection is working. While empirical studies may be powerful to address this, it is also interesting to look at polymorphism data surrounding the sex-determining locus. My simulations (Figure 4.8) provide insight into how to distinguish the mode of selection at a linked locus. Shortly after turnover, if divergence between male and female haplotypes is restricted in a very narrow region around the sex-determining locus, it may be likely that the sex-determining allele has become established with no help from

linked selection (i.e., Myosho *et al.* (2012), Kamiya *et al.* (2012), Koyama *et al.* (2019)). On the other hand, if a highly diverged region spreads surrounding the sex-determining locus, then either the sex-determining allele has become established together with a linked allele at a sexually antagonistic locus, or sexually antagonistic loci arose after the establishment of the sex-determining locus.

4.5 Appendices

Appendix A: Details of simulation model

The details of the simulation model are presented. The life cycle is assumed to be in the order of mating (random genetic drift), selection, gamete production (recombination) and mutation.

First, the details of simulations for establishment probabilities are provided. Let s_{ijk} and e_{ijk} be the frequency of genotype ijk among sperm and egg population at the beginning of the generation, respectively, where $i \in \{\mathrm{A}, \mathrm{a}\}$, $j \in \{\mathrm{B}, \mathrm{b}\}$ and $k \in \{\mathrm{X}, \mathrm{Y}\}$. In a mating step, N individuals are produced by random mating. Denote by $f_0(ijk/lmn)$ the frequency of zygotes between a sperm of genotype ijk and an egg of genotype lmn. $E[f_0(ijk/lmn)]$ is given by $s_{ijk}e_{lmn}$. According to this probability, N zygotes are produced by multinomial sampling. Then, sex is determined by a combination of loci A/a and X/Y (see Figure 4.1B and C).

During the selection step, fitness of each genotype is determined by locus B/b. Let F be a set of genotypes that grow into a female. The fitness of genotype $X = ijk/lmn$, $W(X)$, is given by

$$W(X) = \begin{cases} 1 & \text{if } (j,m) = (b,b) \\ 1 + h_f s_f & \text{if } (j,m) = (B,b) \text{ or } (b,B) \\ 1 + s_f & \text{if } (j,m) = (B,B), \end{cases} \tag{4.16}$$

for females (i.e., $X \in F$) and

$$W(X) = \begin{cases} 1 & \text{if } (j,m) = (b,b) \\ 1 + h_m s_m & \text{if } (j,m) = (B,b) \text{ or } (b,B) \\ 1 + s_m & \text{if } (j,m) = (B,B), \end{cases} \tag{4.17}$$

for males (i.e., $X \notin F$). For $X \in F$, the genotype frequency among female population, $f_1^f(X)$, is

$$f_1^f(X) = \frac{f_0(X)W(X)}{\sum_{Y \in F} f_0(Y)W(Y)}. \tag{4.18}$$

For $X \notin F$, the genotype frequency among male population, $f_1^m(X)$, is

$$f_1^m(X) = \frac{f_0(X)W(X)}{\sum_{Y \notin F} f_0(Y)W(Y)}. \tag{4.19}$$

In gamete production, genotype ijk/lmn produce 8 kinds of gametes, ijk, ijn, imk, imn, ljk, ljn, lmk and lmn, with proportion $\frac{1-r}{4}$, $\frac{1-r}{4}$, $\frac{r}{4}$, $\frac{r}{4}$, $\frac{r}{4}$, $\frac{r}{4}$, $\frac{1-r}{4}$ and $\frac{1-r}{4}$, respectively. After that, proportion u of allele B mutates to allele b while proportion v of allele b mutates to

allele B. Then, the frequency s_{ijk} and e_{ijk} at the beginning of the next generation is defined.

Initial condition of simulations are determined as follows. In simulations for conditional probability, initial frequency of each gamete is set as

$$s_{ijk} = \begin{cases} \frac{1-p_0}{2} & \text{if } (i,j,k) = \text{(a, b, X) or (a, b, Y)} \\ \frac{p_0}{2} & \text{if } (i,j,k) = \text{(a, B, X) or (a, B, Y)} \\ 0 & \text{otherwise,} \end{cases} \tag{4.20}$$

and

$$e_{ijk} = \begin{cases} 1-p_0 & \text{if } (i,j,k) = \text{(a, b, X)} \\ p_0 & \text{if } (i,j,k) = \text{(a, B, X)} \\ 0 & \text{otherwise.} \end{cases} \tag{4.21}$$

After the mating step of first generation, an allele A is introduced. To investigate the fate of allele A arising in linkage with allele i ($i \in \{\text{B, b}\}$), an allele i is randomly chosen and the linked allele a is changed into allele A. The simulation is run until either locus X/Y or locus A/a becomes monomorphic. In simulations for unconditional probability, I first run simulations without introducing allele A to obtain stationary distribution of $s_{\text{a}jk}$ and $e_{\text{a}jk}$. After a burn-in period of $10N$ generations, $s_{\text{a}jk}$ and $e_{\text{a}jk}$ are sampled. For each set of $s_{\text{a}jk}$ and $e_{\text{a}jk}$, an allele a is randomly chosen and turned into allele A after the mating step of first generation. The simulation is run until either locus X/Y or locus A/a becomes monomorphic.

Next, the details of simulations for the pattern of neutral polymorphism are provided. A genomic region of relative length 1 is simulated where the locus A/a is located at relative position 0.25 and the locus B/b is located at relative position 0.75. For neutral sites, the infinite-sites model is assumed. Although the basic assumptions are the same as the three loci model, implements are slightly different to improve efficiency of simulations such that all events are incorporated into the mating step.

In a mating step, a father and a mother are chosen from individuals in previous generation to form an offspring. To incorporate selection, the probability that an individual is chosen as a parent is proportional to its relative fitness among individuals of the same sex. For each parent, a haplotype is made through recombination where a constant rate of recombination across the simulated region is assumed. By combining two haplotypes, an offspring is formed. Mutation is finally introduced in both the locus B/b and neutral sites. These procedures are repeated N times to generate individuals of the present generation.

The dynamics of polymorphism are simulated as follows. First, to simulate the polymorphism just before turnover, I run simulations for $200N$ generations without introducing allele A. Then, allele A is introduced at the locus A/a. If turnover occurs, simulation continues until $50N$ generations pass since the turnover.

Appendix B: Derivation of Equations 4.1 and 4.15

The details for the derivation of Equations 4.1 and 4.15 are provided. First, Equation 4.1 is derived. I here focus on deterministic changes of allele frequency while allele A is rare and ignore stochastic changes. At the beginning of each generation, the frequencies of haplotypes A-B and A-b in the sperm population are assumed to be x_B and x_b, respectively. Because

locus B/b is not on the ancestral sex chromosome, I assume that the frequencies of allele B in the two sexes are almost same. By denoting the frequency of genotype i after random mating as $f_0(i)$, the frequencies of four genotypes are given by

$$\begin{aligned} f_0(\text{A-B/a-B}) &= x_B p \\ f_0(\text{A-B/a-b}) &= x_B(1-p) \\ f_0(\text{A-b/a-B}) &= x_b p \\ f_0(\text{A-b/a-b}) &= x_b(1-p). \end{aligned} \tag{4.22}$$

Since allele A has a masculinizing effect, the above genotypes are all male. During allele A is rare, the effect of mutants on the average fitness can be ignored. Then, the average fitness of males is $\bar{w}_m = 1 + s_m p^2 + 2h_m s_m p(1-p)$. The frequency of genotype i after selection, $f_1(i)$, is given by

$$\begin{aligned} f_1(\text{A-B/a-B}) &= \frac{1+s_m}{\bar{w}_m} f_0(\text{A-B/a-B}) \\ f_1(\text{A-B/a-b}) &= \frac{1+h_m s_m}{\bar{w}_m} f_0(\text{A-B/a-b}) \\ f_1(\text{A-b/a-B}) &= \frac{1+h_m s_m}{\bar{w}_m} f_0(\text{A-b/a-B}) \\ f_1(\text{A-b/a-b}) &= \frac{1}{\bar{w}_m} f_0(\text{A-b/a-b}). \end{aligned} \tag{4.23}$$

Note that a half of the population is male. Then, the haplotype frequencies after recombination among the sperm population, x'_B and x'_b, are given by

$$\begin{aligned} x'_B &= f_1(\text{A-B/a-B}) + (1-r) f_1(\text{A-B/a-b}) + r f_1(\text{A-b/a-B}) \\ x'_b &= r f_1(\text{A-B/a-b}) + (1-r) f_1(\text{A-b/a-B}) + f_1(\text{A-b/a-b}). \end{aligned} \tag{4.24}$$

After mutation at locus B/b, the frequency changes in one generation are given by

$$\begin{aligned} \Delta x_B &= (1-u)x'_B + v x'_b - x_B \\ \Delta x_b &= u x'_B + (1-v) x'_b - x_b. \end{aligned} \tag{4.25}$$

By ignoring the second order terms of s_m, r, u and v, Equation 4.25 is reduced to Equation 4.1.

For Equation 4.15, the above derivations are also valid if $\bar{w}_m, h_m$, and s_m are substituted by $\bar{w}_f, h_f$, and s_f, because I assumed that allele A has a strong feminizing effect such that genotype XYAa grows up into females. It is obvious from the derivation that Equation 4.15 takes the same form as Equation 4.1.

Appendix C: Branching process approximations

The derivation for Equations 4.3 and 4.7 are provided. Each evolutionary force is assumed to be relatively weak such that s_m, s_f, r, u, and v are at most the order of magnitude $\varepsilon \ll 1$. Denote by $\lambda(p)$ the leading eigenvalue of the matrix in Equation 4.1. I also assume that $\lambda(p) \gg \frac{1}{N}$ such that allele A increases deterministically once its frequency becomes large. Note that $\varepsilon \gg \frac{1}{N}$ is required for $\lambda(p) \gg \frac{1}{N}$.

To derive the establishment probability, I focus on descendants of an allele A after one

generation. Let a random variable ξ_i^j be the number of offsprings of haplotype A-j that is left by a haplotype A-i ($i, j \in \{\mathrm{B}, \mathrm{b}\}$). Because I assume that allele A is rare, each ξ_i^j can be treated as independent and the probability distribution of ξ_i^j may be approximated by Poisson distribution. Then, the probability generating functions of the number of offspring are given by

$$\begin{aligned} E_\xi[x^{\xi_B^b} y^{\xi_B^B}] &= e^{((1-p)r+u))(x-1)} e^{(1+\alpha(p)-(1-p)r-u))(y-1)} \\ E_\xi[x^{\xi_b^b} y^{\xi_b^B}] &= e^{(1+\beta(p)-pr-v)(x-1)} e^{(pr+v)(y-1)}, \end{aligned} \tag{4.26}$$

where terms of $\mathcal{O}(\varepsilon^2)$ are ignored in the exponent and x and y are indeterminates. Let Δp be the change of p in one generation. Then, establishment probabilities, φ_B and φ_b, satisfy following equation:

$$\begin{aligned} 1-\varphi_B(p) &= E_{\Delta p}\Big[E_\xi\Big[\big(1-\varphi_b(p+\Delta p)\big)^{\xi_B^b}\big(1-\varphi_B(p+\Delta p)\big)^{\xi_B^B}|\Delta p\Big]\Big] \\ &= E_{\Delta p}\Big[e^{-((1-p)r+u))\varphi_b(p+\Delta p)} e^{-(1+\alpha(p)-(1-p)r-u))\varphi_B(p+\Delta p)}\Big] \\ 1-\varphi_b(p) &= E_{\Delta p}\Big[E_\xi\Big[\big(1-\varphi_b(p+\Delta p)\big)^{\xi_b^b}\big(1-\varphi_B(p+\Delta p)\big)^{\xi_b^B}|\Delta p\Big]\Big] \\ &= E_{\Delta p}\Big[e^{-(1+\beta(p)-pr-v)\varphi_b(p+\Delta p)} e^{-(pr+v)\varphi_B(p+\Delta p)}\Big]. \end{aligned} \tag{4.27}$$

Assume that $\varphi_B(p)$, $\varphi_b(p)$ are the order of ε. Then, Equation 4.27 is expanded as

$$\begin{aligned} [(1-p)r+u]E_{\Delta p}[\varphi_b(p+\Delta p)] + [1+\alpha(p)-(1-p)r-u]E_{\Delta p}[\varphi_B(p+\Delta p)] - \varphi_B(p) - \frac{1}{2}E_{\Delta p}[\varphi_B(p+\Delta p)^2] = \mathcal{O}(\varepsilon^3) \\ [1+\beta(p)-pr-v]E_{\Delta p}[\varphi_b(p+\Delta p)] + [pr+v]E_{\Delta p}[\varphi_B(p+\Delta p)] - \varphi_b(p) - \frac{1}{2}E_{\Delta p}[\varphi_b(p+\Delta p)^2] = \mathcal{O}(\varepsilon^3) \end{aligned} \tag{4.28}$$

Noting that evolutionary forces are so weak that the frequency of allele B changes slowly, $E_{\Delta p}[\varphi_i(p+\Delta p)]$ and $E_{\Delta p}[\varphi_i(p+\Delta p)^2]$ can be approximated by

$$\begin{aligned} E_{\Delta p}[\varphi_i(p+\Delta p)] &\approx E_{\Delta p}\Big[\varphi_i(p) + \Delta p\frac{d\varphi_i(p)}{dp} + \frac{(\Delta p)^2}{2}\frac{d^2\varphi_i(p)}{dp^2} + \cdots\Big] \\ &= \varphi_i(p) + M_p\frac{d\varphi_i(p)}{dp} + \mathcal{O}(\frac{\varepsilon}{N}), \\ E_{\Delta p}[\varphi_i(p+\Delta p)^2] &\approx E_{\Delta p}\Big[\varphi_i(p)^2 + 2\Delta p\varphi_i(p)\frac{d\varphi_i(p)}{dp} + \cdots\Big] \\ &= \varphi_i(p)^2 + \mathcal{O}(\varepsilon^3). \end{aligned} \tag{4.29}$$

Recall that $\varepsilon \gg \frac{1}{N}$ is assumed such that $\lambda(p) \gg \frac{1}{N}$ is satisfied. By substituting Equation 4.29 into Equation 4.28 and taking terms up to ε^2, Equation 4.7 is derived. By assuming M_p is negligible (i.e., $\sim \frac{1}{N}$), Equation 4.3 is also derived.

The scope and the limitation of the approximation are discussed. Equation 4.3 and 4.7 are accurate if terms of order $\frac{1}{N}$ are ignored, as long as $\lambda(p) \gg \frac{1}{N}$. Noting that $\varphi_i(p) \sim \frac{1}{N}$ when $\lambda(p) \sim \frac{1}{N}$, they are generally accurate if the order of $\frac{1}{N}$ can be ignored. Since such small terms can be ignored in many cases, my approximations may be valid in broad situations.

However, there are exceptional situations, for which terms of order $\frac{1}{N}$ become too large to be ignored. Such situations occur when $\lambda(p) \sim \frac{1}{N}$ when $p \approx p^*$ while $\lambda(p) \gg \frac{1}{N}$ otherwise. Typical situations are that negative selection works on allele B and r is large, or positive

selection works. In such cases, it is probable that the number of allele A may increase $\sim N$ before p reaches p^*, especially in small populations. Although $\varphi_i(p)$ are still proportional to $\frac{1}{N}$, the absolute value of establishment probability may become large. For the details of these cases, see Appendix E.

Appendix D: Explicit solution for Equation 4.3

The details for the derivation of Equations 4.4 and 4.5 are provided. The first equation of Equation 4.3 is rearranged to Equation 4.5. By substituting Equation 4.5 into the second equation of Equation 4.3, a quartic equation can be obtained:

$$\varphi_B(p)\Big[\varphi_B(p)^3 + A_2\varphi_B(p)^2 + A_1\varphi_B(p) + A_0\Big] = 0, \tag{4.30}$$

where A_i are defined in the main text. The largest real root of the Equation 4.30 is the biologically relevant solution (see also Sakamoto and Innan (2019)). The root is expressed by Equation 4.4 (see Abramowitz and Stegun 1970, Oldham *et al.* 2010).

Appendix E: Establishment probability when linked selection is very weak at $p \approx p^*$

I describe the behavior of the establishment probability when linked selection is very weak at $p \approx p^*$. This is a typical situation when negative selection works against allele B and r is large, or positive selection works for allele B, so that the establishment probability is very small (unless p_0 is very different from p^*). I here explore such a case in detail because Equation 4.7 could underestimate the establishment probability (see Figures 4.5 and 4.6). This is because my derivation based on the branching process approximation ignores establishment events occurring in a nearly neutral fashion. In this Appendix, I derive another approximation focusing on the establishment of allele A through a nearly neutral fashion. It is assumed that selection is strong and p_0 is close to p^*.

First, I consider Case 1 (i.e., the turnover without changing heterogametic sex) and negative selection on allele B is assumed. For linked selection to be very weak at $p \approx p^*$, $r > h_m s_m$ is also assumed (see Equation 4.9). Under this condition, the establishment process does not occur simply by increasing the frequency of haplotype A-B: rather, because frequent recombination keeps breaking the linkage between alleles A and B, allele A has to increase without increasing allele B. In practice, negative selection works to reduce the frequency of allele B and allele b is almost fixed. Therefore, establishment occurs such that haplotype A-b increases. In this case, haplotype A-b is selectively neutral, so that I can derive an approximation of the establishment probability by following Equation 4.8. By using $\varphi_b(p^*) \approx \frac{2}{N}$, where $\frac{2}{N}$ is the establishment probability of a neutral masculinizing allele, the establishment probability is approximated by

$$\frac{2}{N} \times E(X_b) \tag{4.31}$$

where X_b is the number of haplotype A-b when p reaches p^*. We can calculate $E(X_b)$ numerically under the branching process approximation as described below.

Next, positive selection on allele B is assumed in Case 1. At equilibrium with $p^* \approx 1$,

haplotype A-B is selectively neutral because the frequency of allele b is very low. Similar to the previous case, we can derive an approximate formula for the establishmemt probability as

$$\frac{2}{N} \times E(X_B), \tag{4.32}$$

where X_B is the number of haplotype A-B when p reaches p^*.

I briefly explain how $E(X_B)$ and $E(X_b)$ can be computed. I here assume that mutation rate is low enough to be ignored. Let $X_j^i(p_0)(i, j \in \{B, b\})$ denote the number of descendant A-j haplotypes at $p = p^*$ originated from the focal single haplotype A-i that arose when $p = p_0$. $E(X_B)$ and $E(X_b)$ depend on p_0 and the allele at locus B/b with which the allele A initially links. By considering the change of the haplotype frequency in one generation, we can obtain the recursion equations:

$$\begin{aligned} E[X_j^B(p)] &= (1 + \alpha(p) - (1-p)r)E[X_j^B(p + \Delta p)] + (1-p)rE[X_j^b(p + \Delta p)] \\ E[X_j^b(p)] &= prE[X_j^B(p + \Delta p)] + (1 + \beta(p) - pr)E[X_j^b(p + \Delta p)] \end{aligned} \tag{4.33}$$

(for each coefficient, see Equation 4.1), where Δp is the expected change of p in one generation. By ignoring the order of $\frac{1}{N}$ and using a continuous time approximation, Equation 4.33 is rearranged as

$$\begin{aligned} \frac{dE[X_j^B(p)]}{dt} &= -(\alpha(p) - (1-p)r)E[X_j^B(p)] - (1-p)rE[X_j^b(p)] \\ \frac{dE[X_j^b(p)]}{dt} &= -prE[X_j^B(p)] - (\beta(p) - pr)E[X_j^b(p)] \\ \frac{dp}{dt} &= \Big[\frac{h_f s_f + h_m s_m}{2} + \frac{(1-2h_f)s_f + (1-2h_m)s_m}{2}p\Big]p(1-p), \end{aligned} \tag{4.34}$$

where t is an auxiliary variable. Then, by setting the initial condition at $t = 0$, we can obtain $E[X_j^i]$ as a function of p.

When negative selection is assumed, the initial condition is set by the values at equilibrium $p^* = 0$ as $E(X_b^B) = \frac{r}{r - h_m s_m}$ and $E(X_b^b) = 1$. However, for a technical reason, we cannot use $p = 0$ at initial state because we cannot calculate Equation 4.34 under $\frac{dp}{dt} = 0$ (see the main text). Instead, I set $p = \varepsilon$ ($\varepsilon \ll 1$) as an initial state. When positive selection is assumed, $E(X_B^B) = 1$, $E(X_B^b) = \frac{r}{r + (1 - h_m)s_m}$ and $p = 1 - \varepsilon$ is used as values at $t = 0$. As long as ε is small, its effect on the numerical value appears to be very subtle.

For the case of negative selection, the establishment probability is plotted for different population sizes $N = 10,000$ and $100,000$ (Figure 4.9). All other parameters are the same as those used for Figure 4.15B, so that Figure 4.9A is identical to Figure 4.15B. In Figure 4.9, simulation results are plotted together with Equations 4.3, 4.7 and 4.31. Note that Equation 4.31 can be applied only when $r > h_m s_m$. It is demonstrated that, when $r < h_m s_m$, as stated in the main text, establishment is driven by selection such that its probability does not depend on the population size ($r = 0.0, 0.005$ in Figure 4.9). On the other hand, when $r > h_m s_m$, the establishment probability is no longer determined by the selection intensity, and proportional to $1/N$ because random genetic drift is the dominant force involved in the establishment. This is shown in the inner panels for $r = 0.01, 0.02$ in Figure 4.9, where Equation 4.31 agrees with the simulation results better than Equations 4.3 and 4.7 especially for a large r (i.e., $r = 0.02$).

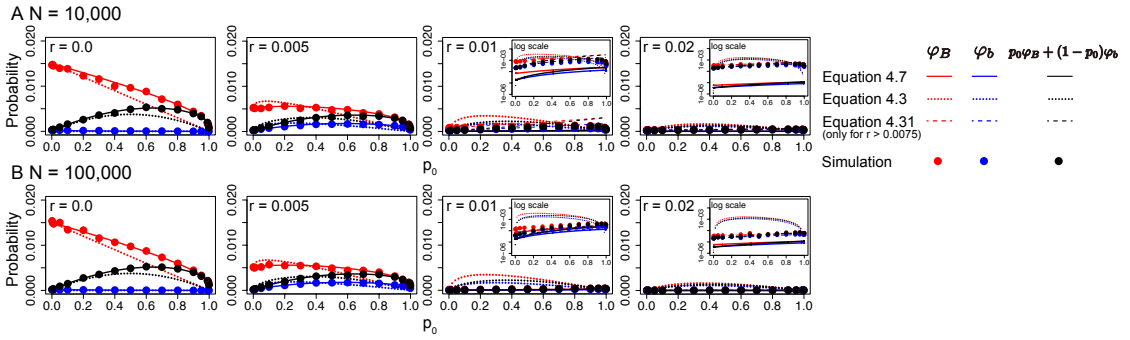

Figure 4.9: Establishment probability for the case of negative selection against allele B in Case 1. Different population sizes are assumed: (A) $N = 10,000$, and (B) $N = 100,000$. Other parameters are $s_m = 0.015, s_f = -0.03, h_m = h_f = 0.5$ and $u = v = 1.0 \times 10^{-6}$. Note that Equation 4.31 is plotted only for $r = 0.01, 0.02$. In the inner panels, the y-axis is log-scaled. Error bars on the red and blue circles represent the 95 % confidence interval, but they are too small to be seen.

Figure 4.10 shows the establishment probability for the case of positive selection. Simulation results are plotted together with Equations 4.3, 4.7 and 4.32. Two population sizes ($N = 10,000, 100,000$) are considered, and all other parameters are the same as those used for Figure 4.6 so that Figure 4.10A is identical to Figure 4.6 except that the establishment probability is log-scaled in Figure 4.10. For all recombination values, as the establishment process depends on random genetic drift, the establishment probability is on the order of $1/N$ (see Figure 4.10). Equation 4.32 agrees very well with simulations unless p_0 is very small.

Finally, I consider Case 2 that involves a turnover of the heterogametic sex. Approximation formulae can be derived in a similar way to Case 1. By noting that the establishment probability of a neutral feminizing allele is $1.07/N$ (Veller *et al.* 2017), the establishment probability can be approximated by,

$$\frac{1.07}{N} \times E(X_b) \tag{4.35}$$

when negative selection works and $r > h_f s_f$, and

$$\frac{1.07}{N} \times E(X_B) \tag{4.36}$$

when positive selection works. $E(X_B)$ and $E(X_b)$ are calculated by using Equation 4.34 with substituting h_m and s_m by h_f and s_f. These equations agree with simulation results (see Figure 4.11 and 4.12).

Appendix F: Relationship with van Doorn and Kirkpatrick (2007, 2010)

I here attempt to relate my results with the previous theory of van Doorn and Kirkpatrick (2007, 2010). Because their results based on a completely different model (i.e., an infinite-size population model), it is difficult to directly compare my results and theirs. To do so, I focus on the establishment probability in a finite size population, which may be comparable to the growth rate obtained by van Doorn and Kirkpatrick (2007, 2010) assuming an infinite population model. First, I briefly overview van Doorn and Kirkpatrick (2007, 2010), and then, I provide a simple, intuitive interpretation of the difference between my results and van Doorn and Kirkpatrick (2007, 2010).

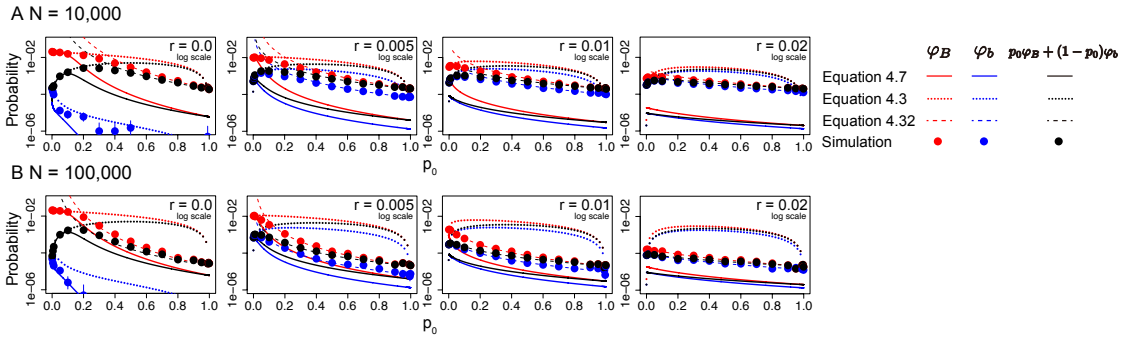

Figure 4.10: Establishment probability for the case of positive selection for allele B in Case 1. Different population sizes are assumed: (A) $N = 10,000$, and (B) $N = 100,000$. Other parameters are $s_m = 0.02, s_f = -0.01, h_m = h_f = 0.5$ and $u = v = 1.0 \times 10^{-6}$. The y-axis is log-scaled. Error bars on the red and blue circles represent the 95 % confidence interval, but they are too small to be seen.

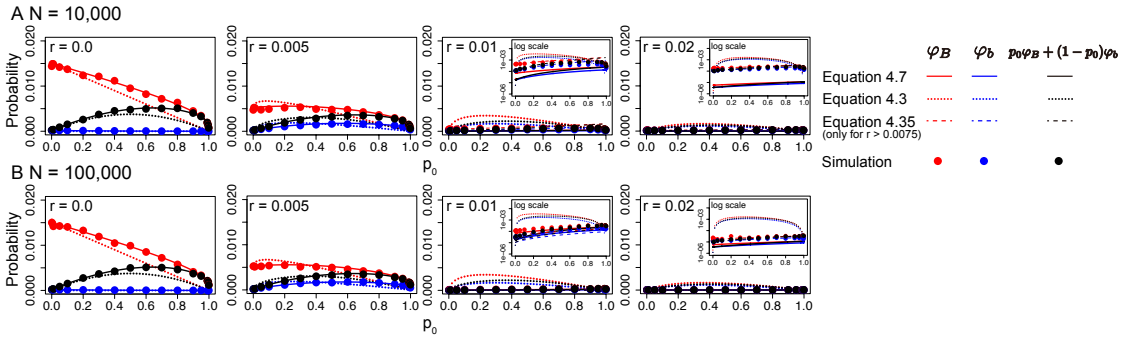

Figure 4.11: Establishment probability for the case of negative selection against allele B in Case 2. Different population sizes are assumed: (A) $N = 10,000$, and (B) $N = 100,000$. Other parameters are $s_f = 0.015, s_m = -0.03, h_m = h_f = 0.5$ and $u = v = 1.0 \times 10^{-6}$. Note that Equation 4.35 is plotted only for $r = 0.01, 0.02$. In the inner panels, the y-axis is log-scaled. Error bars on the red and blue circles represent the 95 % confidence interval, but they are too small to be seen.

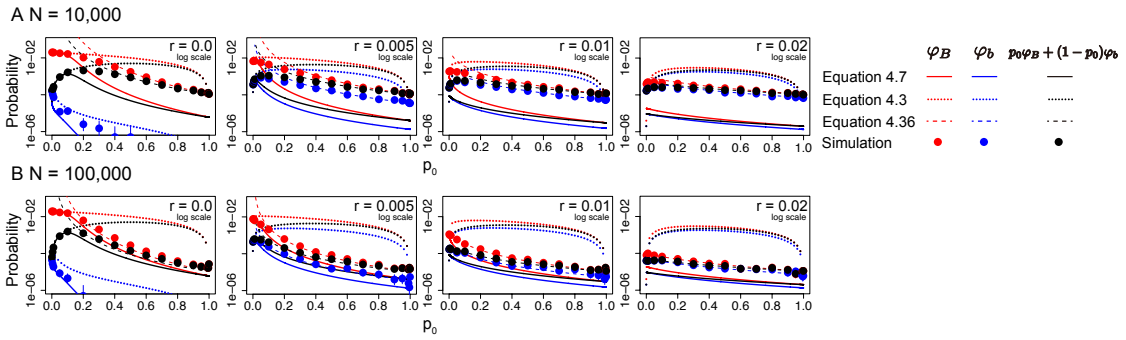

Figure 4.12: Establishment probability for the case of positive selection for allele B in Case 2. Different population sizes are assumed: (A) $N = 10,000$, and (B) $N = 100,000$. Other parameters are $s_f = 0.02, s_m = -0.01, h_m = h_f = 0.5$ and $u = v = 1.0 \times 10^{-6}$. The y-axis is log-scaled. Error bars on the red and blue circles represent the 95 % confidence interval, but they are too small to be seen.

Overview of van Doorn and **Kirkpatrick (2007, 2010):**

I briefly introduce the infinite-size population models of van Doorn and Kirkpatrick (2007, 2010). Initially, the X/Y locus is the sex-determining locus, at which females have genotype XX and males have genotype XY. There is another potentially sex-determining locus A/a, at which allele a is initially fixed. Then, their model considers that a new sex-determining allele A arises at locus A/a. It is also assumed that sexually antagonistic selection works at some other loci. The model allows that there can be more than one loci under sexually antagonistic selection and that the X/Y locus can also link with one of the sexually antagonistic loci, whereas my model has only one sexually antagonistic locus. In order for their results to be comparable with ours, I here set the model of van Doorn and Kirkpatrick (2007, 2010) such that there is only one sexually antagonistic locus (corresponding to the B/b locus in my model).

Under this model, van Doorn and Kirkpatrick (2007, 2010) derived the "invasion fitness" of a newly arisen allele A with considering the effect of linked selection. The invasion fitness is defined as the growth rate of allele A when the frequency of allele A is very low. They derived the invasion fitness both for a masculinizing allele (van Doorn and Kirkpatrick 2007) and for a feminizing allele (van Doorn and Kirkpatrick 2010). Although the two articles consider different situations, the formulae are in the same form if we interchange the parameters of selection in male and female, which is analogous to my results. Therefore, in the following, I arbitrarily chose to focus on the invasion of a feminizing allele, while the same argument will hold for a masculinizing allele.

Although they derived several approximations, I here focus on the tight linkage approximation because they demonstrated that it is most accurate. In Equations 5 and 8 in van Doorn and Kirkpatrick (2010), the invasion fitness of a feminizing allele was derived as

$$\lambda_A = (1-2r)a^f \frac{p_W(1-p_W)(a^f-a^m) - [p^*(1-p^*) - p_W(1-p_W)](a^f+a^m)}{2(r+u+v)}, \qquad (4.37)$$

where $a^f = s_f[h_f + p^*(1-2h_f)]$, $a^m = s_m[h_m + p^*(1-2h_m)]$ and p_W is a solution of

$$-(-p^*+p_W)r + p_W(1-p_W)a^f + [(1-p_W)v - p_W u] = 0$$

(see also the supplementary materials of van Doorn and Kirkpatrick 2010).

Reinterpretation of van Doorn and **Kirkpatrick (2007, 2010):**

I here attempt to interpret Equation 4.37 in the context of my stochastic model. Although the invasion fitness is based on an infinite-size population model, several studies (Connallon and Clark 2010, Yeaman and Otto 2011, Charlesworth *et al.* 2014) suggested that the establishment probability is strongly correlated with the invasion fitness, that is, the establishment probability of a single mutant allele with an invasion fitness of λ is given by

$$\begin{aligned} f &= \frac{1-e^{-2\lambda}}{1-e^{-4N\lambda}} \\ &\approx 2\lambda, \end{aligned}$$

where N is the population size.

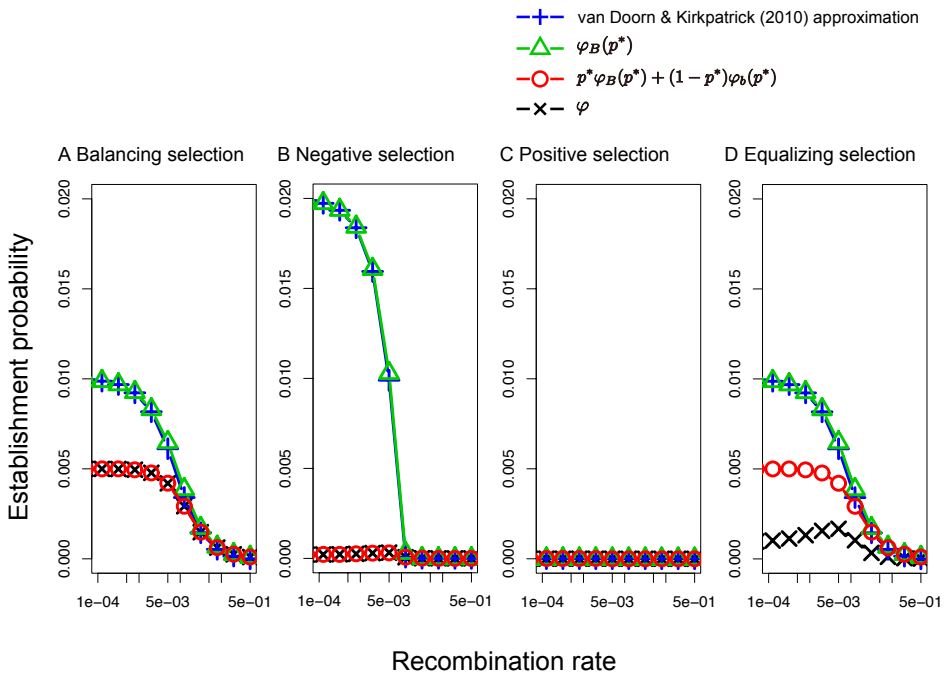

Figure 4.13: Equation 8 of van Doorn and Kirkpatrick (2010) is plotted together with my theoretical results. $N = 100,000$ and $u = v = 1.0 \times 10^{-6}$ are assumed. Other parameters are (A) $s_f = 0.02, s_m = -0.02, h_f = 1.0, h_m = 0.0$, (B) $s_f = 0.02, s_m = -0.025, h_f = h_m = 0.5$, (C) $s_f = 0.02, s_m = -0.01, h_f = h_m = 0.5$ and (D) $s_f = 0.02, s_m = -0.02, h_f = h_m = 0.5$. Error bars on the red and blue circles represent the 95 % confidence interval, but they are too small to be seen.

I find that $2\lambda_A$ is quantitatively in very good agreement with my $\varphi_B(p^*)$, the establishment probability of allele A arising in linkage with beneficial allele B, as demonstrated in Figure 4.13 (the blue line with + and green line with △ in Figure 4.13). Note that I here use a fairly large N to reduce the effect of random genetic drift so that $2\lambda_A$ can be better understood in my framework. It appears that $2\lambda_A$ does not take into the case that allele A arises in linkage with allele b because $2\lambda_A$ does not agree with $p^*\varphi_B(p^*) + (1-p^*)\varphi_b(p^*)$ (the red line with ◯ in Figure 4.13). It may be concluded that their λ_A should well reflect the behavior of allele A when (i) the frequency of allele B is p^* and (ii) the focal allele A is linked with allele B, rather than the general establishment probability with no conditions that correspond to my φ (the black line with × in Figure 4.13). The first condition (i) makes sense because p would be at the equilibrium frequency, p^*, in a deterministic treatment. The second one (ii) may be understood if the case that allele A links with allele b is ignored because the invasion fitness for this case is smaller than 1.

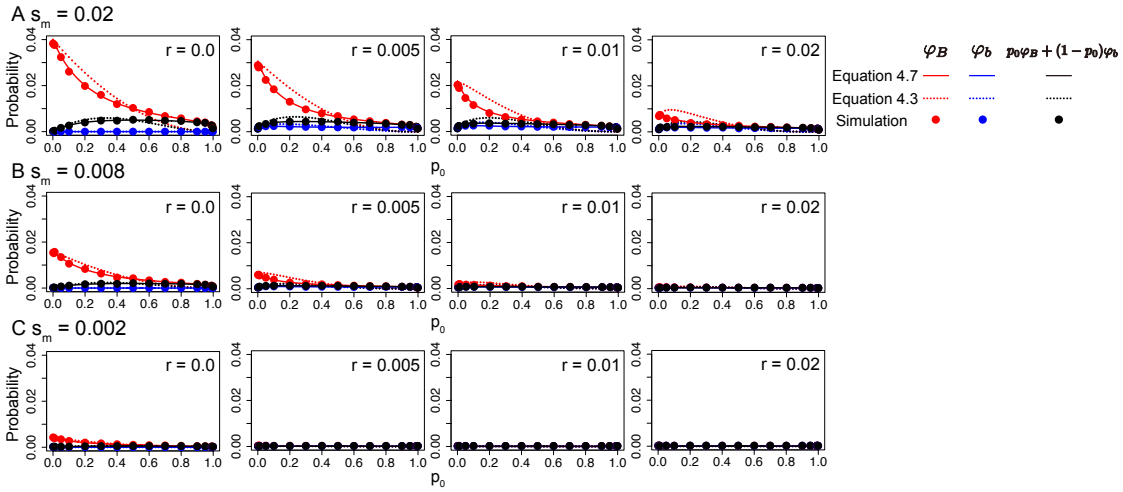

Figure 4.14: Establishment probability for the case of balancing selection on allele B. Different strengths of selection are assumed: (A) $s_m = -s_f = 0.02$, (B) $s_m = -s_f = 0.008$ and (C) $s_m = -s_f = 0.002$. Other parameters are assumed to be $h_m = 1.0, h_f = 0.0, N = 10,000, u = v = 1.0 \times 10^{-6}$. Error bars on the red and blue circles represent the 95 % confidence interval, but they are too small to be seen.

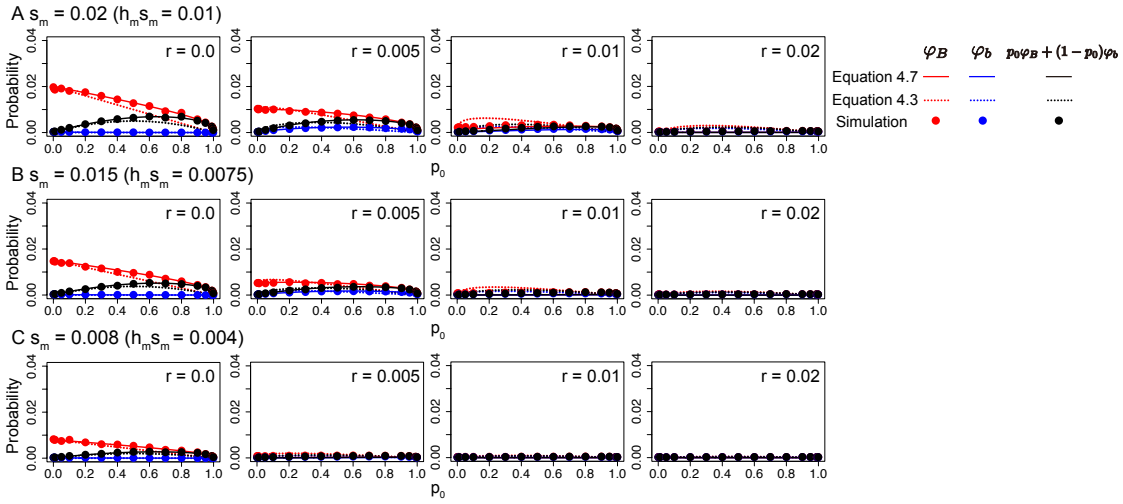

Figure 4.15: Establishment probability for the case of negative selection against allele B. Different strengths of selection are assumed: (A) $s_m = 0.02$, (B) $s_m = 0.015$ and (C) $s_m = 0.008$. Other parameters are assumed to be $s_f = -2s_m, h_m = h_f = 0.5$, $N = 10,000$, and $u = v = 1.0 \times 10^{-6}$. Error bars on the red and blue circles represent the 95 % confidence interval, but they are too small to be seen.

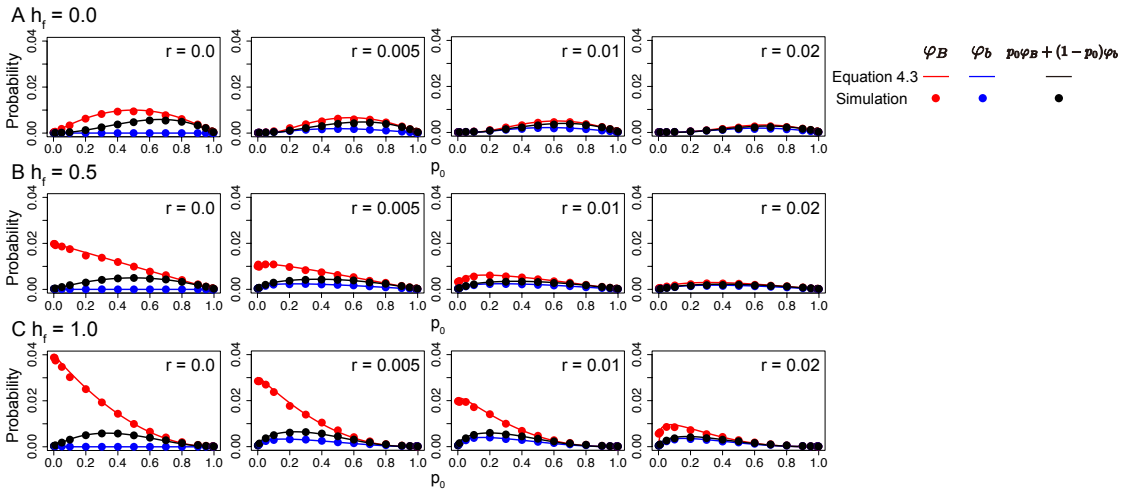

Figure 4.16: Establishment probability of allele A for different dominance and recombination rates in Case 2. Three dominance coefficients are assumed: (A) $h_f = 0.0$, (B) $h_f = 0.5$ and (C) $h_f = 1.0$. Other parameters are as follows: $s_f = -s_m = 0.02, h_m = h_f, N = 10000, u = v = 1.0 \times 10^{-6}$. Error bars on the red and blue circles represent the 95 % confidence interval, but they are too small to be seen.

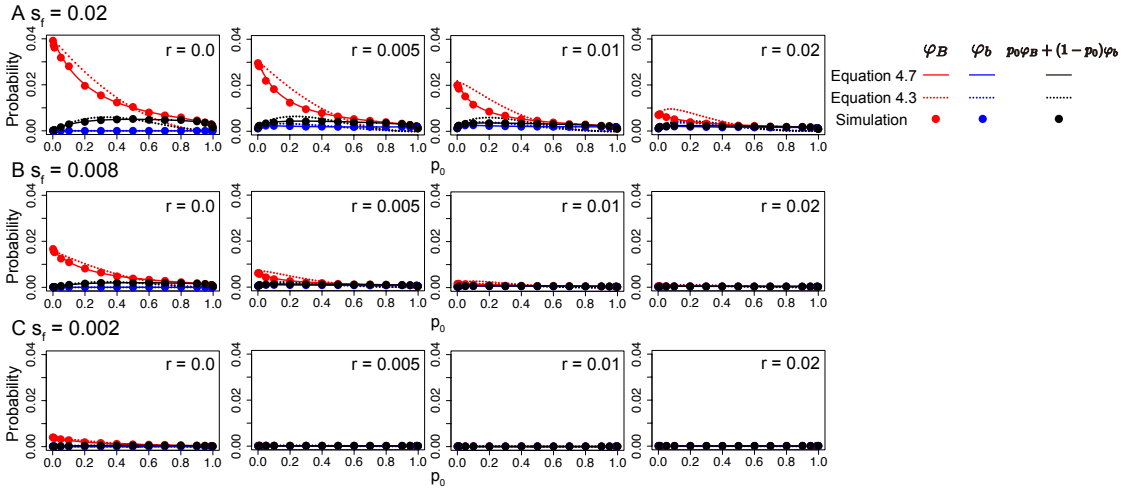

Figure 4.17: Establishment probability for the case of balancing selection for allele B in Case 2. Different strengths of selection are assumed: (A) $s_f = -s_m = 0.02$, (B) $s_f = -s_m = 0.008$ and (C) $s_f = -s_m = 0.002$ are assumed. Other parameters are $h_f = 1.0, h_m = 0.0, N = 10000, u = v = 1.0 \times 10^{-6}$. Error bars on the red and blue circles represent the 95 % confidence interval, but they are too small to be seen.

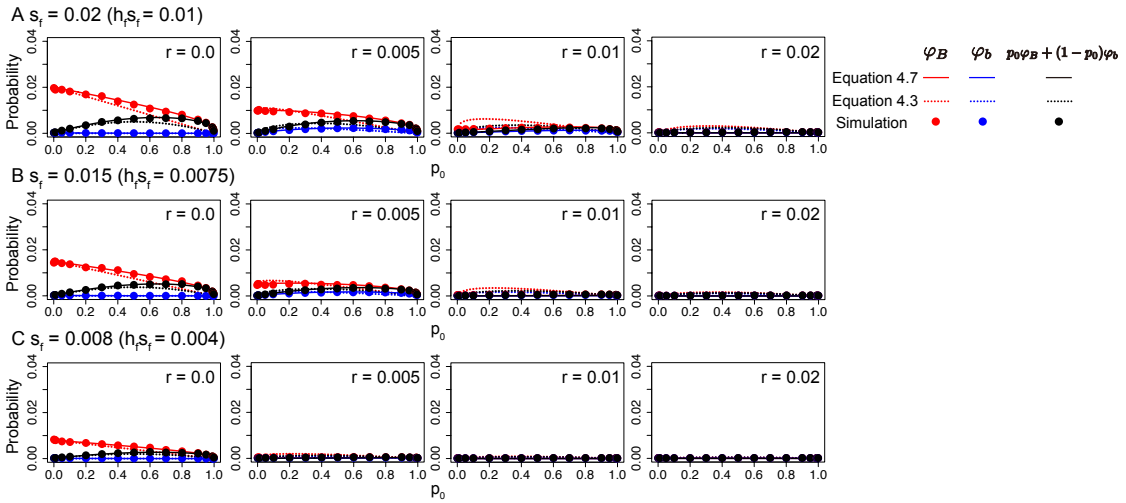

Figure 4.18: Establishment probability for the case of negative selection against allele B in Case 2. Different strengths of selection are assumed: (A) $s_f = 0.02$, (B) $s_f = 0.015$ and (C) $s_f = 0.008$. Other parameters are $s_m = -2s_f, h_m = h_f = 0.5$, $N = 10,000$, and $u = v = 1.0 \times 10^{-6}$. Error bars on the red and blue circles represent the 95 % confidence interval, but they are too small to be seen.

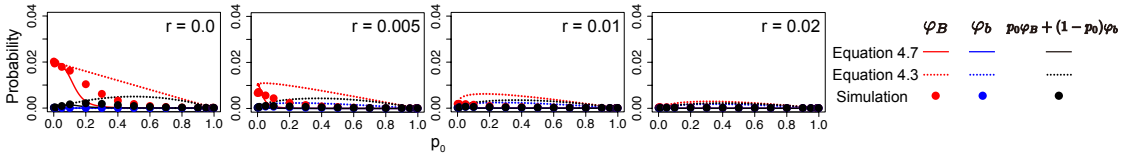

Figure 4.19: Establishment probability for the case of positive selection for allele B in Case 2. Other parameters are $s_f = 0.02, s_m = -0.01, h_m = h_f = 0.5$, $N = 10,000$, and $u = v = 1.0 \times 10^{-6}$. Error bars on the red and blue circles represent the 95 % confidence interval, but they are too small to be seen.

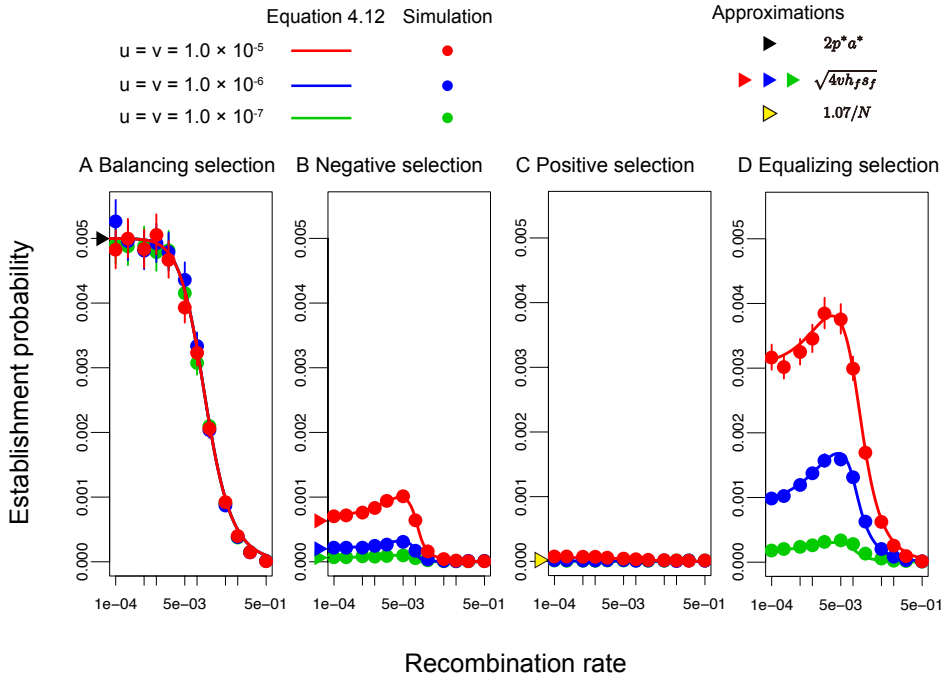

Figure 4.20: Establishment probability of a feminizing allele for different modes of sexually antagonistic selection. $N = 100,000$ and $u = v$ are assumed. Other parameters are (A) $s_f = 0.02, s_m = -0.02, h_f = 1.0, h_m = 0.0$, (B) $s_f = 0.02, s_m = -0.025, h_m = h_f = 0.5$, (C) $s_f = 0.02, s_m = -0.01, h_m = h_f = 0.5$ and (D) $s_f = 0.02, s_m = -0.02, h_m = h_f = 0.5$. Error bars on the red and blue circles represent the 95 % confidence interval.

Chapter 5

Muller's ratchet of the Y chromosome with gene conversion

5.1 Introduction

Non-recombining chromosomes such as Y chromosome often degenerate rapidly because deleterious mutations accumulate irreversibly. This process called Muller's ratchet (Muller 1964) has been investigated extensively in many theoretical studies (Haigh 1978, Stephan *et al.* 1993, Gessler 1995, Charlesworth and Charlesworth 1997, Gordo and Charlesworth 2000a,b, Jain 2008, Rouzine *et al.* 2008, Waxman and Loewe 2010, Neher and Shraiman 2012, Goyal *et al.* 2012, Metzger and Eule 2013). Although these studies used models of single-copy genes, recent sequencing of the Y chromosome has revealed that many genes have acquired multiple copies through gene duplication. These theoretical results therefore cannot be directly applied to the Y chromosome, because the evolution of duplicated genes is not as simple as that of single-copy genes. Duplicated genes are likely to undergo concerted evolution, during which the duplicated copies coevolve by exchanging their DNA sequences with each other by gene conversion (Ohta 1983, Arnheim 1983). The major effect of gene conversion during concerted evolution is that, under neutrality, the level of divergence between the duplicated copies is kept low, while the level of polymorphism within each copy is increased (Innan 2002, 2003, Teshima and Innan 2004). It has been theoretically demonstrated that the effect of selection is enhanced in duplicated genes; deleterious mutations are more efficiently removed, and beneficial mutations are more likely to become fixed in both of the duplicated copies (Mano and Innan 2008). However, the way in which gene conversion affects the degeneration of the Y chromosome, in which single-copy genes and duplicated genes coexist with complete linkage, is not fully understood.

The aim of this study was to theoretically understand the degeneration process of duplicated genes with special interest in the Y chromosome. Y chromosomes have a unique evolutionary history. They usually evolve from an autosome, on which a sex-determining locus arises. After recombination with the X chromosome is suppressed, the Y chromosome gradually loses functional genes by the accumulation of deleterious mutations (Charlesworth and Charlesworth 2000, Bachtrog 2013). During this process, many genes undergo gene duplication (Skaletsky *et al.* 2003, Hughes *et al.* 2010, 2012, 2020, Soh *et al.* 2014). Duplicated gene copies are either in large palindrome structures, as found in primates (Skaletsky *et al.* 2003, Hughes *et al.* 2010, 2012), or arranged in tandem, as found in mouse (Soh *et al.* 2014), bull (Hughes *et al.* 2020) and fruit fly (Bachtrog *et al.* 2019). Since homologous copies of-

ten show high sequence identity, frequent gene conversion should have occurred between the copies (Rozen *et al.* 2003, Hallast *et al.* 2013, Skov *et al.* 2017). These findings indicate that the degeneration of the Y chromosome involves both single-copy and duplicated genes. In this work, I develop a theory to address the following questions: (i) After gene duplication, will the degeneration rate become faster or slower? and (ii) How does gene duplication affect the rate of degeneration of linked single-copy genes?

To investigate these questions, I used a model of Muller's ratchet. In a broad sense, Muller's ratchet is a process by which deleterious mutations are fixed irreversibly in the absence of recombination (Muller 1964). In theoretical reports, it is commonly assumed that all mutations have the same effect on fitness (but see Söderberg and Berg (2007)). Under these conditions, the fitness of an individual depends only upon how many deleterious mutations it has, therefore individuals in the population can be classified based on the number of deleterious mutations (d), as illustrated in Figure 5.2A, in which all haploid individuals have four functional genes, represented by different colored boxes. The class $d = 0$ consists of individuals with no deleterious mutations, which have the highest fitness in the population (i.e., the least-loaded class in this situation). The second class is that of individuals with one deleterious mutation ($d = 1$), and those who have two deleterious mutations belong to the class $d = 2$. Because I assume that all mutations are irreversible (i.e., back mutation is ignored), the class of an individual can shift down (e.g., $d = 0 \rightarrow 1 \rightarrow 2$) as it accumulates mutations. Under these assumptions, the population can be structured according to d, and Muller's ratchet proceeds as these classes turn over and over. In practice, if the least-loaded class ($d = 0$ in Figure 5.2A) goes extinct, the ratchet clicks and the class of $d = 1$ becomes the least-loaded class.

I here extend the model of Muller's ratchet to the case of duplicated genes. Figure 5.2B illustrates an example in which all haploid individuals have four genes which have been duplicated. Again, the population can be structured based on the number of deleterious mutations, and the process of Muller's ratchet proceeds along the turnover of the classes. The major difference is that a new deleterious mutation which has occurred in the duplicated genes is not "irreversible" because gene conversion could remove it. If the original part of the intact copy without the corresponding mutation is transferred, the mutated copy will lose the mutation. However, if gene conversion occurs in the opposite direction—from the mutated copy to the intact version—the mutation becomes irreversible in this individual, because gene conversion cannot remove it any more, under the assumption of no back mutation. I refer to the former and latter types of mutations as reversible and irreversible mutations, respectively (presented by yellow and red circles in Figure 5.2B). Thus, when a new mutation arises in one copy, its fate is not determined, and we can consider that the mutation can contribute to an irreversible click of Muller's ratchet when the mutation is shared in both copies. In this model, we can simplify the process of Muller's ratchet if we assume that all mutations are recessive and have the same fitness effect. Individuals can therefore be classified according to the number of irreversible mutations they carry. Note that reversible mutations have no fitness effect. Intuitively, gene conversion should have two opposite effects on the degeneration process (Graves 2004). If gene conversion mutates both copies, producing an irreversible mutation, the degeneration process is accelerated. If, however, gene conversion removes the mutation and restores both copies to the original form, the speed of degeneration is slowed. I

used this model to explore the way in which gene conversion affects the degeneration of duplicated genes. I was particularly interested in the interactions between the two counteracting effects of gene conversion. I provide analytical expressions of the speed of Muller's ratchet under this simplified model with a constant selection coefficient. I also consider the effect of variable selection coefficients and the degree of dominance, using mathematical analysis and simulations.

Several studies have investigated the effect of gene conversion on the degeneration of Y chromosomes (Connallon and Clark 2010, Marais *et al.* 2010), but their focuses have been different from those of the present study. Connallon and Clark (2010) investigated the role of gene conversion on the conservation of duplicated pairs. Because their model assumes that deleterious mutations have lethal effects, a mutation cannot be shared by both duplicated copies, because this situation would be lethal. Therefore, there is no gene loss through the accumulation of deleterious mutations. Marais *et al.* (2010) investigated the evolution of the human Y chromosome using simulations, in which gene conversion between duplicated genes was taken into account. Their focus was on the process of fixation of a modifier of the gene conversion rate, rather than the long-term degeneration process.

5.2 Model

5.2.1 General model

I used a discrete-generation Wright–Fisher model of a haploid population with size N. Each chromosome consists of L_1 single-copy genes and L_2 pairs of duplicated genes (Figure 5.1A). I assume no inter-chromosomal recombination, or crossing-over, so all genes on the same chromosome are completely linked. A chromosome therefore behaves as a single haploid individual. I am interested in the way in which the genes lose their functions through Muller's ratchet, resulting in a reduction in the number of functional genes on the chromosome. To this end, I applied a simple loss-of-function model to each gene and gene pair. For the i-th single-copy gene, I assume the fitness effect of losing the gene function to be s_i. I only consider loss-of-function mutations, so that one mutation is sufficient to make a gene a pseudogene, with loss of the gene function. Throughout this article, I say a gene is "lost" when it loses the function. The rate of loss-of-function mutation is u per copy per generation, and no back mutation is allowed. Every mutation therefore results in an irreversible loss of the gene (see the right state with a red circle in Figure 5.1B).

For a pair of duplicated genes (Figure 5.1C), I set the fitness as follows. To be comparable with the case of single-copy genes, the fitness of the state with one functional copy is 1 (middle in Figure 5.1C). The other copy is inactivated by a loss-of-function mutation, which is shown by a yellow circle in Figure 5.1C because it is not irreversible, but "reversible". A reversible mutation can disappear when the intact sequence is transferred from the other functional copy by gene conversion. If gene conversion occurs in the opposite direction, the loss-of-function mutation is transferred to the functional copy, resulting in a state in which the loss-of-function mutation is shared by both copies (the right state with red circles in both copies in Figure 5.1C). In this state, the gene has completely lost its function, because the mutation became irreversible, since gene conversion cannot rescue the gene function anymore, and the fitness is given by $1 - t_{2,i}$ for the i-th pair of duplicated genes. The fitness of the

state with two intact copies (left in Figure 5.1C) is given by $1 + t_{1,i}$. Having two copies therefore confers a selective advantage by $t_{1,i}$. It is well documented that Y chromosomes have a number of duplicated genes, some of which seem to provide an advantage by increasing the dosage of the gene product (Hughes *et al.* 2010, 2012, 2020, Soh *et al.* 2014). Under this model, if we assume $t_{1,i} = 0, t_{2,i} > 0$, the functional allele is in complete dominance, whereas if $t_{1,i} = t_{2,i} > 0$ is assumed, the dominance effect is additive. Loss-of-function mutations arise at a rate of u per copy per generation, and no back mutation is allowed. Gene conversion occurs at a rate of c per copy per generation in both directions between the duplicated copies. I assume that a gene conversion event transfers the entire genic region (represented by a single box in Figure 5.1C).

It should be noted that two independent mutations can cause a loss of the gene function, as illustrated in the lower case of the right part of Figure 5.1C. This situation is more complex, because the gene function is lost but the two mutations are still reversible. Nevertheless, I treat this situation as if the gene function is irreversibly lost, which is true in my model, in which a gene conversion event transfers the entire genic region.

The fitness of a haploid individual (chromosome) is determined by the multiplicative effect of all genes. That is,

$$f = \prod_{i=1}^{L_1} w_{1,i} \prod_{i=1}^{L_2} w_{2,i}, \tag{5.1}$$

where $w_{1,i}$ and $w_{2,i}$ are determined as follows:

$$w_{1,i} = \begin{cases} 1 & \text{(if } i\text{-th single-copy gene is functional)} \\ 1 - s_i & \text{(if } i\text{-th single-copy gene is lost)} \end{cases}$$

and

$$w_{2,i} = \begin{cases} 1 + t_{1,i} & \text{(if both copies of the } i\text{-th duplicated genes are functional)} \\ 1 & \text{(if one copy of the } i\text{-th duplicated genes is lost)} \\ 1 - t_{2,i} & \text{(if both copies of the } i\text{-th duplicated genes are lost)} \end{cases}$$

Based on the fitness of all individuals in the current population, the next generation is generated following the Wright–Fisher model.

5.2.2 Simplification for mathematical analyses

Since the general model described above is too complicated for mathematical analysis, we make the following two simplifying assumptions. First, I assume that all genes have the same fitness effect. Therefore, $s_i = s$, $t_{1,i} = t_1$, $t_{2,i} = t_2$ for all i. Second, we assume that the fitness effect of losing the function is the same for a single-copy gene and a pair of duplicated genes ($s = t_2$). Under these assumptions, I derive the rate of gene loss in two special cases: one in which the functional copy is in complete dominance ($t_1 = 0$), and one in which it is additive ($t_1 = t_2$). In the complete dominance case, the fitness of an individual depends on the number of irreversible mutations, d, and the population can be structured based on d (Figure 5.2). In the additive case, the fitness of an individual depends on the total number of mutations, d^*, and individuals can be classified based on d^* (Figure 5.3).

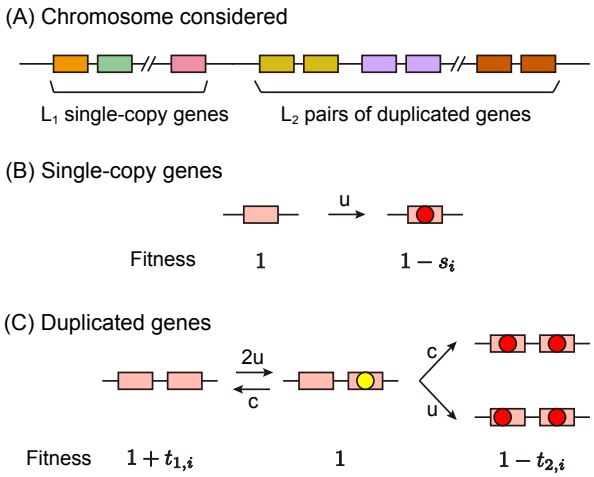

Figure 5.1: Summary of the model. (A) Chromosome considered in the model. (B, C) Fitness models for a single-copy gene (B) and a pair of duplicated gene (C). Red and yellow circles are, respectively, irreversible and reversible mutations.

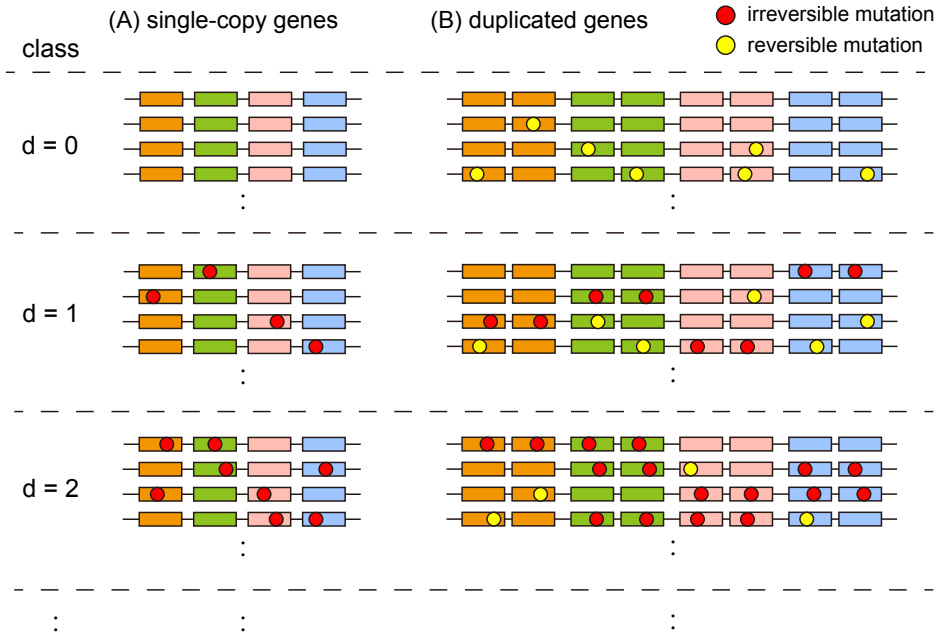

Figure 5.2: Illustration of the population structure based on d, the number of irreversible mutations for (A) the case of all single-copy genes and (B) all duplicated genes. Boxes in different colors represents genes, or genic regions. Boxes in the same color in (B) indicate duplicated gene pairs. Red and yellow circles are, respectively, irreversible and reversible mutations.

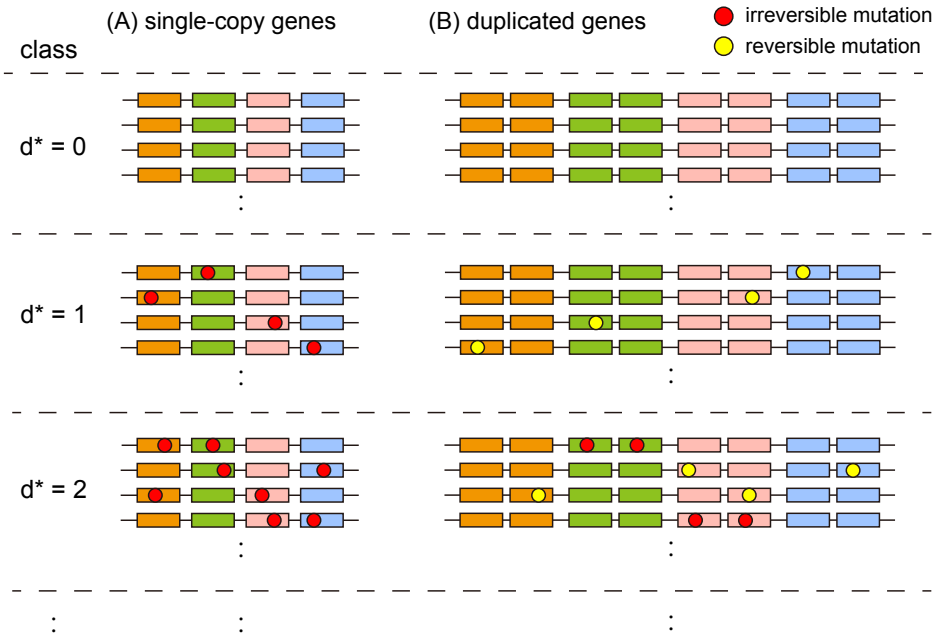

Figure 5.3: Illustration of the population structure based on d^*, the number of deleterious mutations for (A) the case of all single-copy genes and (B) all duplicated genes. Boxes in different colors represents genes, or genic regions. Boxes in the same color in (B) indicate duplicated gene pairs. Red and yellow circles are, respectively, irreversible and reversible mutations.

5.3 Results

I investigated the way in which a non-recombining chromosome loses functional genes through Muller's ratchet. My model assumes a chromosome carrying L_1 single-copy genes and L_2 pairs of duplicated genes, and I compared the rates of gene loss for single-copy genes and duplicated genes. I theoretically consider the speed of gene loss per gene, conditional on L_1 and L_2. The most part of the following is a theoretical analysis, to which the simplifying assumptions detailed above apply. These assumptions are relaxed in the simulation-based analysis, where I mention it.

5.3.1 Duplication with no fitness effect of dosage

I first consider the case in which the presence of two copies, which have arisen by duplication, confers no selective advantage in comparison with having only one copy ($t_1 = 0$). In this case, the fitness of each individual is specified only by the number of irreversible mutations, d, as defined in Figure 5.2, and reversible mutations can be ignored. I first derive the equilibrium size of the least-loaded class ($d = 0$), N_e, conditional on L_1 and L_2, which is the most important quantity with which to determine the evolutionary dynamics of the population. Let U be the total rate of production of irreversible mutations per chromosome (haploid individual). Irreversible mutations arise at rate uL_1 in single-copy genes, while the rate for duplicated genes is $(u + c)H_j$, where H_j is the number of reversible mutations in the j-th individual. If we ignore the variance of H_j among individuals, U is given by $U = uL_1 + (u + c)\bar{H}$ where $\bar{H}$ is the average of H_j. We can ignore irreversible mutations segregating in the population, because they exist at low frequencies under the conditions I consider in this work, $u \ll U \sim s$. Following Haigh (1978), N_e is then expressed as

$$N_e = N \exp(-U/s), \tag{5.2}$$

indicating we need to derive $\bar{H}$ to obtain N_e. It is obvious that $\bar{H}$ largely depends on the frequency of individuals having one reversible mutation in each gene pair, which is denoted by p_i for the i-th gene pair. p_i is mainly determined by the frequency dynamics in the least-loaded class, and the deterministic change of p_i per generation in the least-loaded class is given by

$$\begin{aligned} E[\Delta p_i] &= \frac{p_i + 2u(1-p_i) - (u+2c)p_i}{1-(u+c)p_i} - p_i \\ &\approx 2u(1-p_i) - cp_i - (u+c)p_i(1-p_i), \end{aligned} \tag{5.3}$$

where the term $(u+c)p_i$ in the denominator represents the proportion of individuals that are removed from the least-loaded class by an irreversible mutation, by additional mutation or gene conversion that occurred in individuals that already had one mutation. Therefore, by using Wright's formula (Wright 1931), the stationary distribution of p_i, $\phi(p_i)$, is given by

$$\phi(p_i) = Ce^{-2N_e(u+c)p_i} p_i^{4N_e u - 1}(1-p_i)^{2N_e c - 1}, \tag{5.4}$$

where C is a constant determined such that $\int_0^1 \phi(p_i)dp_i = 1$. Then, considering L_2 pairs of duplicated genes, $\bar{H}$ can be approximately as

$$\begin{aligned} \bar{H} &\approx L_2 \int_0^1 p\phi(p)dp \\ &= L_2 \frac{2u}{2u+c} \frac{{}_1F_1(4N_e u + 1; 4N_e u + 2N_e c + 1; -2N_e(u+c))}{{}_1F_1(4N_e u; 4N_e u + 2N_e c; -2N_e(u+c))} \end{aligned} \tag{5.5}$$

where ${}_1F_1(\cdot)$ is a confluent hypergeometric function. We now have $\bar{H}$ as a function of N_e. We can therefore obtain N_e as a solution of Equations 5.2 where $\bar{H}$ in U is replaced by Equation 5.5.

With N_e from Equation 5.2, it is straightforward to derive T, the expected waiting time for the first click, conditional on L_1 and L_2 by using the common approach in the theory of Muller's ratchet for single-copy genes (Gordo and Charlesworth 2000a, Jain 2008, Rouzine *et al.* 2008). When $N_e s > 1$ (i.e., slow ratchet regime), T is approximated by

$$T \approx \frac{e^{\alpha s N_e}}{\alpha s} \sqrt{\frac{\pi}{\alpha s N_e}} \tag{5.6}$$

(Jain 2008), where $\alpha = \sqrt{s/U}$ (Goyal *et al.* 2012). When $N_e s < 1$ (i.e., fast ratchet regime), following Rouzine *et al.* (2008), T is approximately given by

$$T \approx \frac{1}{Uv}, \tag{5.7}$$

where v is a solution of the following equation:

$$\alpha^2 \log(NU\alpha^3) = \left(1 - \frac{v}{2}\left((1-\log v)^2 + 1\right)\right) - \alpha^2 \log\left[\sqrt{\frac{v^3}{1-v}} \frac{1-\log v}{1 - v(1-\log v) + 5\alpha^2/6}\right].$$

Then, the gene loss rate per gene for a single-copy gene and that for a pair of duplicated

genes (R_1 and R_2, respectively) can be derived as

$$\begin{aligned} R_1 &= \frac{uL_1}{U}\frac{1}{L_1 T} \\ &= \frac{u}{U}\frac{1}{T} \\ R_2 &= \frac{(u+c)\bar{H}}{U}\frac{1}{L_2 T}, \end{aligned} \tag{5.8}$$

because these rates are proportional to $1/T$ and the rates of irreversible mutation.

To verify the performance of Equation 5.8, I carried out forward simulations, and part of the result is shown in Figures 5.4 and 5.5. My simulation assumed a Wright–Fisher population with N haploid individuals with L_1 single-copy genes and L_2 pairs of duplicated genes. Mutation and gene conversion rates and their fitness effects were as described in the Model section. I assumed that $N = 10,000$ and $u = 1.0 \times 10^{-5}$. Then, in every generation, a random N haploid individuals were generated based on the fitness of the individuals in the previous generation (see Equation 5.1). The selection parameters were assumed such that $s = 0.01$ for a strong selection case, and $s = 0.0025$ for a weak selection case. The purpose of this simulation was to obtain $\bar{T}_1$ and $\bar{T}_2$, the average time required for one click of the ratchet at single-copy genes and duplicated genes, respectively, conditional on L_1 and L_2. From them, the two gene loss rates per gene, R_1 and R_2, can be computed as $R_1 = \frac{1}{L_1 \bar{T}_1}$ and $R_2 = \frac{1}{L_2 \bar{T}_2}$, respectively. However, if we simply run a simulation, L_1 and L_2 decreases along the run, making it difficult to evaluate T conditional on a specified pair of L_1 and L_2. To solve this problem, in my simulation, I used an ad-hoc method, in which L_1 and L_2 were kept constant by adding an intact gene (or a pair of duplicated genes) when I observed a loss of a gene (or a gene pair). This treatment allowed us to approximately obtain the expectation of T conditional on L_1 and L_2. See Appendix A, in which I demonstrate that this heuristic treatment worked quite well. In each simulation run, after a burn-in period of $100N$ generations, I scored the waiting time T for every click for both classes of gene, and the run was terminated when we observed 10,000 clicks or $10{,}000N$ generations had passed.

Figure 5.4 compares the results of two extreme cases: In one, the simulated chromosome consists only of duplicated genes ($L_1 = 0$ and $L_2 = 2,000$), and in the other, only single-copy genes are present in the chromosomes ($L_1 = 2,000$ and $L_2 = 0$). In the case of all duplicated genes, three levels of dominance were considered ($t_1 = 0, t_2/2$, and t_2 presented in blue, green and red, respectively), and the gene conversion rate was changed from 10^{-7} to 10^{-3}. The result for the case of all single-copy genes is shown by the black broken line in Figure 5.4.

Let us focus on the simulation result of no dominance presented by blue circles ($t_1 = 0$), to which Equation 5.8 (blue line) is applicable. Equation 5.8 is in a good agreement with the simulation result, except when the gene conversion rate is very large ($c > 10^{-4}$). In the strong selection case, where the ratchet proceeds so slowly that each click occurs almost independently, R_2 in the case of all duplicates is largely affected by the gene conversion rate (Figure 5.4A). When the gene conversion rate is very small ($c = 10^{-7}$), R_2 is almost identical to R_1 in the case of all single-copy genes. This is because the ratchet process in duplicated genes is quite similar to that of single-copy genes. The pattern illustrated, with two independent mutations, in Figure 5.1C, applies to this case. In a pair of duplicated genes, a first mutation itself is neutral and rarely transferred to the other copy, because of

a very small c, and only a secondary mutation contributes to the ratchet, behaving as if it occurs in a single-copy gene. R_2 increases as the gene conversion rate increases. This can be explained by the increase of U in Equation 5.2. Because Equation 5.5 is approximately given by $\bar{H} \approx \frac{2uL_2}{2u+c}$ when $N_e u, N_e c \ll 1$, U becomes:

$$U \approx u(L_1 + L_2) + \frac{uc}{2u+c} L_2. \tag{5.9}$$

This equation indicates that, when the mutation and gene conversion rates are not large ($N_e u, N_e c \ll 1$), U for the case of all duplicates is the same as that for the case of all single-copy genes when $c = 0$, and R_2 increases as c increases. For a very large c ($N_e c \sim 1$), R_2 decreases with increasing c, because a high c keeps p_i very low and reduces U (see Equation 5.4). At an extremely high gene conversion rate, the fate of a reversible mutation is determined very quickly. In such a case, a reversible mutation arises at a rate of $2u$, and half become irreversible mutations. These mutations then behave like mutations in a single-copy gene that arises at rate u. Therefore, R should be as low as the expectation for a single-copy gene (the dashed line). This explains why R decreases as c becomes very high. Since the size of the least-loaded class, N_e, is reduced significantly as U increases, the gene loss rate is quite sensitive to the change in c in this regime.

Figure 5.4B shows the result for the weak selection case, in which selection is so weak that multiple clicks occur in a sequential manner with overlapping fixation processes. The qualitative effect of gene conversion on R_2 appears similar to that in Figure 5.4A: If c is very small, R_2 is almost identical to R_1 in the case of all single-copy genes (black dashed line). With increasing c, R_2 increases up to an intermediate c, and then decreases. The overall quantitative effect of gene conversion is smaller in comparison with Figure 5.4A, because N_e is always very small in this regime, and the effect of U on R_2 is small.

Figure 5.5 assumes that single-copy genes and duplicated genes coexist. In this simulation, it was assumed that $L_1 = L_2 = 1,000$, and the other parameters were the same as those used in Figure 5.4. The gene loss rates are shown by open circles for single-copy genes (R_1) and by filled circles for duplicated genes (R_2). Let us focus on the results of no dominance (blue circles). Equation 5.8 (blue dashed line in the left panel for R_1, blue solid line for R_2 in the right panel in Figure 5.5) agrees well with the simulation results, unless the gene conversion rate is very large.

In the strong selection case (Figure 5.5A), R_1 and R_2 are very similar to each other. The increase in R_1 and R_2 from that for the case of all single-copy genes (black dashed line) is smaller than that in Figure 5.4A, which is merely due to the smaller L_2 assumed in Figure 5.5. R_2 is slightly larger than R_1 because the rate of generation of irreversible mutations is larger for duplicated genes (see Equation 5.9).

In the weak selection case (Figure 5.5B), R_1 is less sensitive to c and almost identical to R_1 for the case of all single-copy genes, while R_2 shows a similar behavior to that for the case of all duplicates in Figure 5.4B. This is because weak selection causes a small N_e, a situation in which random genetic drift dominates. In such a case, the gene loss rate is roughly proportional to the rate of generation of irreversible mutations, which is constant at u in single-copy genes for any value of c.

I next consider the ratchet process over the long term, where a chromosome gradually

loses its functional genes. Let $L_1(\tau)$ and $L_2(\tau)$ be the number of remaining single-copy and duplicated genes at time τ, respectively. Using Equation 5.8, the differential equations for $L_1(\tau)$ and $L_2(\tau)$ are given by

$$\begin{aligned} \frac{dL_1(\tau)}{d\tau} &= -L_1 R_1 \\ \frac{dL_2(\tau)}{d\tau} &= -L_2 R_2, \end{aligned} \tag{5.10}$$

from which we can numerically compute $L_1(\tau)$ and $L_2(\tau)$. To check the performance of Equation 5.10, I ran forward simulations, and the results are shown in Figure 5.6. For this purpose, I simply ran the above simulation without keeping $L_1(\tau)$ and $L_2(\tau)$ constant (see above for details), so that the number of genes monotonically decreased during the process. I assumed that each chromosome initially had $L_1(0)$ intact single-copy genes and $L_2(0)$ intact pairs of duplicated genes. It was also assumed that $N = 10,000$, $L_1(0) = L_2(0) = 1,000$, $u = 1.0 \times 10^{-5}$ and $s = t_2 = 0.0025$, and three levels of dominance were used ($t_1 = 0, t_2/2, t_2$). Two different gene conversion rates were considered: $c = 1.0 \times 10^{-4}$ (deep green) and $c = 1.0 \times 10^{-6}$ (orange). In each panel, the result is compared with that for the case of all single-copy genes presented by black circles (i.e., $L_1(0) = 2,000$, and $L_2(0) = 0$), which was obtained by additional simulations.

As I consider the case of no dominance in this section, let us focus on Figure 5.6A. Equation 5.10 (solid lines) is in good agreement with the simulation results. When the gene conversion rate is low ($c = 10^{-6}$), the gene loss rates for both single-copy genes and duplicated genes are very similar to those in the case of all single-copy genes, consistent with the results in Figure 5.5. When the gene conversion rate is high ($c = 10^{-4}$), the gene loss process is slightly accelerated in duplicated genes, consistent with Figure 5.5B. I also consider the case where s_i and $t_{2,i}$ are heterogeneous among loci in Appendix B and obtained qualitatively similar patterns (see Appendix B for details).

5.3.2 Duplication with an additive fitness effect of dosage

I consider the case of $t_1 = t_2 = s$, in which duplication has an additive effect on fitness. In this case, the fitness of individuals can be specified by the sum of the number of reversible mutations and irreversible mutations, d^*. The treatment for single-copy genes is the same as in the previous section, while some modifications are needed for duplicated genes. Unlike the previous section, a single irreversible mutation in duplicated genes should be counted as two deleterious mutations, because having an irreversible mutation is as deleterious as having two reversible mutations. Based on d^*, the Muller's ratchet process is illustrated in Figure 5.3. This ratchet is different from that in the previous section (see Figure 5.2) because a ratchet click can occur in either direction. Let us consider the situation where the least-loaded class has $d^* = d_0$ mutations. A ratchet click occurs in the forward direction when the class $d^* = d_0$ goes extinct, as in the previous section. We also need to consider a click in the backward direction, when an individual with $d^* = d_0 - 1$ mutations arises by gene conversion, and its descendants become the majority of the population, thereby constituting the new least-loaded class, with $d^* = d_0 - 1$. Clicks in both directions simply change the number of reversible mutations, and only a part of the forward clicks can cause gene loss. The analytical approach

I use here is quite different from that in the previous case, but is similar to that of Goyal *et al.* (2012), who incorporated back mutations into the model of Muller's ratchet for single-copy genes. Following Goyal *et al.* (2012), I consider the click process in each direction separately.

I first consider clicks in the forward direction, which increases d^*. I derive the expected waiting time until the next click in the forward direction, T_F, from which the rate of gene loss will be derived. Let $\bar{H}$ be the average number of reversible mutations per individual, and denote the total rate of production of deleterious mutations per chromosome as U^*. We need to incorporate the following three types of deleterious mutation to derive U^*: irreversible mutations that arise in single-copy genes at the rate uL_1, irreversible mutations that arise in duplicated genes at the rate $(u+c)\bar{H}$, and reversible mutations that arise in duplicated genes at the rate $2u(L_2 - \bar{H})$. U^* is then given by

$$U^* = uL_1 + (u+c)\bar{H} + 2u(L_2 - \bar{H}) \tag{5.11}$$

as a sum of the three types, and the size of the least-loaded class is

$$N_e^* = N\exp(-U^*/s). \tag{5.12}$$

From N_e^*, T_F can be obtained in a similar manner to the previous section. When $N_e^* s > 1$ (i.e., the slow ratchet regime), T_F, can be obtained from Equation 5.6 by substituting U with U^* and T with T_F. When $N_e^* s < 1$ (i.e., the fast ratchet regime), T_F is given by Equation 5.7 by substituting U with U^* and T with T_F. Therefore, the gene loss rate per gene for a single-copy gene and that for a pair of duplicated genes (R_1 and R_2, respectively) can be derived as

$$\begin{aligned} R_1 &= \frac{uL_1}{U^*}\frac{1}{L_1 T_F} \\ &= \frac{u}{U^*}\frac{1}{T_F} \\ R_2 &= \frac{(u+c)\bar{H}}{U^*}\frac{1}{L_2 T_F}, \end{aligned} \tag{5.13}$$

because these rates are proportional to $1/T_F$ and the rates of mutation.

It should be noted that R_1 and R_2 are functions of $\bar{H}$, which can be obtained as follows. The dynamics of $\bar{H}$ involve both forward and backward processes. That is, if we let ΔH_F and ΔH_B be the expected changes in $\bar{H}$ per generation in the forward and backward processes, respectively, the expected change in $\bar{H}$ per generation is given by

$$\frac{d\bar{H}}{d\tau} = \Delta H_F + \Delta H_B. \tag{5.14}$$

I here explain how $\bar{H}$ behaves when a forward click occurs. $\bar{H}$ increases by one when a forward click occurs by the fixation of a reversible mutation in duplicated genes, and decreases by one when it occurs by the fixation of an irreversible mutation in duplicated genes. Because these events occur at rates $\frac{2u(L_2-\bar{H})}{U^* T_F}$ and $L_2 R_2$, respectively, ΔH_F is given by

$$\Delta H_F = \frac{2u(L_2 - \bar{H})}{U^* T_F} - L_2 R_2. \tag{5.15}$$

I will below obtain ΔH_B in the following derivation for the backward process.

I next consider clicks in the backward direction, where $\bar{H}$ decreases by one. I first derive the expected waiting time until the next click in the backward direction, T_B. A backward click usually occurs when a reversible mutation is removed by gene conversion in an individual in the least-loaded class and its descendants become the majority of the population, resulting in a new least-loaded class. When $N_e^* s > 1$, the treatment of the new least-loaded class is relatively simple because its fate is determined quickly. Suppose a new least-loaded class with $d^* - 1$ arises by gene conversion in the population where the least-loaded class is d^*. Because of strong selection, the new least-loaded class spreads in the population quickly with probability $\approx 2s$ (Haldane 1927), otherwise becomes extinct. Therefore, T_B is given by

$$T_B \approx (2sc\bar{H}N_e^*)^{-1}, \tag{5.16}$$

because gene conversion creates a new least-loaded class at rate $c\bar{H}N_e^*$ per generation.

When $N_e^* s < 1$, the treatment of the new least-loaded class is not straightforward. Because selection is weak, the frequency of the newly arisen least-loaded class with $d^* - 1$ fluctuates because of genetic drift. The newly arisen least-loaded class could be maintained in the population for a while and become extinct by genetic drift, or it could increase in frequency to some extent when a backward click occurs (but it does not necessarily mean that the new least-loaded class becomes the majority). It is technically difficult to distinguish the two situations. Rouzine *et al.* (2008) proposed that the least-loaded class can be considered to be lost when its frequency is smaller than $\frac{1}{S^* N}$, where $S^* = U^* v(1 - \log v)$. Following this proposition, I assume that the frequency of the new least-loaded class is significantly increased (i.e., it is considered as a backward click) when the frequency reaches $\frac{1}{S^* N}$, an event which occurs with probability S^*. Then, because the expected size of the least-loaded class is approximately given by $N_e^* \approx \frac{\exp(S^* T_F) - 1}{S^{*2} T_F}$ (see Rouzine *et al.* 2008), T_B is approximately given by

$$\begin{aligned} T_B &\approx \Big(\frac{\exp(S^* T_F) - 1}{S^* T_F} c\bar{H} \Big)^{-1} \\ &= \frac{1 - \log v}{(e/v - 1) c\bar{H}}, \end{aligned} \tag{5.17}$$

where e is Euler's number. From T_B, it is straightforward to obtain ΔH_B. Because a backward click always reduces $\bar{H}$ by one, which occurs at rate $1/T_B$, we have

$$\Delta H_B = -1/T_B. \tag{5.18}$$

Together with Equations 5.14 and 5.15, we are now ready to compute $\frac{d\bar{H}}{d\tau}$. This treatment is general, in that we can obtain the temporal change in $\bar{H}$ from any initial condition.

To check the performance of Equation 5.13, I compare it with simulation results in Figures 5.4 and 5.5 (see above for details about the simulations). Although we can compute R_1 and R_2 using Equation 5.13 for any initial values of $\bar{H}$, I use a treatment with no initial conditions specified, because I am interested in R_1 and R_2 conditional on L_1 and L_2 in a steady state, in which the initial condition is relatively unimportant. To obtain R_1 and R_2 conditional on L_1 and L_2, I assume that the frequency of reversible mutation is in equilibrium.

Then, $\bar{H}$ is determined from Equations 5.13 and 5.14 such that $\frac{d}{d\tau}\frac{\bar{H}}{L_2} = \frac{1}{L_2}\frac{d\bar{H}}{d\tau} + \frac{\bar{H}}{L_2}R_2 = 0$. Using this $\bar{H}$, I derived R_1 and R_2 by Equation 5.13.

Figure 5.4 shows the results of two extreme cases: In one case, the chromosome consists only of duplicated genes ($L_1 = 0, L_2 = 2,000$), and in the other case, it consists only of single-copy genes ($L_1 = 2,000, L_2 = 0$). In the case of all duplicates, since Equation 5.13 is applicable to the case of $t_1 = t_2$, let us focus on the result represented by the red circles. The result for the case of all single-copy genes is represented by black broken lines. Equation 5.13 agrees well with the simulation results, unless the gene conversion rate is very high.

In the strong selection case (Figure 5.4A), R_2 is strongly affected by the gene conversion rate. When the gene conversion rate is very low ($c = 10^{-7}$), R_2 is much higher than R_1 in the case of all single-copy genes, because U^* is elevated due to the increase in copy number caused by duplication (see Equation 5.11). As the gene conversion rate increases, R_2 decreases, and then drops dramatically when $c \sim 10^{-4}$, producing a bad fit between Equation 5.13 and the simulation result. This situation arises because reversible mutations at duplicated genes are quickly removed by gene conversion in this regime. Individuals with a reversible mutation in the second most loaded class are quickly transferred into the least-loaded class, which increases the size of the least-loaded class and retards its extinction. In this situation, d^* in the population does not follow a Poisson distribution, explaining why the simulation result is not well explained by my derivation (Equation 5.12), in which a Poisson distribution is used for the distribution of d^*.

In the weak selection case (Figure 5.4B), R_2 is relatively robust to the gene conversion rate. In this regime, N_e^* is small enough for random genetic drift to dominate, and R_2 is roughly proportional to the rate of generation of irreversible mutations per gene, $(u+c)\bar{H}/L_2$ (see Equation 5.13). When the gene conversion rate is very low ($c = 10^{-7}$), R_2 is almost identical to R_1 in the case of all single-copy genes (Figure 5.4B). This phenomenon can be explained by considering the fate of a newly arisen mutation, as shown in Figure 5.1C, in which gene conversion should be ignored. If a mutation arises in one copy, given a small N_e^*, the mutation can become fixed in one copy with a specific probability. Once it is fixed, as my model does not allow back mutation, the state with one reversible mutation (middle in Figure 5.1C) is prolonged, because this mutation cannot be removed (if gene conversion is ignored). The next event that could happen is that an independent mutation fixes in the other copy, causing a loss of the duplicated genes (the lower case in the right part in Figure 5.1C). Thus, if we consider a chromosome with L_2 pairs of duplicates in a steady state, it is likely that most pairs would be in this state ($\bar{H} \sim L_2$), because genes with their functions already lost are out of the system. Given this situation, the rate at which another mutation causing a gene loss is generated is approximately u per gene, which is identical to that of the all single-copy case, explaining the similar gene loss rates in the two cases. As the gene conversion rate increases, R_2 decreases because gene conversion removes reversible mutations to some extent, resulting in $\bar{H} \ll L_2$.

In Figure 5.5, I consider a chromosome in which single-copy genes and duplicated genes coexist. It was assumed that $L_1 = L_2 = 1,000$ and other parameters were the same as those used for Figure 5.4. In the additive selection case (red circles), Equation 5.13 is in a good agreement with the simulation results unless the gene conversion rate is very large.

In the strong selection case, R_2 exhibits behavior similar to that shown in Figure 5.4A,

but R_1 is quite different. When the gene conversion rate is very low ($c = 10^{-7}$), R_1 is much higher than that of the all single-copy case, because U^* elevated by gene duplication reduces N_e^*, so that the ratchet clicks in the forward direction occur more frequently (see Equations 5.11–5.13). Unless the gene conversion rate is very high ($c < 10^{-4}$), R_1 is quite robust to c, because gene conversion in duplicated genes should not have a direct effect on mutations in single-copy genes. When the gene conversion rate is very high ($c > 10^{-4}$), R_1 starts decreasing with increasing c. The fit of Equations 5.13 to the simulation result is not good for the same reason as that in Figure 5.4A.

When selection is weak, R_2 is very similar to that in Figure 5.4B. R_1 is less affected by the gene conversion rate, because N_e is small enough for random genetic drift to dominate, and the gene loss rate is roughly proportional to the rate of generation of irreversible mutations, which is constant for u in single-copy genes.

Next, I focus on the long-term degeneration process. $L_1(\tau)$ and $L_2(\tau)$ are the numbers of remaining single-copy genes and duplicated gene pairs, respectively, and $\bar{H}(\tau)$ is the average number of reversible mutations per individual at time τ. By using Equations 5.13 and 5.14, the differential equations for $L_1(\tau)$, $L_2(\tau)$ and $\bar{H}(\tau)$ are given by

$$\begin{aligned} \frac{dL_1(\tau)}{d\tau} &= -L_1 R_1 \\ \frac{dL_2(\tau)}{d\tau} &= -L_2 R_2 \\ \frac{d\bar{H}(\tau)}{d\tau} &= \Delta H_F + \Delta H_B, \end{aligned} \tag{5.19}$$

from which we can compute the way in which $L_1(\tau)$, $L_2(\tau)$ and $\bar{H}(\tau)$ change over time.

To check the accuracy of Equation 5.19, I performed simulations (Figure 5.6C). In the initial state of the simulation, each chromosome had $1,000$ intact single-copy genes and $1,000$ intact duplicated pairs of genes ($L_1(0) = L_2(0) = 1,000$ and $\bar{H}(0) = 0$). Two gene conversion rates ($c = 10^{-4}, 10^{-6}$) were considered. It was found that, at both of the two gene conversion rates, single-copy genes decreased faster and duplicated genes decreased more slowly than in the case of all single-copy genes (black circles in Figure 5.6C), because the rapid decrease in the number of single-copy genes slows ratchet clicks in the forward direction. As a consequence, more duplicated genes remain functional than in the case of all single-copy genes. The deviation from the case of all single-copy genes is larger when the gene conversion rate is higher. A very similar result was obtained when the assumption of constant selection coefficient was violated. See Appendix B for details.

5.3.3 Duplication with an intermediate fitness effect of dosage

Finally, I consider the case of an intermediate degree of dosage effect, where $t_1 = t_2/2$ is assumed. Since it was difficult to obtain analytical results, I investigated this case using simulations. The green circles in Figure 5.4 show R_2, the gene loss rate in the case of all duplicated genes ($L_2 = 2,000$). In the strong selection case, R_2 generally decreases as c increases, whereas in the weak selection case, R_2 is almost identical to R_1 in the case of all single-copy genes. When both single-copy genes and duplicated genes coexist ($L_1 = L_2 = 1,000$, in green in Figure 5.5), the pattern is generally similar to that in Figure 5.4. In the strong selection case, R_1 and R_2 show a similar pattern to the additive case. Figure 5.6B

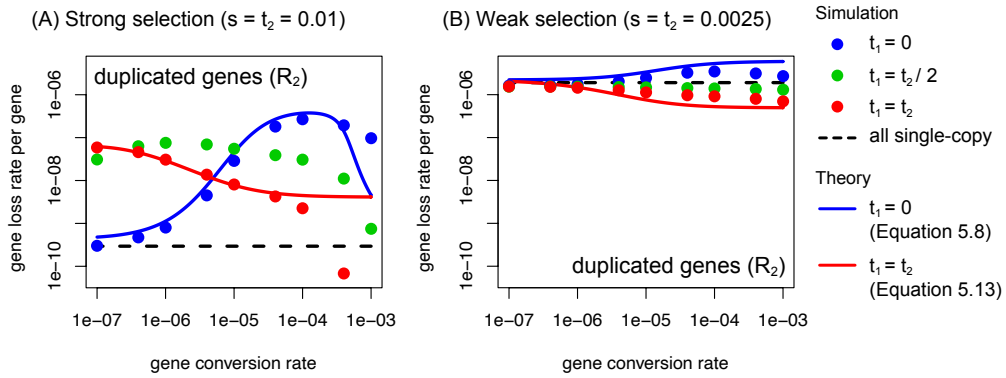

Figure 5.4: Gene loss rates per duplicated gene pair for (A) the strong selection case and (B) the weak selection case when all genes are single-copy ($L_1 = 2,000, L_2 = 0$) or all genes are duplicated genes ($L_1 = 0, L_2 = 2,000$). The closed circles are the simulation results for the case of all duplicated genes (R_2), while the black dashed lines are the simulation results for the case of all single-copy genes (R_1). The solid lines are the theoretical results, which are available for $t_1 = 0$ (blue) and $t_1 = t_2$ (red). $N = 10,000$, $u = 1.0 \times 10^{-5}$, and $s = t_2$ are assumed.

shows the long-term degeneration pattern. In Appendix B, I consider the case where s_i and $t_{2,i}$ are heterogeneous among loci. Overall, the behavior when $t_1 = t_2/2$ seems to be intermediate between those of the cases of no fitness effect of dosage ($t_1 = 0$) and additive effect ($t_1 = t_2$).

5.4 Discussion

Muller's ratchet is a process in which a non-recombining chromosome irreversibly accumulates deleterious mutations (Muller 1964). Muller's ratchet has been considered to play an important role in the evolution of Y chromosome (Bachtrog 2008). Previous theories regarding Muller's ratchet considered only single-copy genes, and the way in which Muller's ratchet works in duplicated genes has not been fully understood. Because there are a number of duplicated genes on the Y chromosome in many species (Skaletsky *et al.* 2003, Hughes *et al.* 2010, 2012, 2020, Soh *et al.* 2014, Bachtrog *et al.* 2019, Peichel *et al.* 2020), in this work I developed a theory for the process of Muller's ratchet on a non-recombining chromosome in which single-copy and duplicated genes coexist. Mutations in duplicated genes can be considered to be a kind of epistatic mutations, because the strength of selection on a mutation depends on whether the other copy already has a mutation or not. Several studies have investigated the effect of epistasis on the process of Muller's ratchet (Charlesworth *et al.* 1993b, Kondrashov 1994, Butcher 1995, Jain 2008). However, these studies have focused on more complex epistatic interactions, in which the fitness effect of a mutation depends upon mutations at all other loci.

This work focuses on the role of gene conversion between duplicates, which has two opposite effects on the degeneration process. Degeneration is promoted if gene conversion leads to the mutation of both copies, while degeneration is retarded if gene conversion restores both copies to the original state. My theoretical results demonstrate that the effect of gene conversion is complex, depending on the fitness effect of dosage change by gene duplication. When duplication has no fitness effect by dosage, gene conversion increases the rates of loss of both single-copy and duplicated genes (see Figure 5.5). In the case of an additive dosage effect on fitness, the gene loss rate of single-copy genes is elevated by gene duplication, while gene conversion prevents duplicated genes from losing their functions (see Figure 5.5). These

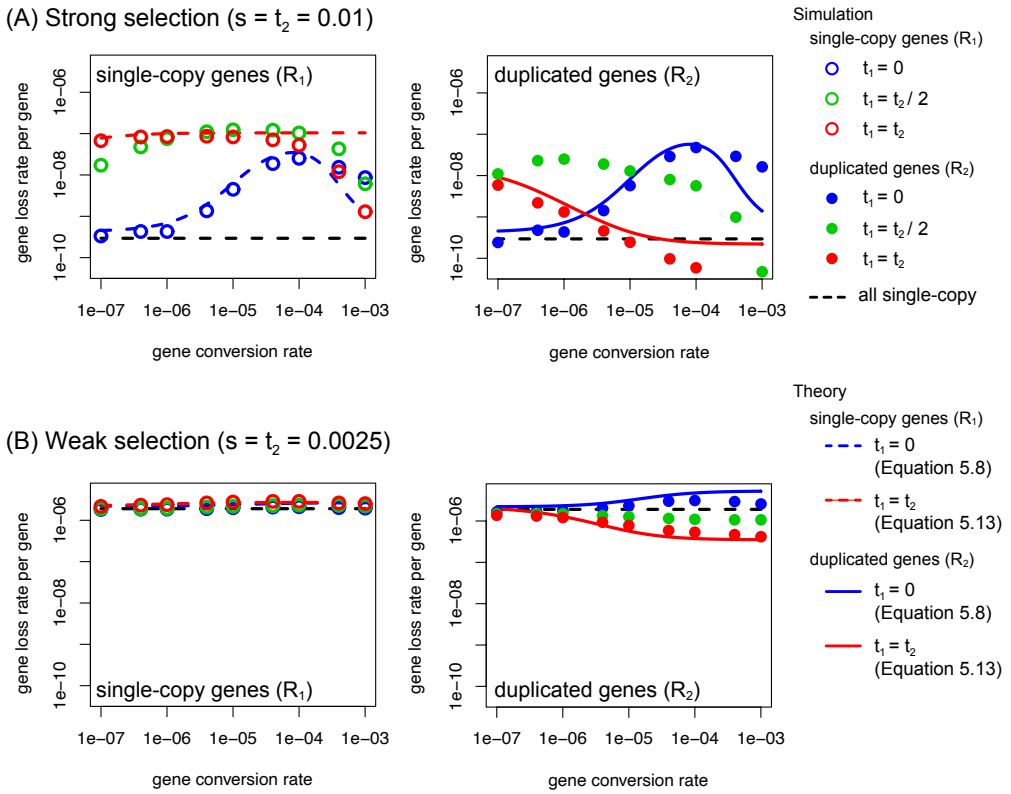

Figure 5.5: Gene loss rates per gene (or gene pair) for (A) the strong selection case and (B) the weak selection case when single-copy genes and duplicated genes coexist ($L_1 = L_2 = 1,000$). The left panels show the gene loss rate of single-copy genes (R_1) and the right panels show that of duplicated genes (R_2). The open and closed circles are the simulation results, and the colored lines show the theoretical results, which are available for $t_1 = 0$ (blue) and $t_1 = t_2$ (red). The black dashed lines are the simulation results for the case of all single-copy genes. $N = 10,000$, $u = 1.0 \times 10^{-5}$ are assumed.

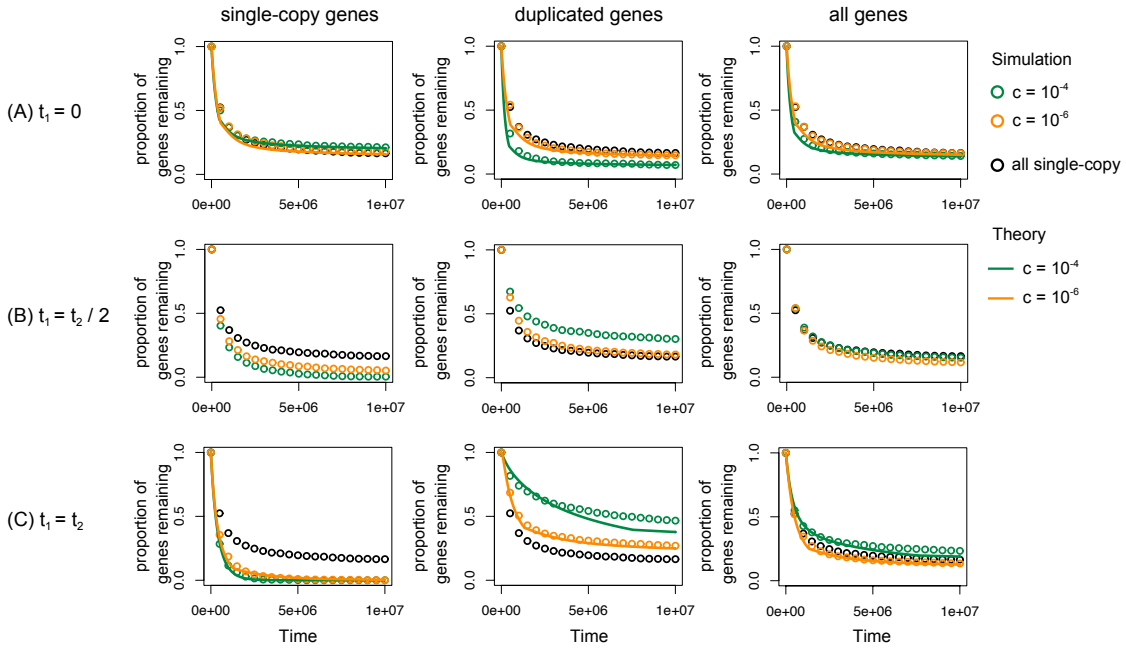

Figure 5.6: Long-term degeneration process with different dominance: (A) $t_1 = 0$, (B) $t_1 = t_2/2$, and (C) $t_1 = t_2$ are assumed. The open circles represent simulation results. The solid lines are theoretical predictions, which are available for (A) and (C). Other parameters are $N = 10,000$, $u = 1.0 \times 10^{-5}$, $s = t_2 = 0.0025$, and $L_1 = L_2 = 1,000$.

patterns are more clearly observed when selection is strong.

This complex nature of the effect of Muller's ratchet on the Y chromosome has not previously been identified. Most of the previous studies have considered only the positive effects of gene conversion. For example, Connallon and Clark (2010) showed that gene conversion works positively in the conservation of essential duplicated genes, assuming mutations are lethal when present in both copies. My work demonstrates that this is not the case when duplicated genes are not essential (see the Introduction for the difference in the models). Mano and Innan (2008) considered a "single" pair of duplicated gene in a Wright-Fisher population, so the effect of linked genes was ignored, and demonstrated that deleterious mutations could be efficiently removed by gene conversion, which suggests that gene conversion could slow the degeneration process of duplicated genes (similar to Connallon and Clark (2010)). However, I found that, when multiple genes are completely linked and multiple mutations exist simultaneously, gene duplication can accelerate the degeneration process in some cases.

My results suggest that understanding the way in which the Y chromosome evolves requires the consideration of a number of parameters, including the number of duplicated genes and their fitness effect through dosage increase. Unfortunately, there are very few empirical data that allow us to estimate those parameters. Theory suggests that dosage increase of many duplicated genes may be beneficial because duplication is more likely to be fixed in the population when it has a direct selective advantage (Clark 1994, Connallon and Clark 2010, Innan and Kondrashov 2010). If so, my theory predicts that duplicated genes are well-conserved by gene conversion, while linked single-copy genes are lost rapidly. However, the situation should be much more complicated, particularly in the early stages of the evolution of the Y chromosome, when duplication-rich Y chromosomes may be developed. Duplicated genes with no dosage effect on fitness may be fixed with a linked gene which has a selective advantage due to a dosage effect. More data with reliable estimates of those selection parameters will give us deeper insights into the evolution of the Y chromosome.

Another important parameter is the gene conversion rate, which has been relatively well estimated in the palindrome regions of the human Y chromosome. Rozen *et al.* (2003) estimated the gene conversion rate of human palindrome as $2c = 2.2 \times 10^{-4}$ per nucleotide per generation, based on the amount of divergence between duplicates. Hallast *et al.* (2013) used a phylogenetic approach, and reported a similar but slightly smaller value ($2c = 2.9$ - 8.4×10^{-5}). At such a high gene conversion rate, my theory predicts that gene conversion plays a significant role in the degeneration of the Y chromosome. Although the gene conversion rate in other species has not been as well investigated, high sequence identity between duplicated copies is observed in many species (Soh *et al.* 2014, Hughes *et al.* 2020), suggesting that my theory would apply to a wide range of species.

5.5 Appendices

Appendix A: On the ad-hoc treatment in the simulation to keep L_1 and L_2 constant

In the simulation to obtain R_1 and R_2 conditional on L_1 and L_2 in a steady state, I used an ad-hoc treatment in which an intact single-copy gene, or an intact pair of duplicated genes, suddenly appears in all individuals when an irreversible mutation is fixed in the population.

The problem is that this method skips a burn-in period, in which some mutations could be accumulated. The performance of this ad-hoc method was verified using the following simulation. Let us assume that we would like to obtain R_1 and R_2 conditional on L_1^* and L_2^*. Then, we need to consider a degeneration process of a chromosome on which $L_1^0 = L_1^* + \Delta L_1$ single-copy genes and $L_2^0 = L_2^* + \Delta L_2$ duplicated genes are initially located, where $\Delta L_1, \Delta L_2$ should be sufficiently large. Then, the system waits for the state with the focal pair $(L_1, L_2) = (L_1^*, L_2^*)$, and we can continue the simulation run to obtain the waiting time for the next click. Very few simulation runs hit $(L_1, L_2) = (L_1^*, L_2^*)$, and all other runs are terminated when $L_1 < L_1^*$ or $L_2 < L_2^*$. This method is honest and correct, but requires a very large number of runs to accumulate a reasonable number of simulation runs that hit $(L_1, L_2) = (L_1^*, L_2^*)$. This is why I used the ad-hoc treatment in the main text. I here show how the ad-hoc treatment works in comparison with the correct simulation with a limited set of parameters.

I assumed that $N = 500$, $u = 2.0 \times 10^{-4}$ and $L_1 = L_2 = 1,000$. The gene conversion rate changed from 2.0×10^{-6} to 2.0×10^{-2}. In Figure 5.7A I assumed strong selection ($s = t_2 = 0.2$), while in Figure 5.7B, weak selection ($s = t_2 = 0.05$) was assumed. All population scaled parameters (Nu, Nc, Ns, Nt_1, and Nt_2) are identical to those in Figure 5.5 if scaled by the population size N. This process demonstrates that the results of the two methods are almost identical, indicating that my ad-hoc method works well.

Appendix B: Variable selection coefficients across loci

In this Appendix, I relax the assumption that all genes have identical effects on fitness, and explore the effect of varying fitness selection coefficients across genes on the long-term degeneration process. Three types of dosage effect on duplication are considered: $t_{1,i} = 0$, $t_{1,i} = t_{2,i}/2$, and $t_{1,i} = t_{2,i}$. I performed simulations for these three types of dosage effect, with variation allowed between individual gene pairs. I randomly chose s_i and $t_{2,i}$, assuming they follow an exponential distribution with mean $\bar{s}$, and they were shared by the simulations for the three types of dosage effect to focus on the effect due the dosage type alone. I simulated the case of all single-copy genes, in which I also used the parameters determined above ($s_i = t_{2,i-L_1}$ is assumed for $L_1 + 1 \leq i \leq L_1 + L_2$). All other parameters are the same as those used in the main text. Figure 5.8 shows the simulation result, which is qualitatively very similar to Figure 5.6.

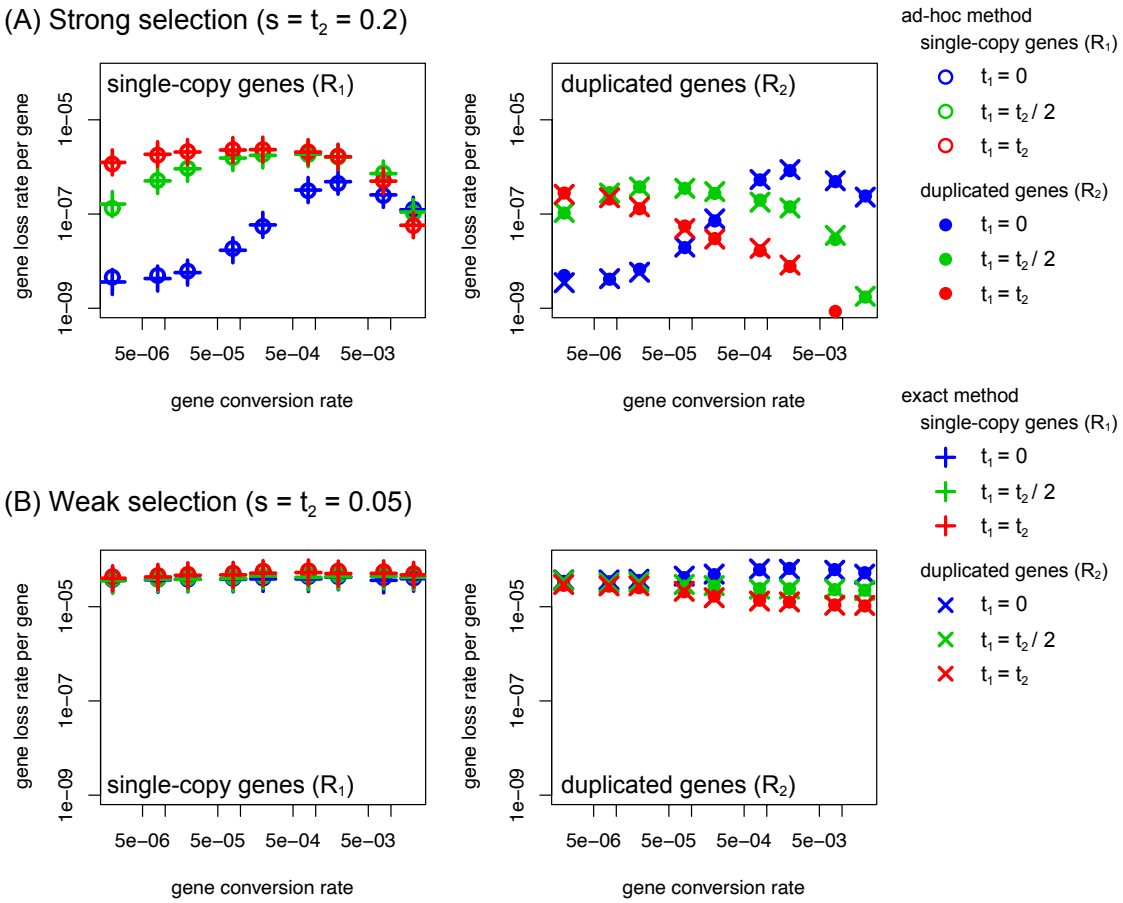

Figure 5.7: Verification my ad-hoc method. The results of my ad-hoc method (circles) are compared with the results of the exact method (crosses). $N = 500$, $u = 2.0 \times 10^{-4}$, $L_1 = L_2 = 1,000$ were assumed in the simulations.

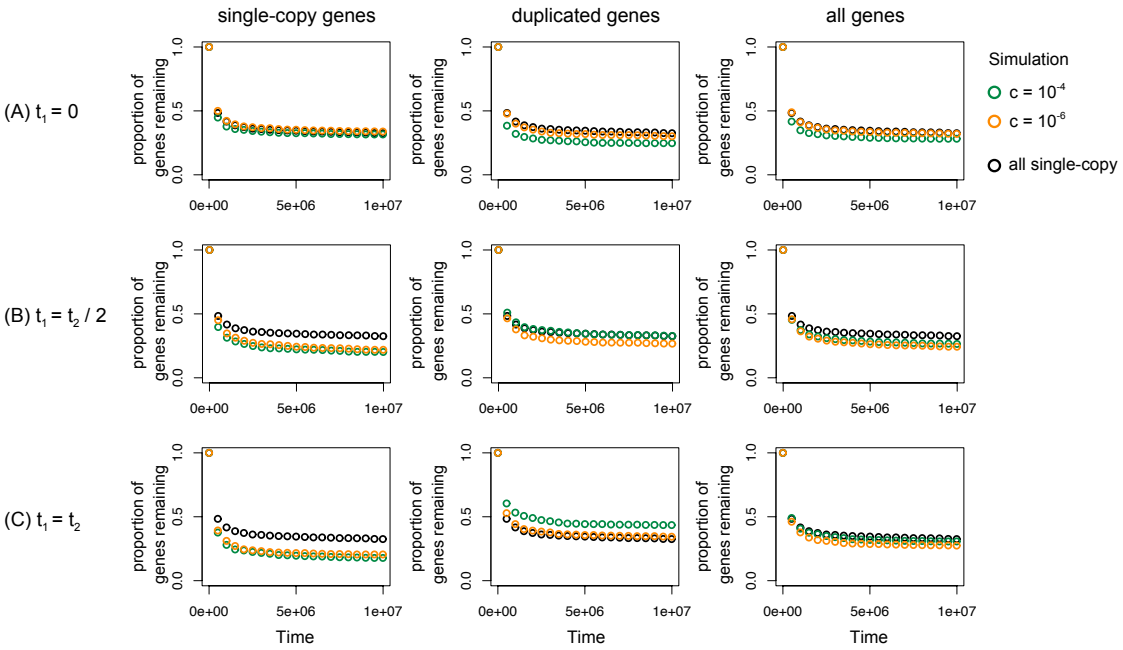

Figure 5.8: Long-term degeneration process for different dominances when the selection coefficients are not constant over genes: (A) $t_{1,i} = 0$, (B) $t_{1,i} = t_{2,i}/2$, and (C) $t_{1,i} = t_{2,i}$ are assumed. The strength of selection (s_i, $t_{2,i}$) is randomly drawn from an exponential distribution with mean $\bar{s} = 0.0025$ (see text). Other parameters are $N = 10,000$, $u = 1.0 \times 10^{-5}$, and $L_1 = L_2 = 1,000$.

Chapter 6

General Discussion

Many evolutionary events are results of interactions among multiple loci and multiple populations. Therefore, it is very important to understand these interactions theoretically. However, when natural selection is at work, analysis of evolutionary dynamics in these situations are generally difficult and theoretical studies are still not sufficient. In this thesis, I focused on two examples of such unresolved situations, local adaptation and the evolution of sex chromosomes, and mathematically described their evolutionary dynamics. In these complex situations, rigorous and general mathematical analysis is yet not possible, but I overcame this difficulty by developing approximate formulas that are valid over a biologically important range of parameters.

The approximations used in this thesis can be classified into three categories: (i) the branching process approximation for alleles in low frequency, (ii) reduction to a one-dimensional model, and (iii) reduction to a neutral model. In the branching process approximation (i), second and higher order terms of the allele frequency are ignored. This approach is useful when the evolutionary dynamics are largely determined while the focal allele is at low frequency. A typical example of such evolutionary process is the fixation (or establishment) probability of alleles that are subject to positive selection. In this thesis, I used this approximation to derive the establishment probability of locally adaptive alleles (Chapter 2) and the establishment probability of new sex-determining alleles (Chapter 4).

The second kind of approximation is the reduction to a one-dimensional model (ii). Although a full multi-dimensional model is not tractable, if the dynamics can be successfully approximated by a combination of one-dimensional models, it may be possible to describe the dynamics. I took this strategy to derive the establishment probability of magic trait alleles (Chapter 3). In this study, I approximated the dynamics in a population in which a magic trait allele is disfavored. When the allele has low frequency, I used the branching process approximation to derive the number of surviving alleles that successfully move to a favorable subpopulation. I then used "effective selection coefficient" (Yeaman and Otto 2011) and considered the subsequent dynamics as if the allele were effectively subject to selection in a one-population model. I also used the approximation by a one-dimensional model to derive the speed of Muller's ratchet (Chapter 5). In this study, I first approximated the generation rate of deleterious mutations at duplicated genes, using the one-dimensional diffusion approximation. Then, previous theories about one-dimensional Muller's ratchet were applied. These results demonstrate that this type of approximation is very useful.

The reduction to a neutral model is also an attractive strategy. I used this approximation to derive changes of nucleotide diversity during the local adaptation process (Chapter 2). In

this study, I used "effective migration rate" (Bengtsson 1985), which incorporates the effect of natural selection into migration rates. Using this approximation, the dynamics become neutral evolution in a two-population model. Although the analysis of the neutral two-population model is still limited, we can use Ohta-Kimura equation (Ohta and Kimura 1969) to derive moments of allele frequencies. This method is very effective when only neutral forces are at work. I show that this approximation works very well to describe the local adaptation process.

In summary, I have developed theories to consider evolutionary processes involving multiple population and multiple loci, using various approximations. In general, building theories of complex evolutionary processes is difficult due to mathematical constraints, but making appropriate approximations is a good way to understand such evolutionary processes. Species in nature live in a much more complex world than the models in this thesis. Further development of useful approximations will be needed in the future to understand evolutionary dynamics in the real world.

Acknowledgments

First of all, I would sincerely like to thank my supervisor Dr. Hideki Innan. I first met him when he visited my high school festival. He was interested in my (immature) research on the genetics of racehorse coat color and invited me to the field of population genetics. I can confidently say that without his enthusiastic invitation, I would never have thought of becoming a researcher. After the entrance into SOKENDAI, I had a very happy time thanks to his tremendous supports. I am deeply grateful to him for showing me the wonderful world of theoretical population genetics.

I would thank to my prior supervisors, Dr. Shohei Takuno. He helped me a lot, including genome data analysis and scientific writing. His kind advice in the early stages of my PhD program was necessary for me to have a satisfactory PhD program. I would also like to express thanks to my current sub-supervisors, Dr. Tatsuya Ota and Dr. Yukinori Onishi. Dr. Ota encouraged my research and gave me advice to improve my presentations. Dr. Onishi is my supervisor of sub-thesis and introduced me the field of philosophy of science. The study that I conducted for sub-thesis program improves my skills as a theoretical biologist. I would like to thank to my committee member Dr. Kosuke Teshima. Without his kind cooperation, I could not have completed this thesis.

I have been supported by Innan lab members and the people in ESB. They have made my everyday life enjoyable. I also thank to my parents. They arranged an environment where I could focus on my research. This work was partly supported by Japan Society for the Promotion of Science (JSPS) research fellowship for young scientists (DC1) and SOKENDAI.

References

Abramowitz, M. and I. A. Stegun, 1970 *Handbook of mathematical functions with formulas, graphs, and mathematical tables*. Dover.

Aeschbacher, S. and R. Bürger, 2014 The effect of linkage on establishment and survival of locally beneficial mutations. Genetics **197**: 317–336.

Akerman, A. and R. Bürger, 2014 The consequences of gene flow for local adaptation and differentiation: a two-locus two-deme model. J. Math. Biol. **68**: 1135–1198.

Arnegard, M. E. and A. S. Kondrashov, 2004 Sympatric speciation by sexual selection alone is unlikely. Evolution **58**: 222–237.

Arnheim, N., 1983 Concerted evolution of multigene families. In *Evolution of Genes and Proteins*, edited by M. Nei and R. K. Koehn, pp. 38–61, Sinauer, Sunderland, MA.

Bachtrog, D., 2008 The temporal dynamics of processes underlying Y chromosome degeneration. Genetics **179**: 1513–1525.

Bachtrog, D., 2013 Y-chromosome evolution: emerging insights into processes of Y-chromosome degeneration. Nat. Rev. Genet. **14**: 113–124.

Bachtrog, D., S. Mahajan, and R. Bracewell, 2019 Massive gene amplification on a recently formed drosophila Y chromosome. Nat. Ecol. Evol. **3**: 1587–1597.

Bachtrog, D., J. E. Mank, C. L. Peichel, M. Kirkpatrick, S. P. Otto, T.-L. Ashman, M. W. Hahn, J. Kitano, I. Mayrose, R. Ming, *et al.*, 2014 Sex determination: why so many ways of doing it? PLoS Biol. **12**: e1001899.

Barton, N. H., 1987 The probability of establishment of an advantageous mutant in a subdivided population. Genet. Res. **50**: 35–40.

Barton, N. H., 1995 Linkage and the limits to natural selection. Genetics **140**: 821–841.

Barton, N. H., 1998 The effect of hitch-hiking on neutral genealogies. Genet. Res. **72**: 123–133.

Bengtsson, B. O., 1985 The flow of genes through a genetic barrier. In *Evolution: Essays in Honor of John Maynard Smith.*, edited by J. J. Greenwood, P. H. Harvey, and M. Slatkin, pp. 31–42, Cambridge University Press, New York.

Beukeboom, L. W. and N. Perrin, 2014 *The evolution of sex determination*. Oxford University Press, Oxford.

Blaser, O., C. Grossen, S. Neuenschwander, and N. Perrin, 2013 Sex-chromosome turnovers induced by deleterious mutation load. Evolution **67**: 635–645.

Blaser, O., S. Neuenschwander, and N. Perrin, 2014 Sex-chromosome turnovers: the hot-potato model. Am. Nat. **183**: 140–146.

Bull, J. J. and E. L. Charnov, 1977 Changes in the heterogametic mechanism of sex determination. Heredity **39**: 1–14.

Bürger, R. and K. A. Schneider, 2006 Intraspecific competitive divergence and convergence under assortative mating. Am. Nat. **167**: 190–205.

Butcher, D., 1995 Muller's ratchet, epistasis and mutation effects. Genetics **141**: 431–437.

Charlesworth, B. and D. Charlesworth, 1997 Rapid fixation of deleterious alleles can be caused by Muller's ratchet. Genet. Res. **70**: 63–73.

Charlesworth, B. and D. Charlesworth, 2000 The degeneration of Y chromosomes. Philos. Trans. R. Soc. Lond. B **355**: 1563–1572.

Charlesworth, B., C. Y. Jordan, and D. Charlesworth, 2014 The evolutionary dynamics of sexually antagonistic mutations in pseudoautosomal regions of sex chromosomes. Evolution **68**: 1339–1350.

Charlesworth, B., M. Morgan, and D. Charlesworth, 1993a The effect of deleterious mutations on neutral molecular variation. Genetics **134**: 1289–1303.

Charlesworth, B., M. Nordborg, and D. Charlesworth, 1997 The effects of local selection, balanced polymorphism and background selection on equilibrium patterns of genetic diversity in subdivided populations. Genet. Res. **70**: 155–174.

Charlesworth, D., M. Morgan, and B. Charlesworth, 1993b Mutation accumulation in finite outbreeding and inbreeding populations. Genet. Res. **61**: 39–56.

Clark, A. G., 1994 Invasion and maintenance of a gene duplication. Proc. Natl. Acad. Sci. USA **91**: 2950–2954.

Connallon, T. and A. G. Clark, 2010 Gene duplication, gene conversion and the evolution of the Y chromosome. Genetics **186**: 277–286.

Connallon, T. and A. G. Clark, 2012 A general population genetic framework for antagonistic selection that accounts for demography and recurrent mutation. Genetics **190**: 1477–1489.

Cotto, O. and M. R. Servedio, 2017 The roles of sexual and viability selection in the evolution of incomplete reproductive isolation: From allopatry to sympatry. Am. Nat. **190**: 680–693.

Coyne, J. A. and H. A. Orr, 2004 *Speciation*. Sinauer.

Crow, J. F. and M. Kimura, 1970 *An introduction to population genetics theory*. Blackburn Press, New Jersey.

Dieckmann, U. and M. Doebeli, 1999 On the origin of species by sympatric speciation. Nature **400**: 354–357.

Doebeli, M. and U. Dieckmann, 2003 Speciation along environmental gradients. Nature **421**: 259–264.

Durrett, R. and J. Schweinsberg, 2004 Approximating selective sweeps. Theor. Popul. Biol. **66**: 129–138.

Etheridge, A., P. Pfaffelhuber, and A. Wakolbinger, 2006 An approximate sampling formula under genetic hitchhiking. Ann. Appl. Probab. **16**: 685–729.

Ewens, W., 1973 Conditional diffusion processes in population genetics. Theor. Popul. Biol. **4**: 21–30.

Ewens, W. J., 2004 *Mathematical population genetics*. Springer, New York.

Feder, J. L., S. P. Egan, and P. Nosil, 2012a The genomics of speciation-with-gene-flow. Trends Genet. **28**: 342–350.

Feder, J. L., R. Gejji, S. Yeaman, and P. Nosil, 2012b Establishment of new mutations under divergence and genome hitchhiking. Philos. Trans. R. Soc. Lond. B Biol. Sci. **367**: 461–474.

Fisher, R. A., 1930 *The genetical theory of natural selection*. Clarendon Press.

Gavrilets, S., 2004 *Fitness landscapes and the origin of species*. Princeton University Press.

Gavrilets, S. and N. Gibson, 2002 Fixation probabilities in a spatially heterogeneous environment. Popul. Ecol. **44**: 51–58.

Gessler, D. D., 1995 The constraints of finite size in asexual populations and the rate of the ratchet. Genet. Res. **66**: 241–253.

Gordo, I. and B. Charlesworth, 2000a The degeneration of asexual haploid populations and the speed of Muller's ratchet. Genetics **154**: 1379–1387.

Gordo, I. and B. Charlesworth, 2000b On the speed of muller's ratchet. Genetics **156**: 2137–2140.

Goyal, S., D. J. Balick, E. R. Jerison, R. A. Neher, B. I. Shraiman, and M. M. Desai, 2012 Dynamic mutation–selection balance as an evolutionary attractor. Genetics **191**: 1309–1319.

Graves, J. A. M., 2004 The degenerate Y chromosome–can conversion save it? Reprod. Fertil. Dev. **16**: 527–534.

Haigh, J., 1978 The accumulation of deleterious genes in a population–Muller's ratchet. Theor. Popul. Biol. **14**: 251–267.

Haldane, J. B. S., 1927 A mathematical theory of natural and artificial selection, part V: selection and mutation. Proc. Camb. Philos. Soc. **23**: 838–844.

Hallast, P., P. Balaresque, G. R. Bowden, S. Ballereau, and M. A. Jobling, 2013 Recombination dynamics of a human Y-chromosomal palindrome: rapid GC-biased gene conversion, multi-kilobase conversion tracts, and rare inversions. PLoS Genet. **9**: e1003666.

Higashi, M., G. Takimoto, and N. Yamamura, 1999 Sympatric speciation by sexual selection. Nature **402**: 523–526.

Hudson, R. R. and N. L. Kaplan, 1988 The coalescent process in models with selection and recombination. Genetics **120**: 831–840.

Hudson, R. R. and N. L. Kaplan, 1995 Deleterious background selection with recombination. Genetics **141**: 1605–1617.

Hughes, J. F., H. Skaletsky, L. G. Brown, T. Pyntikova, T. Graves, R. S. Fulton, S. Dugan, Y. Ding, C. J. Buhay, C. Kremitzki, *et al.*, 2012 Strict evolutionary conservation followed rapid gene loss on human and rhesus Y chromosomes. Nature **483**: 82–86.

Hughes, J. F., H. Skaletsky, T. Pyntikova, T. A. Graves, S. K. Van Daalen, P. J. Minx, R. S. Fulton, S. D. McGrath, D. P. Locke, C. Friedman, *et al.*, 2010 Chimpanzee and human Y chromosomes are remarkably divergent in structure and gene content. Nature **463**: 536–539.

Hughes, J. F., H. Skaletsky, T. Pyntikova, N. Koutseva, T. Raudsepp, L. G. Brown, D. W. Bellott, T.-J. Cho, S. Dugan-Rocha, Z. Khan, *et al.*, 2020 Sequence analysis in *Bos taurus* reveals pervasiveness of X–Y arms races in mammalian lineages. Genome Res. **30**: 1716–1726.

Innan, H., 2002 A method for estimating the mutation, gene conversion and recombination parameters in small multigene families. Genetics **161**: 865–872.

Innan, H., 2003 The coalescent and infinite-site model of a small multigene family. Genetics **163**: 803–810.

Innan, H. and F. Kondrashov, 2010 The evolution of gene duplications: classifying and distinguishing between models. Nat. Rev. Genet. **11**: 97–108.

Jain, K., 2008 Loss of least-loaded class in asexual populations due to drift and epistasis. Genetics **179**: 2125–2134.

Kamiya, T., W. Kai, S. Tasumi, A. Oka, T. Matsunaga, N. Mizuno, M. Fujita, H. Suetake, S. Suzuki, S. Hosoya, *et al.*, 2012 A trans-species missense snp in amhr2 is associated with sex determination in the tiger pufferfish, takifugu rubripes (fugu). PLoS Genet. **8**: e1002798.

Kaplan, N. L., T. Darden, and R. R. Hudson, 1988 The coalescent process in models with selection. Genetics **120**: 819.

Kaplan, N. L., R. R. Hudson, and C. H. Langley, 1989 The "hitchhiking effect" revisited. Genetics **123**: 887–899.

Kim, Y. and T. Maruki, 2011 Hitchhiking effect of a beneficial mutation spreading in a subdivided population. Genetics **189**: 213–226.

Kimura, M., 1954 Process leading to quasi-fixation of genes in natural populations due to random fluctuation of selection intensities. Genetics **39**: 280–295.

Kimura, M., 1957 Some problems of stochastic processes in genetics. Ann. Math. Statist. **28**: 882–901.

Kimura, M., 1962 On the probability of fixation of mutant genes in a population. Genetics **47**: 713–719.

Kimura, M. *et al.*, 1955 Stochastic processes and distribution of gene frequencies under natural selection. Cold Spring Harb. Symp. Quant. Biol. **20**: 33–53.

Kimura, M. and T. Ohta, 1969 The average number of generations until fixation of a mutant gene in a finite population. Genetics **61**: 763.

Kirkpatrick, M. and R. F. Guerrero, 2014 Signatures of sex-antagonistic selection on recombining sex chromosomes. Genetics **197**: 531–541.

Kirkpatrick, M. and S. L. Nuismer, 2004 Sexual selection can constrain sympatric speciation. Proc. R. Soc. Lond. B **271**: 687–693.

Kirkpatrick, M. and S. Peischl, 2013 Evolutionary rescue by beneficial mutations in environments that change in space and time. Philos. Trans. R. Soc. Lond. B Biol. Sci. **368**: 20120082.

Kirkpatrick, M. and V. Ravigné, 2002 Speciation by natural and sexual selection: models and experiments. Am. Nat. **159**: S22–S35.

Kisdi, É. and T. Priklopil, 2011 Evolutionary branching of a magic trait. J. Math. Biol. **63**: 361–397.

Kondrashov, A. S., 1994 Muller's ratchet under epistatic selection. Genetics **136**: 1469–1473.

Kopp, M., M. R. Servedio, T. C. Mendelson, R. J. Safran, R. L. Rodríguez, M. E. Hauber, E. C. Scordato, L. B. Symes, C. N. Balakrishnan, D. M. Zonana, *et al.*, 2018 Mechanisms of assortative mating in speciation with gene flow: connecting theory and empirical research. Am. Nat. **191**: 1–20.

Koyama, T., M. Nakamoto, K. Morishima, R. Yamashita, T. Yamashita, K. Sasaki, Y. Kuruma, N. Mizuno, M. Suzuki, Y. Okada, *et al.*, 2019 A SNP in a steroidogenic enzyme is associated with phenotypic sex in seriola fishes. Curr. Biol. **29**: 1901–1909.

Kozielska, M., F. Weissing, L. Beukeboom, and I. Pen, 2010 Segregation distortion and the evolution of sex-determining mechanisms. Heredity **104**: 100–112.

Krone, S. M. and C. Neuhauser, 1997 Ancestral processes with selection. Theor. Popul. Biol. **51**: 210–237.

Maan, M. E. and O. Seehausen, 2011 Ecology, sexual selection and speciation. Ecol. Lett. **14**: 591–602.

Mano, S. and H. Innan, 2008 The evolutionary rate of duplicated genes under concerted evolution. Genetics **180**: 493–505.

Marais, G. A., P. R. Campos, and I. Gordo, 2010 Can intra-Y gene conversion oppose the degeneration of the human Y chromosome? A simulation study. Genome Biol. Evol. **2**: 347–357.

Maruyama, T., 1970 On the fixation probability of mutant genes in a subdivided population. Genet. Res. **15**: 221–225.

Maruyama, T., 1974 The age of an allele in a finite population. Genet. Res. **23**: 137–143.

Matessi, C., A. Gimelfarb, and S. Gavrilets, 2001 Long-term buildup of reproductive isolation promoted by disruptive selection: how far does it go? Selection **2**: 41–64.

Maynard Smith, J. and J. Haigh, 1974 The hitch-hiking effect of a favourable gene. Genet. Res. **23**: 23–35.

Metzger, J. J. and S. Eule, 2013 Distribution of the fittest individuals and the rate of Muller's ratchet in a model with overlapping generations. PLoS Comput. Biol. **9**: e1003303.

Muller, H. J., 1964 The relation of recombination to mutational advance. Mutat. Res. **1**: 2–9.

Myosho, T., H. Otake, H. Masuyama, M. Matsuda, Y. Kuroki, A. Fujiyama, K. Naruse, S. Hamaguchi, and M. Sakaizumi, 2012 Tracing the emergence of a novel sex-determining gene in medaka, oryzias luzonensis. Genetics **191**: 163–170.

Nagylaki, T., 1980 The strong-migration limit in geographically structured populations. J. Math. Biol. **9**: 101–114.

Nagylaki, T. and Y. Lou, 2008 The dynamics of migration-selection models. In *Tutorials in Mathematical Biosciences IV: Evolution and Ecology*, Lecture Notes in Mathematics., pp. 117–170, Springer.

Neher, R. A. and B. I. Shraiman, 2012 Fluctuations of fitness distributions and the rate of Muller's ratchet. Genetics **191**: 1283–1293.

Neuhauser, C. and S. M. Krone, 1997 The genealogy of samples in models with selection. Genetics **145**: 519–534.

Newberry, M. G., D. M. McCandlish, and J. B. Plotkin, 2016 Assortative mating can impede or facilitate fixation of underdominant alleles. Theor. Popul. Biol. **112**: 14–21.

Nordborg, M., 1997 Structured coalescent processes on different time scales. Genetics **146**: 1501–1514.

Nosil, P., 2012 *Ecological speciation*. Oxford University Press.

Ohta, T., 1983 On the evolution of multigene families. Theor. Popul. Biol. **23**: 216–240.

Ohta, T. and M. Kimura, 1969 Linkage disequilibrium at steady state determined by random genetic drift and recurrent mutation. Genetics **63**: 229–238.

Oldham, K. B., J. Myland, and J. Spanier, 2010 *An atlas of functions: with equator, the atlas function calculator*. Springer.

Otto, S. P., M. R. Servedio, and S. L. Nuismer, 2008 Frequency-dependent selection and the evolution of assortative mating. Genetics **179**: 2091–2112.

Peichel, C. L., S. R. McCann, J. A. Ross, A. F. Naftaly, J. R. Urton, J. N. Cech, J. Grimwood, J. Schmutz, R. M. Myers, D. M. Kingsley, *et al.*, 2020 Assembly of the threespine stickleback Y chromosome reveals convergent signatures of sex chromosome evolution. Genome Biol. **21**: 1–31.

Pennings, P. S., M. Kopp, G. Meszéna, U. Dieckmann, and J. Hermisson, 2008 An analytically tractable model for competitive speciation. Am. Nat. **171**: E44–E71.

Pollak, E., 1966 On the survival of a gene in a subdivided population. J. Appl. Prob. **3**: 142–155.

Rettelbach, A., M. Kopp, U. Dieckmann, and J. Hermisson, 2013 Three modes of adaptive speciation in spatially structured populations. Am. Nat. **182**: E215–E234.

Ritchie, M. G., 2007 Sexual selection and speciation. Annu. Rev. Ecol. Evol. Syst. **38**: 79–102.

Rouzine, I. M., É. Brunet, and C. O. Wilke, 2008 The traveling-wave approach to asexual evolution: Muller's ratchet and speed of adaptation. Theor. Popul. Biol. **73**: 24–46.

Rozen, S., H. Skaletsky, J. D. Marszalek, P. J. Minx, H. S. Cordum, R. H. Waterston, R. K. Wilson, and D. C. Page, 2003 Abundant gene conversion between arms of palindromes in human and ape Y chromosomes. Nature **423**: 873–876.

Sakamoto, T. and H. Innan, 2019 The evolutionary dynamics of a genetic barrier to gene flow: From the establishment to the emergence of a peak of divergence. Genetics **212**: 1383–1398.

Santiago, E. and A. Caballero, 2005 Variation after a selective sweep in a subdivided population. Genetics **169**: 475–483.

Saunders, P. A., S. Neuenschwander, and N. Perrin, 2018 Sex chromosome turnovers and genetic drift: a simulation study. J. Evol. Biol. **31**: 1413–1419.

Saunders, P. A., S. Neuenschwander, and N. Perrin, 2019 Impact of deleterious mutations, sexually antagonistic selection, and mode of recombination suppression on transitions between male and female heterogamety. Heredity **123**: 419–428.

Schweinsberg, J. and R. Durrett, 2005 Random partitions approximating the coalescence of lineages during a selective sweep. Ann. Appl. Probab. **15**: 1591–1651.

Scott, M. F., M. M. Osmond, and S. P. Otto, 2018 Haploid selection, sex ratio bias, and transitions between sex-determining systems. PLoS Biol. **16**: e2005609.

Servedio, M. R., 2011 Limits to the evolution of assortative mating by female choice under restricted gene flow. Proc. R. Soc. Lond. B **278**: 179–187.

Servedio, M. R. and J. W. Boughman, 2017 The role of sexual selection in local adaptation and speciation. Annu. Rev. Ecol. Evol. Syst. **48**: 85–109.

Servedio, M. R. and R. Bürger, 2015 The effects of sexual selection on trait divergence in a peripheral population with gene flow. Evolution **69**: 2648–2661.

Servedio, M. R., G. S. Van Doorn, M. Kopp, A. M. Frame, and P. Nosil, 2011 Magic traits in speciation:'magic'but not rare? Trends Ecol. Evol. **26**: 389–397.

Skaletsky, H., T. Kuroda-Kawaguchi, P. J. Minx, H. S. Cordum, L. Hillier, L. G. Brown, S. Repping, T. Pyntikova, J. Ali, T. Bieri, *et al.*, 2003 The male-specific region of the human Y chromosome is a mosaic of discrete sequence classes. Nature **423**: 825–837.

Skov, L., M. H. Schierup, D. P. G. Consortium, *et al.*, 2017 Analysis of 62 hybrid assembled human Y chromosomes exposes rapid structural changes and high rates of gene conversion. PLoS Genet. **13**: e1006834.

Slatkin, M., 1981 Fixation probabilities and fixation times in a subdivided population. Evolution pp. 477–488.

Slatkin, M., 1982 Pleiotropy and parapatric speciation. Evolution **36**: 263–270.

Slatkin, M. and T. Wiehe, 1998 Genetic hitch-hiking in a subdivided population. Genet. Res. **71**: 155–160.

Söderberg, R. J. and O. G. Berg, 2007 Mutational interference and the progression of Muller's ratchet when mutations have a broad range of deleterious effects. Genetics **177**: 971–986.

Soh, Y. S., J. Alföldi, T. Pyntikova, L. G. Brown, T. Graves, P. J. Minx, R. S. Fulton, C. Kremitzki, N. Koutseva, J. L. Mueller, *et al.*, 2014 Sequencing the mouse Y chromosome reveals convergent gene acquisition and amplification on both sex chromosomes. Cell **159**: 800–813.

Song, Y. S. and M. Steinrücken, 2012 A simple method for finding explicit analytic transition densities of diffusion processes with general diploid selection. Genetics **190**: 1117–1129.

Stephan, W., L. Chao, and J. G. Smale, 1993 The advance of Muller's ratchet in a haploid asexual population: approximate solutions based on diffusion theory. Genet. Res. **61**: 225–231.

Stephan, W., T. H. Wiehe, and M. W. Lenz, 1992 The effect of strongly selected substitutions on neutral polymorphism: analytical results based on diffusion theory. Theor. Popul. Biol. **41**: 237–254.

Takimoto, G., M. Higashi, and N. Yamamura, 2000 A deterministic genetic model for sympatric speciation by sexual selection. Evolution **54**: 1870–1881.

Teshima, K. M. and H. Innan, 2004 The effect of gene conversion on the divergence between duplicated genes. Genetics **166**: 1553–1560.

Thibert-Plante, X. and S. Gavrilets, 2013 Evolution of mate choice and the so-called magic traits in ecological speciation. Ecol. Lett. **16**: 1004–1013.

Tomasini, M. and S. Peischl, 2018 Establishment of locally adapted mutations under divergent selection. Genetics **209**: 885–895.

Turner, G. F. and M. T. Burrows, 1995 A model of sympatric speciation by sexual selection. Proc. R. Soc. Lond. B **260**: 287–292.

Turner, T. L., M. W. Hahn, and S. V. Nuzhdin, 2005 Genomic islands of speciation in anopheles gambiae. PLoS Biol. **3**: e285.

van Doorn, G. S. and M. Kirkpatrick, 2007 Turnover of sex chromosomes induced by sexual conflict. Nature **449**: 909–912.

van Doorn, G. S. and M. Kirkpatrick, 2010 Transitions between male and female heterogamety caused by sex-antagonistic selection. Genetics **186**: 629–645.

Veller, C., P. Muralidhar, G. W. Constable, and M. A. Nowak, 2017 Drift-induced selection between male and female heterogamety. Genetics **207**: 711–727.

Via, S., 2012 Divergence hitchhiking and the spread of genomic isolation during ecological speciation-with-gene-flow. Philos. Trans. R. Soc. Lond. B Biol. Sci. **367**: 451–460.

Wakeley, J., 2009 *Coalescent Theory: An Introduction*. Roberts & Company, Greenwood Village, Colorado.

Waxman, D. and L. Loewe, 2010 A stochastic model for a single click of Muller's ratchet. J. Theor. Biol. **264**: 1120–1132.

Weissing, F. J., P. Edelaar, and G. S. Van Doorn, 2011 Adaptive speciation theory: a conceptual review. Behav. Ecol. Sociobiol. **65**: 461–480.

Whitlock, M. C. and R. Gomulkiewicz, 2005 Probability of fixation in a heterogeneous environment. Genetics **171**: 1407–1417.

Wright, S., 1931 Evolution in mendelian populations. Genetics **16**: 97–159.

Wright, S., 1938 The distribution of gene frequencies under irreversible mutation. Proc. Natl. Acad. Sci. USA **24**: 253–259.

Wu, C.-I., 1985 A stochastic simulation study on speciation by sexual selection. Evolution **39**: 66–82.

Wu, C.-I., 2001 The genic view of the process of speciation. J. Evol. Biol. **14**: 851–865.

Yamamichi, M. and A. Sasaki, 2013 Single-gene speciation with pleiotropy: effects of allele dominance, population size, and delayed inheritance. Evolution **67**: 2011–2023.

Yeaman, S., S. Aeschbacher, and R. Bürger, 2016 The evolution of genomic islands by increased establishment probability of linked alleles. Mol. Ecol. **25**: 2542–2558.

Yeaman, S. and S. P. Otto, 2011 Establishment and maintenance of adaptive genetic divergence under migration, selection, and drift. Evolution **65**: 2123–2129.